T-PM-SymIII-1 SYNAPTIC AND NON-SYNAPTIC INTEGRATION IN FINE NEURAL PROCESSESS.
I. Parnas, Neurobiology, Hebrew University, Jerusalem, Israel.

Axons do not always behave as simple transmission lines. Instead, at bifurcations or regions in which the neurite changes its diameter, propagation of action potentials my be altered and even blocked. Thus, under some conditions a neuron and its ramifications may function as a single unit, but under other circumstances sections of the same neuron may function independently, providing a degree of plasticity not normally attributed to axons. Some examples will be given and the contribution of synaptic activity to such behavior will be demonstrated.

A depolarizing wave, finally reaches the axon terminal where it induces transmitter release. Its amplitude at the terminal may be controlled by the mechanisms described. Recent findings, both theoretical and experimental, indicate that processess governing release of neurotransmitter are more complicated than previously thought. In particular, the critical effects of membrane potential on the onset and termination of transmitter release will be demonstrated.

T-PM-SymIII-2 STRUCTURAL ANALYSIS OF NEURONAL INTEGRATION. R.S. Eisenberg, Department of Physiology, Rush Medical College, 1750 W. Harrison Street, Chicago, IL 60612.

The electrical properties of cells and tissues are determined by the resistance of cytoplasm and the capacitance and conductance of membranes and channels. In cells of complex structure, like neurons or skeletal muscle fibers, the cytoplasmic path between different patches of membrane can offer as much resistance to current flow as the channels in that patch. Such cells, like syncytial tissues consisting of many cells, have nonuniform distributions of current flow and active membrane potential, perhaps even resting potential. Thus, the functional consequences of channels in syncytial tissues like epithelia depend as much on their location as their properties.

Systematic methods have been developed to study the spatial distribution of the linear electrical properties of complex tissues (e.g. skeletal and cardiac muscle; lens; gall bladder epithelium) and these can be used, at least in principle, to analyze the electrical properties of neurons with elaborate dendritic trees. First, the structure is described qualitatively (i.e., topologically) and quantitatively, using morphometric techniques. Second, the linear properties expected from such a structure are predicted using singular perturbation theory to understand and solve the appropriate electrodiffusion field equations. Third, impedance measurements are used to determine the linear properties of the cellular components. Direct measurements of the spatial distribution of potential (using voltage sensitive dyes) or current (using a wideband version of the vibrating probe) will probably be needed to map out the distribution of channels in dendritic trees and thus to determine the relative contributions of dendritic structure, channel distribution, and channel properties to neuronal integration.

T-PM-SymIII-3 ELECTRORESPONSIVE PROPERTIES OF CENTRAL NEURON DENDRITES AND THEIR CONTROL IN NEURONAL INTEGRATION. R. R. Llinás. Dept. Physiol. & Biophys., New York Univ. Med. Ctr., New York 10016.

Over the last decade intracellular recordings from dendrites (especially in the Purkinje cells of the cerebellum) have yielded direct measurements concerning the electroresponsiveness of central dendrites. These studies have been performed both *in vivo* and *in vitro*. The *in vitro* studies indicate that the dendrites of Purkinje cells have at the very least 3 distinct voltage dependent ionic conductances. These consist of (a) 2 inward currents carried by Ca++, one of which does not inactivate and can generate very prolonged all-or-none plateau activations, (b) a Ca++ conductance capable of generating fast rising action potentials, and (c) a Ca-dependent K+ conductance which regulates both the duration of the Ca++ spikes as well as the duration and amplitude of the plateau potentials. In addition, the somata of these cells demonstrate the Na+ and K+ conductances which generate fast action potentials, and a slower non-inactivating Na+ conductance which may be separated from the fast inward Na+ current and which may also generate plateau potential responses, in this case at somatic level. These different conductances and the strategic way in which they are distributed over the soma-dendritic area of central neurons indicate that integration emerges as a rather complex interaction between linear and nonlinear properties of membrane conductances. Furthermore, it is evident that variation and modulation of such conductance is central in understanding the mechanisms which ultimately must encode long-term storage of information. Examples of other types of dendritic electroresponsiveness will be given, as exemplified by electrical activity of neurons in the mammalian inferior olive and thalamus *in vitro*. [Supported by NS13742, NINCDS]

T-PM-SymIII-4 OPTICAL MEASUREMENT OF ELECTRICAL ACTIVITY IN FINE PROCESSES OF THE NERVOUS SYSTEM.
B.M. Salzberg. University of Pennsylvania, Philadelphia, PA 19104.

Optical methods that employ linear potentiometric probes are now capable of recording electrical activity from fine neuronal processes that are too small to be impaled with microelectrodes and too far, electrically, from the somata to be reflected there. Multiple Site Optical Recording of Transmembrane Voltage (MSORTV), using computer linked two-dimensional photodetector arrays, should permit increasingly sophisticated analyses of the electrical properties of otherwise inaccessible regions of neurons in situ and in tissue culture. The time course of the membrane potential changes that occur in the less accessible reaches of the nervous system (e.g., in the dendritic trees and axonal terminals of vertebrate central neurons, in the secretory endings of neuroendocrine cells, in neuroglia, and in the neuropil jungles of invertebrates), and the effects of the cable properties of these structures on integration, are becoming amenable to study using molecular probes.

Recent applications of MSORTV and other optical techniques will be discussed, including studies in tissue culture of the processes of single cells, and recordings of the action potential, under a variety of conditions, from the small (0.5 - 1.0 μm) nerve terminals in the neurohypophyses of frog and mouse. Current techniques and their limitations, as well as eventual prospects will be considered.

Supported by USPHS grant NS 16824.

T-PM-A1 ELASTIC SIDE-FORCES BETWEEN THICK FILAMENTS IN VERTEBRATE STRIATED MUSCLE AND THE POSSIBLE ROLE OF C-PROTEIN. Alan Magid, Theda Kontis, H.P. Ting-Beall and Carmen Lucaveche, Department of Anatomy, Duke University Medical Center, Durham, North Carolina 27710

Relaxed myofibrils retain their 3-D coherency, implying that non-actomyosin structural links are intrinsic. Here we consider the forces which hold thick filaments together sideways in the A-band. Theoretical analysis (Maughan & Godt, Biophys. Struct. Mech. 7: 17) indicates that van der Waals' force is much too small to balance the swelling pressure present in the A-band and that elastic crosslinks are far more important. Skinned frog fibers stretched to non-overlap of A- and I-bands were studied by EM. In thin sections, abundant densities (~ 8 nm wide) apparently connecting neighboring thick filaments were seen. They occur roughly every 20-30 nm. Study of stereo pairs prepared by the deep-etch method confirm that these structures, which we call side-struts, attach to filaments. We developed methods for preparing non-overlap myofibrils (from frog muscle). Exposure to 2 mM ionic strength caused A-bands to swell about 70%, from which they largely recover when returned to std. salt (.15 M i.s.). Brief digestion with pancreatic elastase (1.2 μg/ml) caused an irreversible loss of this elasticity. The action of elastase on slack length rabbit psoas myofibrils was studied by SDS gel electrophoresis. C-protein was digested, yielding a fragment ~ 5 Kdl smaller. Actin, α-actinin, tropomyosin, and the very high mol. wt. proteins seemed unaffected, but myosin was slightly degraded. Since C-protein is present as transverse stripes in the A-band, we suggest that it provides part of the passive radial elasticity. Experiments correlating the functional and structural effects of elastolysis are in progress. Supported by NIH Grant AM27763.

T-PM-A2 THE RATE OF FORCE REDEVELOPMENT IN SINGLE SKINNED RABBIT PSOAS FIBERS. Bernhard Brenner Institute of Physiology II, University of Tübingen, FRG, and the Laboratory of Physical Biology, NIH, Bethesda, MD. 20205

The rate of recovery of isometric force was measured either immediately after unloaded shortening of a fiber or after the fiber was stretched back to its isometric length at the end of lightly loaded isotonic contraction. With both methods the recovery of force starts from near zero level. The approach to the steady state isometric force is well fitted by a single exponential function and it appears to be the same for both methods within the accuracy of the experiment. The rate of recovery is about 4 to 6 s^{-1} at 5°C, 170 mM ionic strength (μ), and 1 mM MgATP. Decreasing the ionic strength to 50 mM reduces this rate by a factor of about 1.5. Increasing the temperature to 25°C causes about a 6-7 fold increase. At 50 μM MgATP the rate of recovery is 50 to 75% of the value measured in the presence of 1 mM MgATP. At 15°C, μ = 170 mM and 1 mM MgATP the rate of recovery is 12-15 s^{-1} which compares favourably with the maximum actin activated ATPase rate of 6 s^{-1} measured in solution under the same conditions using myosin subfragment-1 cross linked to actin (Mornet et al., Nature, 292, 301 - 306; Stein and Eisenberg, unpublished data). It is concluded that the step which determines the rate of force development in the cross-bridge cycle (i.e., the rate constant "f" defined by A. F. Huxley, 1957) may be the same as the rate limiting step in the actomyosin ATPase cycle in solution.

T-PM-A3 THE FORCE-SARCOMERE LENGTH RELATIONS OF PERCH (PERCA FLUVIATILIS L.) MUSCLE FIBERS HAVING DIFFERENT ACTIN FILAMENT LENGTH. H.L.M. Granzier, H.E.D.J. te Keurs, H.A. Akster, Dept. of Exp. Cardiology, State University Leiden, the Netherlands.

Isometric force (F) - sarcomere length (SL) relations were studied in 8 bundles of fast twitch fibers from the hyohyoid muscle (HH) and in 7 bundles of slow twitch fibers from the levator operculi anterior (LOP). Bundles of 3-20 fibers were bathed in oxygenated saline, pH 7.4, 20°C. Mean active SL (laser-diffraction and light microscopy) and plateau F were measured during maximal tetani. Filament lengths in these fibers were determined by electronmicroscopy and corrected for shrinkage using actin periodicity. The F-SL relations showed a plateau at 2.00-2.20 μm (HH) and 2.50-2.70 μm (LOP), and their descending limbs were linear. The regression line of HH had zero F at 3.67 μm and at 4.22 μm in LOP. The passive F was less than 1% of maximal active F at 2.4 μm (HH) and at 2.65 μm (LOP), it increased exponentially with longer SL, and was 50% of maximal active F at 3.0 μm (HH) and at 3.22 μm (LOP). In both muscles myosin was 1.45 ± 0.05 μm (± S.D.) long, the bare zone was 0.14 ± 0.01 μm long and the z-line was 0.13 ± 0.01 μm wide. Actin length was 0.90± 0.05 μm in HH and 1.22 ± 0.05 μm in LOP. The shift of the descending limbs of the F-SL relations in these muscles is slightly less than that is expected on the basis of the difference in actin length in a sliding filament/cross-bridge model.

T-PM-A4 THE CHARACTERISTIC FORCE RESPONSE OF UNSTIMULATED INTACT AND SKINNED MUSCLE FIBERS: EFFECT OF SARCOMERE LENGTH WITH RADIAL COMPRESSION. J. Gulati and A. Babu, Depts. of Medicine and Physiology & Biophysics, Albert Einstein College of Medicine, Bronx, N.Y. 10461.

On continuous elongation, unstimulated muscle and isolated fibers give a characteristic force response consisting of a stepwise rise (I), followed by a plateau and a phase (III) that parallels the change in length (Hill, 1968 J Physiol 199, 637; Ford et al, 1977 J Physiol 269, 441; Haugen et al, 1981 Acta Physiol Scand 112, 113). To evaluate the effects of filament overlap and compression we have measured the response in lumbricalis frog fibers to 10%Lo stretch (1) at 2.2μm S.L. in standard solution (240mOsm) at various stretch speeds, (2) varying the osmotic strength (240 to 390mOsm) with sucrose or KCl, (3) varying the S.L. (2.2μm to 3.4μm) at 240-290mOsm. The response was measured on skinned fibers (4) by varying the dextran and glycerol in the relaxing solution. The amplitude of phase I (F_I) increased with speed. Also, F_I increased with osmolality in sucrose (from 1%Po in control to 20%Po in 390mOsm), but was constant with KCl. Thus filament separation (f.s.) is a significant factor in the origination of F_I. In skinned fibers, F_I increased in dextran, where both the fiber was compressed and viscosity was higher; but F_I was constant in glycerol, where only the viscosity was increased. Thus, solution viscosity is not a factor in the F_I response. With S.L., F_I in intact cells increased from 2.2μm to 3.0μm and fell at longer lengths. Subtracting the f.s. dependent factor (found from #2 and #4 above), the remainder of F_I decreased with S.L. according to overlap. This is the most direct evidence that the F_I-part of the characteristic response is due to (unusual) interaction between thin and thick filaments in the relaxed fibers. The above interaction increases with decreasing lateral interfilament separation but diminishes at no overlap. (Supported by NSF & MDA).

T-PM-A5 MECHANICAL SPEED OF TYPE 2A FIBERS TRANSFORMED BY CHRONIC STIMULATION. H.L. Sweeney, M.J. Kushmerick, E. Mabuchi, J. Gergely and F. Sreter. Departments of Physiology & Biophysics, Neurology, and Anesthesiology, Harvard Medical School, Boston, MA 02115, and Department of Muscle Research, Boston Biomedical Research Institute, Boston, MA 02114.

Chronic stimulation of the motor nerve alters the metabolic profile and myofibrillar proteins of the muscle fibers. One of the hind limbs of rabbits was intermittently stimulated via the common peroneal nerve (8 Hz, 8 hr/day) for up to 7 weeks. This protocol resulted in nearly complete transformation of type 2B to type 2A fibers in the tibialis anterior muscle, without the appearance of type 1 fibers. We examined whether the mechanical properties of type 2B and transformed 2A fibers are different. Bundles of fibers were teased from the tibialis anterior muscles of the chronically stimulated side and the unstimulated (control) side of a pentobarbital-anesthetized rabbit, and stored in relaxing solution for up to 14 days. A segment of a single fiber was mounted on a motor lever and force transducer. Its sarcomere length was set to 2.6-2.7 μm using interference contrast microscopy. The slack test was used to estimate the unloaded velocity of shortening at 12°C and 20°C after activation at pCa 4.5. Pieces of the same fiber segment were subjected to pyrophosphate gel electrophoresis to determine their fiber type. Isometric tensions averaged 1.0 kg/cm^2 in both control and stimulated fibers. At 20°C, velocity shortening in units of fiber length/sec in stimulated fibers (all type 2A) was 1.33 ± 0.08 (SEM; n=6), whereas in controls (all type 2B) the velocity was 2.5 ± 0.09 (SEM; n=6). At 12°C, the corresponding values were: stimulated = 0.85 ± 0.10 (n=4), and control = 1.33 ± 0.13 (n=4). Therefore, the velocity of shortening, but not maximum isometric force, changes in the transformation of type 2B to type 2A fibers in concert with the myosin isozyme change. (Supported by NIH Grants AM 32018 and AG 02103.)

T-PM-A6 DIFFERENTIAL MYOSIN REACTIVITY CORRELATED WITH ULTRASTRUCTURAL VARIATION ALONG EXTRAOCULAR MUSCLE FIBERS. J.Davidowitz, S.Shafiq*, A.Onejeme and D.J.Chiarandini, Dept. of Ophthalmology, New York Univ. Medical Center, New York, NY 10016 and *Dept. of Neurology, Downstate Medical Center, Brooklyn, NY 11203

Extraocular muscles (EOM's) in mammals contain various populations of singly innervated fibers (SIF's) and multiply innervated fibers (MIF's) distributed in two layers, global and orbital. We have shown that orbital MIF's of rabbit EOM's are the longest of this muscle layer, and that these fibers display a systematic ultrastructural variation (1). Toward the middle of the muscle's length (nerve entry region), these fibers exhibit a well developed sarcoplasmic reticulum (SR), small myofibrils and elevated mitochondrial content. This 'twitch-like' morphology is associated with a large endplate-like nerve ending. In the muscle's distal third, these fibers exhibit poorly developed SR, large ill-defined myofibrils, and reduced mitochondrial content. This 'tonic-like' structure is associated with small superficial nerve endings (1). We presently examined the distribution of myosin types along the length of orbital MIF's using two monoclonal antibodies (AB), ALD-180 and MF-18, which respectively react against slow (anterior latissimus dorsi) and fast (pectoralis) chicken muscle. Serial frozen sections of superior rectus muscles were taken, and those at the nerve entry region and distal third region of the muscles were stained with fluorescein-conjugated AB. In the nerve entry region, the orbital MIF's were recognized by their characteristic diameter (5-10 μ) which contrasts with the diameter of the orbital SIF's (15-20 μ). In the distal third region, these MIF's were recognized by their being virtually the only orbital fibers there. ALD-180 reactivity was positive only in the distal portion of orbital MIF's. Neither the global MIF's nor any SIF's reacted with this AB. MF-18 reactivity was negative in both orbital regions. In the global layer, MF-18 was the only AB that reacted, staining global white and intermediate SIF's. The present finding that the ALD-180 AB reacts selectively with the distal portion of orbital MIF's, where they display a 'tonic-like' structure, would be compatible with the notion that these fibers may have different contractile properties at different regions of their length. Supported by USPHS grants EY00309 and EY01297.

(1) J.Davidowitz, G.Philips and G.M.Breinin, Invest. Ophthal. 1977, 16:711.

T-PM-A7 THE EFFECTS OF A CALCIUM-ACTIVATED PROTEASE ON THE CONTRACTILE MECHANICS AND ULTRASTRUCTURE OF SKINNED SMOOTH MUSCLE, Joe R. Haeberle, Sharon A. Coolican, and David R. Hathaway, Depts. Physiology and Medicine, Indiana Univ. Sch. Med., Indianapolis, IN 46223

The contraction of smooth muscle involves filamentous actin and myosin as well as cytoskeletal structures (e.g., dense bodies) which are presumably involved in the attachment of actin filaments to each other and to the cell membrane. Digestion of chemically "skinned" smooth muscle by a calcium-activated protease (CAP) resulted in a reduction of isometric force and isotonic shortening velocity as well as a parallel loss of cytoplasmic and membrane-bound dense bodies. Longitudinal uterine smooth muscle from rat uterus was skinned in a buffered solution (pH 7.0) containing 5 mM EGTA and 6 mM MgATP at 5°C for 48 hr and then frozen at -70°C. Muscles were contracted by elevating calcium to 30 uM. The addition of 1 uM CAP resulted in a loss of isometric force (F) and a decrease in lightly loaded (0.1F) isotonic shortening velocity. Reductions in force to 77 $\pm$ 2.6% (mean $\pm$SD), 49 $\pm$ 5.0%, and 27 $\pm$ 2.8% of maximum force (F_o) were accompanied by reductions in shortening velocity to 81 $\pm$ 2.9%, 64 $\pm$ 4.0%, and 36 $\pm$ 3.6% of control velocity (0.012 l_o/s) respectively. Electron microscopic examination of tissues following loss of >95% F_o showed no apparent loss of actin or myosin filaments but almost complete loss of both cytoplasmic and membrane attached dense bodies. Digestion of contracting muscles in the presence of calcium and MgATP resulted in disorientation and central aggregation of actin and myosin filaments. Digestion of contracted muscles in the absence of MgATP prevented the disorientation of myofilaments without preventing the loss of dense bodies. In summary, these results suggest that 1) dense bodies are a substrate for the CAP and 2) dense bodies serve as myofilament attachment sites and are necessary for coordinated cellular contraction.

T-PM-A8 CALCIUM ACTIVATION OF SKINNED BUNDLES OF CARDIAC CELLS CONTAINING RV_1 OR RV_3 MYOSIN. Pagani,ED and Julian,FJ, Dept Anes Res Labs, Brigham and Women's Hosp Boston, MA 02115

Force-pCa curves (pCa 4.22 - pCa 8) and the time to peak tension (TPT) were measured in saponinized bundles of cardiac cells dissected from rabbit hearts which contained RV_1 or RV_3 myosin. SDS gel electrophoresis of the proteins (125,000-10,000 MW) released from segments of cardiac muscle as a result of saponin treatment indicated that none of the major myofibrillar proteins was lost. Force-pCa curves were obtained at average sarcomere lengths of 2.2-2.3 µm. Rapid activation of force was accomplished by using the "calcium jump" method (Moisescu and Thieleczek J Physiol 275 1978) with slight modifications. Bundles could undergo as many as 20 contractions with no decrease in maximum force development or change in the sarcomere pattern. The relation between force and pCa was the same for bundles of cardiac cells which contained either RV_1 or RV_3 myosin. Although the TPT was generally faster for preparations which contained the RV_1 myosin, it was not entirely clear if this was solely due to a more rapid rate of RV_1 cross-bridge formation or rather a result of Ca^{2+}-induced Ca^{2+} release from the sarcoplasmic reticulum (SR). For example, the TPT of fibers that showed tension oscillations (1-7% P_o), which we are assuming to be due to the release and uptake of Ca^{2+} by the SR, while in the pre-activation solution (HDTA), gave a TPT of 1.0 sec. Yet the same fibers, activated under identical conditions, not showing tension oscillations gave a TPT of 2.0 to 3.5 sec. These data suggest that the Ca^{2+} sensitivity of the regulatory system is the same for cardiac cells which contain all RV_1 or RV_3 myosin. The rate of tension development of skinned cardiac cells with a functionally intact SR may not only depend upon the rate of cross-bridge formation but also upon the release of Ca^{2+} from the SR. NIH grants HL30133 (FJJ) and HL06563 (EDP).

T-PM-A9 THE INFLUENCE OF STIMULATION RATE AND TWITCH POTENTIATORS (Zn^{+2} & NO_3^-) ON THE LENGTH-TENSION RELATIONSHIP OF FROG SINGLE MUSCLE FIBERS. Rome L.C.*, Morgan D.L., and Julian F.J. Anes. Res. Labs., Brigham & Women's Hosp., Boston, MA, and *Monash Univ., Australia

Taylor et al (Can J Physiol Pharm 60 1982) observed that exposure to Zn^{2+} substantially increased tension generated during tetani at short sacromere lengths (SL<1.9µ). This suggested to them that as SL decreased, the level of activation produced by electrical stimulation in Ringers decreased as well. Julian & Morgan (J Physiol 319 1981), however, found that exposure to Zn^{2+} resulted in little change in tension, suggesting that activation was essentially complete at all SL (1.7-2.3 µ). To resolve this discrepancy, we measured the effects of stim rate, Zn^{2+} and NO_3^- on isometric tension at SL = 1.7 to 2.3 µ in single living fibers from R. temp. Significant depression in tension levels was observed at submaximal stim rates even though little ripple in the tension record was evident. % Depression/% Ripple increased as SL decreased, and was larger in fibers with low Twitch/Tet. Exposure to 50 µm Zn^{2+} or NO_3^- caused tension at all SL to increase but the tension did not exceed that generated at the maximal stim rate in normal Ringers by more than 2%. These data, with Taylor et al's (1982), suggest that their results were obtained from fibers stimulated at submaximal rates which became maximally activating only in the presence of Zn^{2+}, while Julian & Morgan's (1981) results were from fibers that were stimulated at rates which were maximally activating. Fibers maximally activated, either by high stim rates or by low stim rates in Zn^{2+}, followed the classical force-SL curve. These results support the idea that the decline in tension seen between SL = 2.0 to 1.7 µ is not the result of length-dependent activation, but is caused by mechanical interference resulting from double overlapping of thin filaments (Julian & Morgan 1981). NIH grants HL30133 (FJJ) & AM07046 (LCR), & MSRG #EN7/82 (DLM).

T-PM-A10 NO TENSION FLUCTUATION IN NORMAL AND HEALTHY SINGLE MYOFIBRILS. Tatsuo Iwazumi, Dept. Physiology and Biophysics, University of Texas Medical Branch, Galveston, Texas 77550.

Use of extremely sensitive and wideband transducers and a recently developed method for keeping single myofibrils healthy for many hours permitted measurements of tension noise spectra in long, steady, and strong contractions. Myofibrils were 1 ∿ 2 μm wide and about 30 sarcomere long.

If there were mechanical cycling of N cross-bridges in a half-sarcomere, the total mean tension is proportional to N, but the fluctuation about the mean is proportional to $\sqrt{N}$. In fully overrapped (SL = 2.2 μm) sarcomeres, N ≅ 50,000, but N can be reduced by stretching; for example, N ≅ 5,000 at SL = 3.46 μm, hence 3.16 times more fluctuations.

Actually observed single myofibril tension traces were very smooth, just as smooth as during rest, at all sarcomere lengths tested. Furthermore, the noise spectra taken during rest and during plateau of active tension had no consistent differences with detection uncertainty < 1 ng/$\sqrt{Hz}$ in 2-512 Hz bandwidth with 64 averages. To test if mechanical vibrations were transmitted through the myofibril, the length controller was activated by white noise with comparable noise power expected from above assumption, and the fluctuations were detectable. It was also demonstrated that the water medium did not transmit enough power below 600 Hz.

However, tension fluctuations with Lorentzian-like spectra having about 20 Hz roll-off were clearly detectable in myofibril bundles (> 3 μm) only when their SR were still functional, demonstrating that SR exerts strong effects even in rather small myofibril bundles in EGTA (10 mM) buffered solution.

Therefore, it is highly unlikely that there exists mechanical cycling of cross-bridges as generally assumed in conjunction with the ATPase activity.

T-PM-A11 POST-TETANIC POTENTIATION IN SINGLE MOTOR UNITS OF MOUSE MUSCLE. by D.J. Parry and S.Di Cori. (Dept. Physiol., Univ. Ottawa, Ottawa, Ont. Canada)

Mammalian fast-twitch muscles exhibit post-tetanic potentiation (PTP) whereas slow-twitch muscles show post-tetanic depression (PTP). Mouse soleus (SOL) does not show significant potentiation, however. In adult mice SOL contains a relatively high proportion (about 40%) of type II fibres which might be expected to exhibit fast-twitch characteristics, the remainder being type I (slow-twitch). The absence of PTP may be due to PTD in the type I fibres offsetting the PTP of the type II fibres. Alternatively, SOL fibres may be inherently different from those of fast-twitch muscles regardless of fibre type. We examined PTP in single motor units of SOL and extensor digitorum longus (EDL) of mice aged 3 months. Units were isolated by ventral root splitting and PTP was determined 1 second after a 2-second unfused tetanus (50Hz). Motor unit times to peak twitch tension (CT) ranged from 6 to 40 msec. When PTP was plotted against CT, units with CT < 12 msec showed PTP while those with CT > 12 msec showed either PTD or no effect. The data were fitted by two straight lines suggesting that the extent of PTP and CT are not controlled by a single process. All EDL units had PTP < 12 msec and all showed PTP. When all EDL units were plotted for PTP against CT they fell along the same line as those SOL units with CT < 12 msec. When EDL units were subdivided into types FF and FR it appeared that FF units may show slightly less PTP than FR units with identical CT. (Supported by MDAC).

T-PM-A12 SARCOMERE DYNAMICS IN THE ISOLATED MYOCYTE: THE INTERACTION OF CALCIUM AND THE PATTERN OF STIMULATION. Rashid Nassar, Page A. W. Anderson and Mary C. Reedy. Duke University, Durham, N.C. (Intr. by Andrés Manring.)

Sarcomere motion in untethered isolated intact myocytes from rabbit ventricle was measured in order to understand how alterations in the pattern of stimulation and calcium bring about the force-interval relationship of intact muscle. Sarcomere length was measured from the magnified image of the cell recorded on video tape. The cell was stimulated at a basic interval t_0 (4s). Two extra stimuli were introduced every eighth beat at intervals t_1 and t_2. A first stage curve was obtained by fixing t_2 at 3s and plotting the maximum sarcomere shortening velocity, $\dot{S}_1$, as a function of t_1. A second stage curve was obtained by fixing t_1 at a short interval (e.g. 950 ms) and plotting $\dot{S}_2$ as a function of t_2, t_2 being extended up to 15s to assess the effect of long rest periods. The first stage curve rose monotonically to a plateau equal to $\dot{S}$ at the basic rate. The second stage curve rose faster and to a higher plateau than the first. The plateau was maintained. Increasing calcium concentration increased the rates of rise and the plateau levels of both curves. The effects of these patterns of stimulation on $\dot{S}$ demonstrate that the changes in the maximum rate of rise of force in the isolated papillary muscle and the maximum rate of rise of ventricular pressure in the isolated heart have their basis in sarcomere shortening. These results suggest that the pattern of stimulation and the extracellular calcium concentration modulate the amount of activator calcium. The effects of these previous conditions on the pool of activator calcium are unaltered by long periods of rest. This suggests that from beat to beat during a broad range of rates, no time-dependent depletion of activator calcium occurs.

T-PM-B1 Na^+, K^+-ATPASE ACTIVITY AND ION FLUXES IN INTACT BROWN ADIPOCYTES. LaNoue, K. F., Strzelecki, D., and Koch, C. D. Dept. Physiology, The Milton S. Hershey Medical Center, Penn State Univ., Hershey, PA 17033.

Previous data suggested that brown fat Na^+, K^+-ATPase is hormonally regulated. An increase in Na^+ flux across the plasma membrane may trigger increases in respiration observed when brown fat is exposed to norepinephrine. $^{22}Na^+$ transport across the cell membrane of isolated adipocytes was measured. External sodium rapidly equilibrated with internal sodium in a ouabain insensitive way. The half time of equilibration was between 15 and 30 seconds. Surprisingly, ouabain did not effect the size of the internal sodium pool during 15 minutes of incubation. Effux of $^{22}Na^+$ was also measured in $^{22}Na^+$ loaded cells. A small (~ 20%) ouabain sensitive component of the $^{22}Na^+$ efflux could be detected. Rates of efflux were not altered by norepinephrine.

Since ouabain-sensitive $^{22}Na^+$ fluxes could not be measured accurately, $^{86}Rb^+$ (substituting for K^+) uptake was measured. The K^+ salts in the Krebs Henseleit cell media were replaced with non-radioactive Rb^+ and measurements were initiated by the addition of tracer $^{86}Rb^+$. Rb^+ fluxes were slow; the half time to equilibration of $^{86}Rb^+$ with the intracellular pool of Rb^+ was more than 40 minutes. Rates of uptake were measured during the initial 5 minutes. Over 90% of the $^{86}Rb^+$ fluxes were sensitive to ouabain. Norepinephrine stimulated respiration of the cells 10x but had no effect on $^{86}Rb^+$ fluxes. Although ouabain inhibited 90% of the $^{86}Rb^+$ uptake within one minute, 40% inhibition of the norephinephrine response required 30 minutes preincubation. The effects of amiloride and external Ca^+ and Na^+ on the rapid Na^+ fluxes are being investigated. (Supported by NIH Grant AM-26309).

T-PM-B2 SODIUM PUMP ACTIVITY IN MDCK EPITHELIAL CELL CULTURES. B.G. Kennedy and J.E. Lever. Dept. of Biochemistry and Molecular Biology. The University of Texas Medical School, Houston, TX.

Fluctuations in sodium pump mediated cation exchange have been associated with growth and differentiation in several tissues. We have examined ouabain-sensitive Rb^+ influx, internal Na^+ levels and ouabain-sensitive ATP hydrolysis to characterize the sodium pump in MDCK cells. The MDCK cell line, derived from dog kidney, forms a functioning epithelium capable of vectorial salt and water transport in vitro. Localized bulges of the cell monolayer, termed domes, are morphological manifestations of this transport. Furthermore, a correspondence between processes of cellular differentiation and dome induction has been inferred since compounds such as hexamethylene bisacetamide, (HMBA) and DMSO, known as inducers of mammalian cell differentiation will stimulate dome formation. Ouabain-sensitive ATPase activity and Rb^+ uptake were maximal in subconfluent MDCK cultures and both activities decreased in parallel as cultures grew to confluence. HMBA and DMSO partially inhibited ouabain-sensitive Rb^+ uptake in confluent cultures. This inhibition required the presence of an intact cell membrane since the ATPase activity assayed in disrupted cell suspensions was not altered by inducer treatment. Sodium pump inhibition did cause a measurable rise in internal Na^+ concentration. This increase in internal Na^+, and not pump inhibition per se, may be important in the differentiation response caused by HMBA and DMSO. Thus we observed that elevation of cAMP content would elevate Na^+ concentration and also stimulate dome formation. In this case, the increase in intracellular sodium concentration was mediated by a furosemide-sensitive mechanism and secondarily caused a stimulation of sodium pump activity.

T-PM-B3 P_i PHOSPHORYLATION OF RED CELL (Na^++K^+)-ATPase DURING K:K EXCHANGE. Jack H. Kaplan, Linda J. Kenney, and Martin R. Webb. Departments of Physiology and Biochemistry and Biophysics, University of Pennsylvania, Philadelphia, Pa. 19104.

The sodium pump of human red blood cells mediates a ouabain-sensitive exchange of intracellular and extracellular K^+ (K:K exchange) that requires the presence of both inorganic phosphate (P_i) and an adenosine nucleotide such as ADP. This P_i requirement could involve covalent phosphorylation or just reversible binding. We have prepared resealed red cell ghosts using a gel filtration procedure to contain ADP and $(^{18}O_4)P_i$. Using ^{31}P NMR spectroscopy we have shown that the ghosts mediate a P_i-water-oxygen exchange which is inhibited (ca. 75%) by ouabain ($10^{-4}M$) indicating that the reaction is sodium pump-mediated. This oxygen exchange resulting from reversible E-P formation is stimulated by K^+ and inhibited by Na^+ + oligomycin, although neither agent alone has much effect. Simultaneous measurements of K:K exchange and oxygen exchange show that oxygen exchange is somewhat faster (about ten-fold) and can occur in the absence of transport when the ghosts do not contain ADP. These results suggests that reversible phosphorylation is part of a common pathway shared by both K:K exchange and oxygen exchange, but there are steps in the reaction pathway for K:K exchange that involve ADP which are not required for oxygen exchange. Thus the two reactions are linked, but are not tightly coupled. The relevance of these findings to the sodium pump reaction mechanism will be discussed. (Supported by NIH AM 23030 and HL 30315. JHK is a recipient of RCDA K04-HL01092, and LJK is supported by Training Grant 5T-32-GM07229).

T-PM-B4 CALCIUM TRANSPORT IN TRANSVERSE TUBULES ISOLATED FROM RABBIT SKELETAL MUSCLE. C. Hidalgo and M. E. Gonzalez. Department of Muscle Research, Boston Biomedical Research Institute, and Department of Neurology, Harvard Medical School, Boston, MA.

Transverse tubule (T-tubule) vesicles isolated by loading contaminating SR with calcium phosphate contain significant amounts of Ca^{2+}, and display very low, if any, Ca^{2+} transport. To avoid isolating T-tubules containing Ca^{2+}, we modified the isolation procedure by further fractionating in discontinuous sucrose gradients the light microsomal vesicles, which are enriched in T-tubules. The lightest T-tubule fraction, which is usually devoid of SR contamination as indicated by its lack of measurable ATPase activated by Ca^{2+}, accumulates 110-140 nmol of calcium per mg of protein, at rates of 10-12 nmol $mg^{-1}min^{-1}$. No Ca^{2+} transport was observed in the absence of ATP, indicating that the transport is the result of an ATP-dependent Ca^{2+} pump. Ca^{2+} accumulation by T-tubules is not increased by oxalate or by phosphate, indicating that the T-tubule membrane is impermeable to both anions. Half maximum rates of Ca^{2+} transport were observed at a $[Ca^{2+}]$ of 5 X 10^{-7}M. Arrhenius plots of Ca^{2+} transport rates show a break temperature at 27-30°C for T-tubules and at 15-20°C for SR, with higher activation energies in SR than in T-tubules, both above and below their respective break temperatures. The isolated T-tubules do not seem to have significant Na^{+}-Ca^{2+} exchange, as evidenced by the lack of effect of Na^{+} on Ca^{2+} efflux from vesicles actively loaded with Ca^{2+}. In contrast, addition of the ionophore A23187 rapidly releases the accumulated Ca^{2+}, indicating that it is intravesicular and not simply bound to the T-tubule surface. Supported by NIH grant HL23007.

T-PM-B5 INHIBITION OF OXYGEN-18 EXCHANGE BETWEEN INORGANIC PHOSPHATE AND WATER CATALYZED BY THE GASTRIC H,K-ATPase. L.D. Faller and J. Mendlein (Intr. by G. Sachs) CURE, VA Wadsworth and Dept. of Medicine, University of California, Los Angeles, CA 90073.

The proton translocating ATPase isolated from hog gastric mucosae catalyzes oxygen-18 exchange between inorganic phosphate and water. Inhibition of the exchange reaction by reversible and irreversible inhibitors of the enzyme has been studied. Vanadate ions completely inhibit isotope exchange with an apparent K_I = 1.8 μM. Under similar conditions, 3 nmol of vanadate per mg of Lowry protein bind specifically to microsomal vesicles with an apparent K_d = 0.6 μM. All specifically bound vanadate is displaced by inorganic phosphate with an apparent K_d = 70 μM. Oxygen-18 exchange is also completely inhibited by omeprazole, a substituted benzimidazole which inhibits acid secretion *in vivo* and in isolated gastric glands. 1.5 nmol of fluorescein isothiocyanate (FITC) per mg Lowry protein reversibly inhibits the ATPase activity of gastric microsomes without affecting pNPPase activity (Jackson et al., BBA 731, 9-15, 1983). The rate of oxygen-18 exchange is halved by FITC labeling. 8-Azido ATP (N_3ATP) is a photoaffinity label that irreversibly halves the ATPase activity of gastric microsomes without affecting pNPPase activity. 1.5 nmol mg^{-1} of K^{+}-inert phosphorus-32 is incorporated by photolysis of $[\gamma\text{-}^{32}P]N_3ATP$ (Faller et al., Ann. N.Y. Acad. Sci. 402, 146-163, 1982). Photolabeling with N_3ATP appears to have little effect on the rate of oxygen-18 exchange. These results help to clarify the number of active sites and their ability to catalyze the different partial reactions of the gastric enzyme. (Supported by NSF Grant PCM 83-09756 and NIH Grant AM 32931)

T-PM-B6 CYTOSOLIC $[Ca^{++}]$ DEPENDENT STIMULUS SECRETION COUPLING IN PARIETAL CELLS. S. Muallem, G. Sachs, CURE, VA Wadsworth and Dept. of Medicine, University of California, Los Angeles, CA 90073.

Free cytosolic Ca^{++} was measured fluorimetrically or microspectrophotofluorimetrically using Quin 2 fluorescence changes. After 30 minutes incubation in modified gastric gland medium (containing 10mM pyruvate), the isolated parietal cells were washed and suspended either in 1mM Ca or Ca-free medium with EGTA. The intracytosolic Ca^{++} level was found to be 122±21nM, which increased in the presence of carbachol to 533±81nM. The response to carbachol was blocked or reversed by atropine. In Ca-free medium, carbachol lowered free-cell Ca^{++}. ^{45}Ca flux data show that carbachol enhances membrane Ca^{++} permeability. Gastrin induced transient increase in cell Ca^{++} levels, independent of the presence of carbachol. Histamine or dbcAMP had no effect on free-cell Ca^{++}, but reduction of cell Ca^{++} by the addition of Quin 2 in Ca-free medium showed that also the histamine-cAMP pathway depended on free-cell Ca^{++}. Studies on vesicle preparations enriched in basal-lateral membranes showed that no Na^{+}:Ca^{++} exchange could be detected, but that there was a calmodulin-dependent, ATP-driven Ca^{++} uptake. It appears therefore that, depending on species or preparation, the parietal cell responds to muscarinic agents or gastrin by a change in cell Ca^{++} levels, due to alterations in basal-lateral membrane Ca^{++} permeability. In the parietal cell, it appears that the major extrusion pathway for Ca^{++} is via the calmodulin-regulated Ca^{++} pump. (NIH support)

T-PM-B7 ION PATHWAYS IN GASTRIC CELL MEMBRANES: S. Muallem, C. Burnham, G. Sachs. CURE, VA Wadsworth and Department of Medicine, University of California, Los Angeles 90073.

A fraction enriched in basal-lateral membrane vesicles was prepared from rabbit fundic mucosa by step-gradient centrifugation. Determination of ion pathways was carried out both by optical and ion flux methods. Using acridine orange to detect acidification of the vesicle interior, the presence of Na^+:H^+ exchange that was amiloride-sensitive (100uM) and electroneutral was confirmed. Dilution of K_2SO_4-loaded vesicles into K^+-free medium resulted in acidification which was enhanced by the presence of valinomycin. Neither TCS nor VO_4 affected the response but both TEA (20mM) and Ba^{++} (2.5mM) were inhibitory. The addition of Na^+ to the medium dissipated the H^+ gradient. Thus, by this coupling method the vesicles which contain the Na^+:H^+ exchange also possess H^+ and K^+ conductances. No evidence could be found for a Cl^- conductance. Using the dilution-into-tracer method developed by Garty, Rudy and Karlish (personal communication: cation + impermeant anion-loaded vesicles diluted into tracer quantities of cation under isotonic conditions), K^+ gradient-dependent ^{86}Rb uptake and Na^+ gradient-dependent ^{22}Na uptake were measured. This technique confirmed the presence of a K^+ conductance and Na^+:H^+ exchange. With a similar technique, Cl^- conductance was not detected. Parietal cell suspensions can be used to confirm the physiological relevance of the vesicle data. (NIH support).

T-PM-B8 DEPENDENCE OF pH-REGULATION ON EXTERNAL Na^+ AND HCO_3^- IN SQUID AXONS. Walter F. Boron (Intr. by J.M. Russell), Dept. of Physiology, Yale Univ. School of Medicine, New Haven, CT 06510.

The intracellular pH (pH_i) of the squid giant axon is regulated by an ion-transport system that responds to intracellular acid loads by extruding acid from the cell. The transporter takes up one Na^+ and two HCO_3^- (or an equivalent ion), for each Cl^- ejected. To test whether the apparent uptake of Na^+ and HCO_3^- is actually due to the uptake of a single $NaCO_3^-$ (ion-pair model), I studied the kinetics of acid extrusion as a function of $[Na^+]_o$ and $[HCO_3^-]_o$. Axons were internally dialyzed with Na-free solution containing 400mM Cl^-, and 20mM MES (pH 6.5). When pH_i, measured with a glass microelectrode, fell to ~ 6.6, dialysis was halted. With Na^+ and HCO_3^- in the external solution, pH_i now increased due to acid extrusion. The acid-extrusion rate (J, equivalent H^+ efflux) was calculated from dpH_i/dt, intracellular buffering power, and axon diameter. In each axon, J was determined in four combinations of $[Na^+]_o$ and $[HCO_3^-]_o$. When $[HCO_3^-]_o$=12mM, Km(Na)=70.5 ± 12.1mM and Vmax=17.8 ± 3.1 $pmol.cm^{-2}.s^{-1}$ (pcs). Reducing $[HCO_3^-]_o$ to 6 or 3mM caused Km(Na) to rise to 178.6 ± 14.7 or 363.9 ± 34.3mM, respectively. Vmax was not significantly altered. Conversely, when $[Na^+]_o$=425mM, $Km(HCO_3^-)$ = 2.59 ± .28 mM and Vmax = 18.6 ± 2.0 pcs. When $[Na^+]_o$ was reduced to 212 or 106mM, $Km(HCO_3^-)$ rose to 5.35 ± .95 or 9.66 ± 2.10mM, respectively. Vmax was unchanged. These data are consistent with the ion-pair model. In particular, when the flux J is plotted as a function of $[NaCO_3^-]_o$, data from all six groups of experiments fall along the same Michaelis-Menten curve. Fluxes at a given $[NaCO_3^-]_o$ were never significantly different, regardless of the combination of $[Na^+]_o$ and $[HCO_3^-]_o$ used to achieve that $[NaCO_3^-]_o$. (Supported by NIH grant NS-18400.)

T-PM-B9 VOLTAGE DEPENDENCE OF THE Na/Ca EXCHANGE IN SQUID AXONS. DiPolo, R., Bezanilla, F. and Caputo, C. (Intr. by S. Krasne). CBB, IVIC, Aptdo. 1827, Caracas, Venezuela, Dept. of Physiology, UCLA, Los Angeles, CA 90024 and MBL, Woods Hole, MA 02543.

We report the measurement of Na_o-dependent Ca efflux in voltage clamped squid axons under conditions of internal dialysis or perfusion. There was no significant difference in the operation of the Na/Ca exchange when the axons were dialyzed with standard internal solutions containing K (310 mM) and Na (40 mM) or when these ions were replaced with N-methylglucamine and Tris respectively to reduce leakage. Under both experimental conditions, it was found that changes in the membrane potential in both directions from a holding value of -60 mV, induced changes in the Na_o-dependent Ca efflux. The magnitude of these changes depended on ionic conditions and they were considerably smaller than expected from an electrogenic mode of operation of the exchange mechanism with stoichiometries of 4 Na to 1 Ca or sometimes even 3 Na to 1 Ca. Even when axons were depolarized to +25 mV there remained a sizeable fraction of the Na_o-dependent Ca efflux. In other experiments we have attempted to measure the kinetics of the voltage dependent Na/Ca exchange system. For this, we used hyper- or de-polarizing trains of pulses of varying durations to induce changes in the Ca efflux. Pulses of 200 msec duration had virtually the same effect as steady potential changes, pulses of 100, 50 and 20 msec were increasingly less effective, with barely detectable changes induced by the shorter pulses. These results indicate that the voltage dependent activation of the carrier involved in the Na/Ca exchange has kinetics in the order of tens of milliseconds. (Supported by CONICIT S1-1144 to R.D.,CONICIT S1-1148 to C.C. and UPHS GM30376 to F.B.)

T-PM-B10 FUROSEMIDE-SENSITIVE (FS) K FLUXES IN HUMAN RED CELLS: EQUILIBRIUM POSITION AND STOICHIOMETRIC RATIO WITH THE Na FLUXES. Mitzy Canessa, Carlo Brugnara, Daniele Cusi and Daniel C. Tosteson. Department of Physiology and Biophysics, Harvard Medical School, Boston, MA 02115.

We have shown (J. Gen. Physiol. 1983, 82:28a) that FS Na influx equals FS Na efflux at a set of internal and external Na and K concentrations that gives constant values (K_{eq}= 20) for a transport reaction with a stoichiometry of 2 Na_o + 3 $K_o \rightleftharpoons$ 2 Na_i + 3 K_i. To verify experimentally the predicted stoichiometry from the FS Na fluxes, we have measured K efflux and influx using ^{86}Rb and ^{42}K. Internal Na (Na_i) and K (K_i) were adjusted using the nystatin procedure. External K (K_o) was varied from 0-20 mM at constant external Na (Na_o = 130 mM) in the presence of 0.1 mM ouabain. In cells containing only K, the FS K influx was equal to the Na_o-stimulated K influx. We assumed that the Na_o-stimulated component of the K influx measured the inward movement of Na-K pairs. At Na_i = 5, 12 and 30 mM, the FS K influx was higher than the Na_o-stimulated component and was trans-stimulated by Na_i. The inward transport of Na-K pairs (Na_o-stimulated K influx) was independent from Na_i and the difference with the FS K influx could be accounted by a 1:1 K_i/K_o exchange (Na_i-stimulated and Na_o-independent). These two modes of operation of the Na-K cotransport were chloride-dependent and bumetanide-sensitive. The inward transport of Na-K pairs had different selectivity for Rb and K, being the Na_o-stimulated $^{86}Rb/^{85}Rb$ and $^{42}K/K$ influxes similar, but 50% lower than $^{86}Rb/K$ and ^{85}Rb influxes. The FS K efflux was equal to the K influx at values of Na_o, K_o, Na_i and K_i similar to those at which the FS Na fluxes reach equilibrium. The experimentally measured stoichiometry between FS Na and K fluxes agreed with an electroneutral cotransport reaction involving 2 Na, 3 K and 5 Cl (K_{eq}= 2). Supported by NIH-GM 25685-05 and,Milan, Verona and Harvard University

T-PM-B11 Na^+ IONS HAVE TWO SEPARATE ROLES IN THE ACTIVE TRANSPORT OF NONPOLAR AMINO ACIDS IN CHROMATIUM VINOSUM. Andrea D. Cobb and *David B. Knaff, Department of Chemistry, Texas Tech University, Lubbock, TX 79409.

The energy-dependent transport processes of seven nonpolar amino acids studied to date in the photosynthetic bacterium Chromatium vinosum are each electrogenic and involve Na^+ ions in either a symport mechanism or as an allosteric modulator.

Evidence for the role of Na^+ in an amino acid/Na^+ symport includes the following: 1) a Na^+ gradient ($[Na^+]_{out} > [Na^+]_{in}$) across the membrane drives uptake of L-alanine, D-alanine, AIB (α-aminoisobutyric acid, an alanine analog), L-isoleucine and L-valine. The ability of Na^+ gradients to drive L-ile and L-val uptake exists only at pH $\geq$ 7.5. 2) A gradient ([out]>[in]) of any of the amino acids is capable of driving $^{22}Na^+$ uptake.

Evidence that Na^+ allosteric effects are separate from symport relationships is provided by the following: 1) Although Na^+ decreases the K_m of transport for L-ala, AIB, L-ile, and L-val, no such allosteric effect is observed for D-alanine transport. 2) pH gradients ($pH_{out} < pH_{in}$) (but not Na^+ gradients) provide energy for L-leucine and L-phenylalanine transport. However, the K_m for L-phe and L-leu transport decreases markedly in the presence of Na^+. 3) Although Li^+ acts as a Na^+ analog in the Na^+/amino acid symport, no allosteric effect is noted when Li^+ replaces Na^+ in the above systems.

At least two separate Na^+ sites (symport and allosteric) are suggested.

This research is supported by a grant (to D.B.K.) from the NSF (PCM-8109635).

T-PM-B12 K^+ - AND $\Delta\Psi$-DEPENDENT GLYCINE TRANSPORT IN THE PHOTOSYNTHETIC BACTERIUM CHROMATIUM VINOSUM. *Andrea D. Cobb and David B. Knaff, Department of Chemistry, Texas Tech University, Lubbock, TX 79409.

The photosynthetic bacterium Chromatium vinosum accumulates glycine in an energy-dependent reaction. Uptake is electrogenic and independent of ΔpH. The K_m for glycine uptake is 39 μM.

A K^+ ion gradient ($[K^+]_{in} < [K^+]_{out}$) is able to drive glycine uptake in Chromatium vinosum while gradients of other cations are ineffective. Similarly, a glycine gradient ($[Gly]_{in} < [Gly]_{out}$) is capable of driving K^+ uptake in the absence of any other energy source. No other amino acid tested has any effect on K^+ uptake.

Glycine uptake is also capable of being driven by a membrane potential (outside positive) generated by first loading cells with either K^+ or Na^+, then adding valinomycin or monensin, respectively, to initiate uptake. TPP^+, a lipophilic cation which dissipates $\Delta\Psi$, causes a marked decrease in glycine transport.

Glycine, D-alanine, and L-alanine each compete for transport of the other two amino acids. Because D-alanine and L-alanine appear to be cotransported with Na^+ and because K^+ gradients do not affect their uptake, the possible mode of competitive inhibition may be at the level of binding rather than at the level of transport.

This research is supported by a grant (to D.B.K.) from the NSF (PCM-8109635).

T-PM-C1 WHY ARE ENTROPY-DRIVEN PROCESSES COMMON IN BIOLOGY? Max A. Lauffer. Biophysical Laboratory, Dept. of Biological Sciences, University of Pittsburgh, Pittsburgh, PA 15260.

The structures which give shape to cells, the spindles involved in cell division, the bundles which distort erythrocytes in sickle cell anemia, many structural and contractile aggregates, the protein coat of tobacco mosaic virus and many other biological structures are formed from subunits by entropy-driven processes, as is the interaction of myosin heads with actin. Structure formation is spontaneous because of a net increase in entropy to overbalance a net increase in enthalpy. The increase in entropy results from release of water molecules during polymerization. Crystallographic data frequently show the usual weak bonds between subunits, the formation of which involves a decrease in enthalpy, overbalanced in polymerization by the increase in enthalpy associated with water release. Depolymerization involves water binding with a net decrease in enthalpy; it is enthalpy-driven. Why are entropy-driven, structure-forming processes so frequently found in dynamic biological systems? Such needed structures must be easily reversed at biological temperature, approximately 300 K. The real role of water is to reverse the structure-forming processes to permit the structure to disintegrate when no longer needed. The greater the water binding upon disintegration, the greater can be the enthalpy increase associated with breaking of weak bonds between subunits without sacrificing ready reversibility. Thus, strong, precisely fitting structures with many weak bonds can be formed at biological temperatures when needed and yet be readily reversed by small changes in environment when the structures are no longer needed. This arrangement serves dynamic systems admirably.

T-PM-C2 HYDROGEN BONDED WATER IN COLLAGEN STRUCTURE: A FT-IR SPECTROSCOPIC CORROBORATION. V.Renugopalakrishnan,Harvard Medical School,Children's Hospital Medical Ctr.,Boston,MA 02115 and R.S.Bhatnagar,School of Dentistry,UCSF,San Francisco,CA 94143. Intr. by E.A.Dawidowicz

Ramachandran and Chandrasekharan(1) suggested the participation of water molecules in the stabilization of collagen triple helix by formation of H-bonds between the chains. Recently, Lim(2) has advanced an unique model of collagen where a linear array of H-bonded water molecules sandwiched between the chains stabilize the macromolecular structure by every alternate water molecule forming a H-bond with the carbonyl groups. As a part of continuing investigation of biopolymer structures utilizing FT-IR Photoacoustic (FT-IR PA) spectroscopy,which is ideally suited for biopolymers since it permits investigation of the biopolymer structure per se, we have studied type I collagen from chicken skin using FT-IR PA and Attentuated Total Reflection(ATR) spectroscopic methods. To explain the slightly higher frequency of amide I band in FT-IR PA spectrum, we have performed a Fourier self-deconvolution of the amide I and II region. Amide I band was observed to split into a doublet with frequencies at 1660 and 1634 cm^{-1}whereas amide II band occurred at 1554 cm^{-1} with a tendency for shoulder formation at 1521 cm^{-1}. The doublet structure is quite similar to Raman observations on collagen by Goheen et al(3). Amide I band at 1660 cm^{-1} is quite close to FT-IR PA frequency of 1661 cm^{-1}. The 1634 cm^{-1} seems to arise from the bending mode of H-bonded water in collagen. Implications of our observations to collagen structure will be discussed. Refs. 1. G.N.Ramachandran and R.Chandrsekharan,Biopolymers,6,1649(1968). 2. V.I.Lim FEBS Letters 132,1(1981). 3. S.C.Goheen et al BBA,536,197(1978).

T-PM-C3 NEUTRON SCATTERING STUDIES OF WATER IN MACROMOLECULAR SYSTEMS D. B. Heidorn, H. E. Rorschach, Rice University, Houston, Texas, C. F. Hazlewood, Baylor College of Medicine, Houston, Texas and R. M. Nicklow, Oak Ridge National Laboratory, Oak Ridge, Tennessee.

The microscopic structure and dynamics of water in the presence of macromolecules in water-polymer mixtures and living systems are not well-understood. Much work has been done using various experimental techniques to study the properties of water in these heterogeneous systems, yet there is no generally accepted model which describes the interaction of water with macromolecules. Quasielastic neutron scattering (QNS) is a relatively new technique that is capable of a spatial resolution of 1-10 Å and a frequency resolution of 10^9 to 10^{13} sec^{-1} which cover the ranges of interest for diffusive water motion. The large incoherent scattering cross section of hydrogen relative to other biologically abundant nuclei also makes this technique especially suitable for the study of water dynamics. Our results for water diffusion in agarose and polyox gels and in hydrated cysts of brine shrimp (Artemia salina) were interpreted by using a jump-diffusion model for translational water motion and a simple Brownian rotational model and show that the translational and rotational diffusion coefficients are reduced from the values for pure water, especially in the least hydrated systems. We show that these measured values are consistent with diffusion coefficients and T_1 relaxation times measured by NMR methods.

Funding for this research was provided by the Robert A. Welch Foundation and the Office of Naval Research.

T-PM-C4 THE KINETICS OF MICROTUBULE ASSEMBLY IN VITRO. David C. Clark, Stephen R. Martin and Peter M. Bayley. (Intro. by R.W. Woody). Biophysics Division, NIMR, Mill Hill London, NW7 1AA, U.K.

The kinetics of microtubule (MT) assembly have been studied turbidimetrically for both bovine and porcine protein as a function of pH, temperature, nucleotide and protein concentration. Although the kinetics are dependent upon solution conditions they are in general biphasic, with two processes of similar amplitude but differing in rate by one order of magnitude. However, the two rates become independent of protein concentration and therefore depart from the simple bimolecular kinetics required by the condensation mechanism of MT assembly. Each phase must contain a rate limiting first order process to account for this behaviour.

The rate of dissociation of oligomeric species on dilution of MT-protein closely parallels the fast phase rate in magnitude and temperature dependence and it is proposed that this process represents the upper limit of the rate of the fast phase of assembly. The slow phase rate appears to be rate limited by the availability of microtubule-associated proteins (MAPs) that are complexed in the 'MAP-rich' microtubules formed during the fast phase.

A working model for microtubule assembly in vitro, in agreement with these data, assigns a key-role to the MAP-containing components in determining the kinetics of the two phases of microtubule elongation.

T-PM-C5 MOVEMENT OF AXOPLASMIC VESICLES AND MITOCHONDRIA ON SINGLE FIBERS IN DISSOCIATED AXOPLASM. Ronald Vale, Bruce Schnapp[+], Thomas Reese[+] and Michael P. Sheetz. Marine Biological Labs., Woods Hole, MA.

The movement of endogenous vesicles has recently been observed along filamentous structures on frayed ends of extruded axoplasm from the squid giant axon by Allen et al. (Biol. Bull., in press) and Brady and Lasek (personal communication) using video-enhanced contrast microscopy. We have developed procedures for producing a thin ($< .1$ μM) network of filaments well separated from the main body of axoplasm which support the movement of vesicles and mitochondria. Some filaments support movement in one direction while others are bidirectional. Vesicles in the medium can bind to filaments and subsequently move and are also observed to dissociate from the middle or at the ends of filaments. ATP dependent movements of small and medium size vesicles and mitochondria all occur at a uniform velocity of 2.2 ± 0.2 μm/sec. By contrast, a range of velocities are observed in the intact axoplasm with small and medium size vesicles and mitochondria moving at rates of 2.2 ± 0.3, 1.1 ± 0.2 and 0.4 ± 0.1 μm/sec respectively. This result suggests that the lower rates of movement of larger vesicles in intact axoplasm is due to viscosity (steric hindrance). Since all size classes move at identical rates in a dissociated preparation with no steric hindrance, we propose that the retrograde and anterograde movement of various vesicular elements is driven by a single ATPase motor.

T-PM-C6 THE CYTOPLASMIC MATRIX: ITS STRUCTURE, VOLUME, SURFACE AND SPACE FOR DIFFUSION. N.D. Gershon[+], K.R. Porter[++], B.L. Trus[+], [+]DCRT, NIH, Bethesda, MD 20205, [++]Univ. of Colorado, Boulder, CO 80309.

Small molecules in the cytoplasm diffuse a few times slower than in aqueous solutions, while fluorescent proteins in cells at 22°C diffuse 27-341 times slower than in buffer solution (e.g., 1). To determine whether the cytoplasmic matrix (the microtrabecular lattice (2) or MTL and the cytoskeleton) has a structure that might retard the diffusion to that extent, we developed a novel image analysis method to measure the volume fraction it occupies. We digitize electron micrographs of frozen dried cells, find the area occupied by the structure using a video frame buffer, and correct for the thickness of the cell and the directions of the strands in space. The measured values of the fractional volume of the cytoplasmic matrix in PTK and NRK cells cytoplasm are only 10-30%, which cannot explain the slow cytoplasmic diffusion of proteins. It is possible that the diffusing fluorescent proteins are entangled with, adsorbed or attracted chemically by the network. For the simplest adsorption model, where the concentration of the adsorbed protein is proportional to its concentration in the aqueous space, we obtained a binding free energy of about -2.4 kcal/mole for the MTL and filaments volume fraction of 0.1 in the cytoplasm and diffusion coefficient ratio of 70. The amount of surface associated with the MTL and the cytoskeleton is quite high (our measurement yields estimated values of 40,000 - 130,000 μm^2 in a cytoplasm of a cell of 16 μm in diameter with a 10 μm nucleus). Similar measurements on cells responding to different osmotic environments will be presented. 1. Wojcieszyn, J.W. et al. (1981). PNAS U.S.A. 78:4407-4410.
2. Wolosewick, J.J., and Porter, K.R. (1979). J. Cell Biol. 82:114-139.

T-PM-C7 POLYMORPHISM IN ASSEMBLY OF POLYOMA VIRUS PENTAMERIC CAPSOMERES. D.L.D. Caspar, I. Rayment, Rosenstiel Research Center, Brandeis University, Waltham, MA 02254 and T.S. Baker, Department of Biological Sciences, Purdue University, West Lafayette, IN 47907.

The discovery that all 72 capsomeres in the polyoma virus capsid are pentamers (Rayment et al., 1982, Nature 295, 110) contradicted the presumption that the T=7 icosahedral papova virus capsids should be built of 12 pentameric and 60 hexameric capsomeres arranged to conserve quasi-equivalent bonding (Caspar & Klug, 1962, Cold Spring Harbor Symp. 27, 1). In view of this result, we questioned whether the wide class of polymorphic tubular assemblies of polyoma virus capsomeres, called "hexamer" tubes (Kiselev & Klug, 1969, J. Mol. Biol. 40, 155), was, in fact, built of hexamers. Reexamination of negatively stained tubes by digital image processing has led to a new indexing of the "hexamer" tube diffraction pattern, which indicates that these tubes are assemblies of paired pentamers (Baker et al., 1983, Nature, 303, 446). The packing arrangement of the pentamers in the "hexamer" tubes is simply related to the pentagonal tessellation representing the packing in the narrow "pentamer" tubes. In all the tube structures we have examined, at least one pairwise contact between neighboring pentagonal units closely resembles the edge-to-edge contact between the pentavalent and hexavalent capsomere in the icosahedral capsid. In addition to the edge-to-edge contacts, the pentagonal units in both the "hexamer" tubes and the icosahedral capsid make similar overlapped corner-to-corner and vertex-to-vertex contacts. Similar switching in the bonding of the capsomeres may occur in both capsid and "hexamer" tube assembly. The logic of the all-pentamer assembly can be represented by a pentamer model with switchable bonding specificity that can build the icosahedral capsid and the polymorphic tubes. Supported by NIH grant CA15468.

T-PM-C8 NMR STUDIES OF PROTEIN STRUCTURE IN FD VIRUS. K. Valentine, D. Schneider, T. Cross, S. Opella. "(Intr. by T. Kumosinski)".

The structure of the coat protein in fd virus is being determined by NMR spectroscopy. The protein subunits are immobilized due to the large size and rod shape of the virus. Therefore solid state NMR methods are necessary to study this structure. ^{15}N chemical shift anisotropy and ^{15}N-^{1}H and ^{15}N-^{13}C dipolar couplings elicit the peptide backbone structure in the oriented virus particle.

Specific sites in the protein backbone are labelled with ^{15}N through biosynthetic incorporation of labelled amino acids. The resonance frequencies and dipolar splittings are measured with one and two dimensional experiments. The resonances are assigned using ^{13}C and ^{15}N labelled proteins. The orientation of individual amino acid residues is determined from the analysis of the anisotropic spin interactions for the assigned sites.

A complete turn of an α-helix was mapped at residues 40 through 45. The NMR results are in general agreement with previous fiber diffraction results, with significantly enhanced resolution and structural details that show the helix to be distorted.

T-PM-C9 STABILITY AND DYNAMICS OF TURNIP YELLOW MOSAIC VIRUS BY DIFFERENTIAL SCANNING CALORIMETRY AND ^{31}P NUCLEAR MAGNETIC RESONANCE SPECTROSCOPY. R. Virudachalam*, Philip S. Low*, Patrick Argos†, and John L. Markley*, Departments of Chemistry* and Biological Sciences†, Purdue University, W. Lafayette, IN 47907

Turnip yellow mosaic virus (TYMV) is an RNA-containing T = 3 iscosahedral particle with an external diameter of ∿280 Å. The capsid consists of 180 copies of a single 20-KDa protein. The stability and dynamics of empty capsids and intact virions, which contain the 2.0 x 10^6 Da RNA, at different pH values were analysed by using a differential scanning calorimeter (DSC) and ^{31}P NMR. A single peak was observed in the DSC scan of the intact particle as well as its capsid over a wide range of pH. The endotherm is attributed to the disruption of the quarternary structure of the virion or capsid. The melting temperature (T_m) of the virion and the capsid is pH sensitive; the virion is more stable below neutral pH (T_m = 71 °C at pH 5.5 and 55 °C at pH 8.5) whereas the capsid is more stable above neutral pH (T_m = 70 °C at pH 5.5 and 84 °C at pH 8.5.). The reduction in the stability of the virion above neutral pH is consistent with the conclusions arrived at by ^{31}P NMR that some of the protein-RNA interaction is disrupted above neutrality. The instability of the empty capsid at lower pH is expected to be due to repulsion between positively-charged side chains, one or more of which have pK_a values near 5.7. In the intact particles the repulsive interaction may vanish due to the large number of anionic RNA phosphate groups. The experimental enthalpy at pH 5.5 is about 11 x 10^3 Kcal/mol for the capsid and about 30 x 10^3 Kcal/mol for the virion. During the disruption of the capsid at low pH (5.5) the size of the cooperative unit is a trimer of the capsid protein whereas at high pH (8.0) the cooperative unit is a dimer. (Supported by NIH grants RR01077 and GM 19907.)

T-PM-C10 STRUCTURE OF THE THREE PROGENY VIRIONS PRODUCED BY A BUDDING ENVELOPED PHAGE.

Jack Maniloff, Saibal K. Poddar, Stephen P. Cadden, and Jyotirmoy Das,
Department of Microbiology, University of Rochester Medical Center, Rochester, New York 14642.

Infection of Acholeplasma laidlawii by the temperate enveloped mycoplasma virus L2 results in the production of three morphological forms of progeny L2 virus; L2-I, L2-II, and L2-III. These three forms can be separated by velocity sedimentation and agarose gel electrophoresis. The same distribution of the three forms is found independently of whether infection is with purified L2-I, L2-II, or L2-III; or with an induced lysogen. In addition, the same distribution of particles is found at all times postinfection, so the three forms are not viral assembly intermediates. Agarose gel electrophoresis was used to size the particles: L2-I 74 nm, L2-II is 88 nm, and L2-III is 132 nm in diameter. All three particles have the same surface charge density, which is similar to that reported for A. laidlawii cells. The protein composition of the three L2 particles is the same, although there are differences in the protein stoichiometric ratios. L2-I, L2-II, and L2-III have the same 11.8 kb negatively superhelical, circular, double-stranded DNA genome. However, UV inactivation studies and restriction frequency measurements indicate that L2-I and L2-III each contain one molecule of the viral chromosome, while L2-II contains 2-3 molecules. A variant has been isolated which only produces two particles, sedimenting near L2-II and L2-III. The three L2 particles observed in these studies appear to represent alternate assembly mechanisms for a cell infected by an L2 chromosme. These may result from physical chemical constraints on membrane closure around nucleoprotein complexes during viral assembly.

(Supported by USPHS NIH grant GM32442)

T-PM-D1 EQUILIBRIA BETWEEN IONOPHORE A23187 AND MONOVALENT CATIONS; EFFECTS OF MEMBRANE ASSOCIATION AND SOLVENT COMPOSITION. Douglas R. Pfeiffer and Clifford J. Chapman (Intr. by Gregory Reinhart), The Hormel Institute, University of Minnesota, Austin, MN 55912

The cation binding reactions of ionophore A23187 provide a useful model of complexation-decomplexation reactions which occur at a membrane interface. When associated with DMPC vesicles, the anionic form of A23187 complexes Li^+ and Na^+ according to the relationship $M^+_{aq} + A^-_B \quad MA_B$ where M^+_{aq} refers to cation in the aqueous phase while A^-_B and MA_B refer to the membrane associated anion and 1:1 complex, respectively. The equilibrium constant for this reaction $K^{B'}_{MA}$ is given by the relationship $K^{B'}_{MA} = [MA_B]/[A^-_B][M^+_{aq}]$. Equilibria may be monitored by fluorescence or absorbance measurements. Li^+ vs H^+ competition studies reveal that $K^{B'}_{LiA}$ is related to the true stability constant K^B_{LiA} according to the relationship $K^{B'}_{LiA} = K^B_{LiA}\,(1 + K^B_{HA}a_{H^+})^{-1}$ where K^B_{HA} is the protonation constant of membrane bound A23187 and a_{H^+} is the activity of aqueous phase hydrogen ion.

When determined at 30°C at an aqueous phase pH of 10.5 and an ionic strength of 0.05 M, log $K^{B'}_{MA}$ for the Li^+ and Na^+ complexes are 3.22 ± 0.04 and 1.33 ± 0.04, respectively. This degree of selectivity (∿75 fold for Li^+ over Na^+) is 15 times greater than obtained under comparable conditions when the ionophore is dissolved in MeOH-H_2O solutions. Plots of log $K^{B'}_{MA}$ vs 1/T display a discontinuity of approximately 0.7 log units at the critical temperature of the DMPC vesicles. This behavior is not seen in analogous plots of the protonation constant. Increasing the ionic strength of aqueous phase from 0.005 to 0.085 M (Et_4NClO_4) enhances $K^{B'}_{LiA}$ by 0.4 log units even without correcting for the effect of ionic strength on the activity of Li^+_{aq}. Data are discussed in terms of the interactions of different species in the equilibria with DMPC vesicles (Supp. by GM 24701).

T-PM-D2 A VOLTAMMETRIC INVESTIGATION OF TCNQ-CONTAINING BILAYER LIPID MEMBRANES. Z.K. Lojewska and H. Ti Tien, Department of Physiology/Biophysics, Michigan State University, East Lansing, Mich.

In an earlier investigation (Biophys. J., 41, 182a, 1983) an application of cyclic voltammetry to dye-sensitized bilayer lipid membranes (BLM) was reported, in which electronic processes in as well as across the BLM were considered. It was pointed out that redox reactions at the BLM/solution interfaces are most conveniently studied by the cyclic voltammetric technique. The present studies examined TCNQ-containing BLM in the presence of a variety of redox couples such as ferri-ferro, iodine/iodide, cupric/cuprous, stanic-stanous, nitrate/nitrite, quinhydrone, ASC/dehydro-ASC, etc. Voltammograms obtained clearly indicate that redox reactions are occurring at the interfaces of the BLM with electrons moving transversely across the TCNQ/doped BLM. Cyclic voltammetry is a powerful technique for detecting and characterizing coupled redox reactions at electrode-electrolyte interface and its application to biologically significant compounds in the BLM system is in progress.

(Supported by NIH research grant GM-14971)

T-PM-D3 MEMBRANE BINDING, FLIP-FLOP AND VOLTAGE DEPENDENT SPECTROSCOPY OF CHARGE SHIFT PROBES. E. Fluhler and L.M. Loew, Dept. of Chemistry, State University of N.Y., Binghamton, N.Y. 13901

Transmission, excitation, and emission voltage-response spectra are obtained using an apparatus based on phase-sensitive detection from an oxidized cholesterol hemispherical bilayer for a series of 20 dyes based on the styryl chromophore. All dyes investigated display biphasic response spectra. $\Delta T/T$ and $\Delta F/F$ responses in the ranges 5×10^{-5}-5×10^{-4} and 8.8×10^{-3}-5×10^{-2}, respectively, have been measured and the shapes of the response spectra were similar for all dyes studied. For some of the dyes, the relative fluorescence change decreases with time indicating that the dye may be flipping to the inside of the bilayer. Using lipid vesicles, equilibrium binding parameters have been determined for the dyes; it is clear from these results that binding is very strong and that it is quite sensitive to the length and shape of the hydrophobic region of the dyes while insensitive to the character of the polar region. (Supported by USPHS Grant GM25190 and a NIH RCDA, CA 677, to LML.)

T-PM-D4 NEUTRON DIFFRACTION STUDIES OF SPECIFICALLY DEUTERATED DOL MULTILAYERS. Stephen H. White, Glen King, and Russell Jacobs, Dept. of Physiology and Biophysics, University of California, Irvine, California 92717

We have performed neutron diffraction studies on oriented multilayers of dioleyl lecithin (DOL) specifically deuterated at the double bond. This allows us to locate the double bond in the projected profile structure of the bilayers and gain information on bilayer organization under different conditions. Of particular interest to us is the organization of the bilayer in the presence of dissolved hexane introduced from the vapor phase at different relative humidities. Last year we reported diffraction results based upon measurements using protonated and deuterated hexane and water in protonated lipid. The additional measurements made using the deuterated DOL along with radioisotopically labeled hexane uptake experiments agree very well with the earlier results: (i) The hexane enters the bilayer without changing the hydrocarbon volume (the partial molar volume of the hexane in the bilayer hydrocarbon region is zero) and (ii) The calculated lipid mass density is considerably lower than the measured value for lipids in excess water (0.84 gm/ml vs. 1.0 gm/ml). The mole ratios of water and hexane to lipid are also in good agreement with the values determined by direct radiolabeled water and hexane uptake experiments. Research supported by the NIH and the NSF.

T-PM-D5 ORIENTATIONAL ORDER AND PHASE BEHAVIOUR IN SATURATED MIXED-CHAIN PHOSPHATIDYLCHOLINE-WATER SYSTEMS: A ^2H NMR STUDY. L. M. Strenk[+], M. J. Vaz[+], J. W. Doane*[+] and P. W. Westerman*[+], *Molecular Pathology Program, Northeastern Ohio Universities College of Medicine, Rootstown, Ohio 44272 and [+]Department of Physics and Liquid Crystal Institute, Kent State University, Kent, Ohio 44242.

The effect, on molecular ordering, of varying chain composition in lecithin bilayer membranes was evaluated by ^2H NMR. Four saturated mixed-chain phosphatidylcholines, ^2H-labelled at sites in the sn-1 and 2 chains and glycerol moeity were examined in the L_α phase. At the sites examined and at equivalent reduced temperatures, orientational ordering in mixed-chain lecithins is very similar to that in analogous single chain lecithins.

Changes in molecular ordering at the pre- and main phase transitions in single and mixed-chain lecithins were studied using the terminal C^2H_3 of the sn-1 and 2 chains as probes. Results from the labelled sn-2 chain, in the $P_{\beta'}$ phase, show the spectra to be the superposition of two powder patterns, for both single and mixed-chain lecithins. A model with two populations of motionally inequivalent lipid molecules is proposed for this phase. Data from the labelled sn-1 chain, show only a single splitting at temperatures below the main transition for both single and mixed-chain lecithins. The relative magnitude of the guadrupole splittings in these lecithins support the hypothesis that below the main phase transition, additional conformational flexibility is found in the sn-1 chain of mixed-chain lecithins whose sn-1 chain is 2 carbons longer than their sn-2 chain.

T-PM-D6 ^{13}C-NMR STUDIES OF MOLECULAR MOTION IN DIPALMITOYLPHOSPHATIDYLCHOLINE BILAYERS. J.F. Ellena[+], G.D. Williams[+], M.D. Sefcik*, J. Schaefer*, E.O. Stejskal*, R.A. McKay*, and M.F. Brown[+]. (Intr. by D.S. Cafiso) [+]Department of Chemistry, University of Virginia, Charlottesville, VA 22901, and *Monsanto Company, St. Louis, MO 63166.

It has recently been shown that two types of motion, fast and slow, must be invoked to explain the spin-lattice (T_1) relaxation times of the hydrocarbon region of 1,2-dipalmitoyl-sn-glycero-3-phosphocholine (DPPC)(1). The fast motions most likely include carbon-carbon bond isomerizations which fall into the short correlation time limit ($\omega_0^2\tau_c^2<<1$; $\tau_c \sim 10ps$). The slow motions, which presumably correspond to whole molecule motions, have been modeled in two ways; a) a single correlation time, or b) a continuous distribution of correlation times (continuum model) have been assumed. ^{13}C T_1 measurements employing DPPC vesicles at seven frequencies from 15 to 126 MHz do not allow one to distinguish unequivically between the two models. However, the T_1 measurements together with ^{13}C rotating frame spin-lattice ($T_{1\rho}$) relaxation studies (2) of DPPC multilamellar dispersions, using spin-locking fields of 25 to 50 kHz, best fit the continuum model, and allow one to rule out the possibility of a single correlation time for the slow motions. ^{13}C T_1, $T_{1\rho}$ and NOE data obtained at several different magnetic field strengths will be presented and discussed in terms of the hydrocarbon chain dynamics in the liquid crystalline phase of DPPC.

1) M.F. Brown, J. Chem. Phys. 77, 1576 (1982). 2) M.D. Sefcik et al., BBRC 114, 1048 (1983).

Work supported by NIH Fellowship 1F32EY05635 (to J.F.E.), by NIH grant EY03754 and the Alfred P. Sloan Foundation (to M.F.B.), and by the Monsanto Company.

T-PM-D7 MOLECULAR ORDERING AND DYNAMICS OF SATURATED LIPID BILAYERS USING ^{2}H-NMR. G.D. Williams, J.M. Beach, S.R. Lustig, S.W. Dodd, A. Salmon, and M.F. Brown. Department of Chemistry, University of Virginia, Charlottesville, VA 22901.

A homologous series of 1,2-diacyl-sn-glycero-3-phosphocholines have been synthesized with (i) perdeuterated acyl chains at both the sn-1 and sn-2 positions of the glycerol moiety, and (ii) only the sn-2 fatty acid perdeuterated. ^{2}H NMR studies of 50 wt.% multilamellar dispersions of di(C12:0)PC, di(C14:0)PC, di(C16:0)PC, and di(C18:0)PC in H_2O have been performed at 55 MHz. The quadrupolar echo pulse method was employed using homebuilt, solenoidal-type high power ^{2}H NMR probes. Our measurements of the ^{2}H spin-lattice (T_1^{-1}) relaxation-rates and quadrupolar splittings $\Delta\nu_Q$ are consistent with a square-law dependence of T_1^{-1} on the bond segmental order parameter $|S_{CD}|$, as proposed earlier (1-3). Such a relaxation law of the form $T_1^{-1} \propto |S_{CD}|^2$ is characteristic of a contribution from relatively slow fluctuations in the local bilayer ordering (director fluctuations) to the T_1^{-1} relaxation in the MHz regime. Thus, two broad classes of segmental motions in these saturated lipid bilayers are postulated: fast motions due largely to bond isomerizations and slower motions of a more collective nature. The influence of the acyl chain length and temperature on the ^{2}H T_1^{-1} relaxation rates and $|S_{CD}|$ values will be discussed in terms of models for the physical state and molecular dynamics of saturated phospholipid bilayers in the liquid crystalline phase.

1) M.F. Brown, J. Chem. Phys. 77, 1576 (1982). 2) M.F. Brown et al., PNAS 80, 4325 (1983).
3) M.F. Brown, J. Chem. Phys., in press (1984).

Work supported by an NSF Predoctoral Fellowship (to A.S.), and by NIH Grant EY03754 and the Alfred P. Sloan Foundation (to M.F.B.)

T-PM-D8 THE MECHANISM OF OSMOTIC CONTROL OF LIPID BILAYER FUSION. L.R. Fisher and N.S. Parker CSIRO Division of Food Research, P.O. Box 52, North Ryde, N.S.W. 2113, AUSTRALIA

We have used optical reflectance and capacitance to monitor the interaction and eventual fusion of optically "black" lipid bilayers (BLM's), hydrostatically bulged to approximately hemispherical shape and pushed together mechanically. Optical reflectance yields the thickness of a single bilayer (to ± 0.1 nm) and of the draining aqueous film between two bilayers. Specific capacitance measurements also yield bilayer thickness to ± 0.1 nm, and are used to establish the thicknesses of various regions of the complex bilayer configurations resulting from fusion. A necessary first step in the fusion process is drainage of aqueous solution from between the bilayers to allow close contact of the bilayers. With equiosmolal aqueous solution on both sides of each bilayer, only lateral drainage (i.e. parallel to the bilayers) is possible. In this case, drainage is driven by the hydostatic pressure of the bulged bilayers and is relatively slow. Even after an hour in "contact" there is still a film of aqueous solution more than 30 nm thick between the bilayers; we have never found fusion in this case. When an osmotic difference exists across at least one bilayer, water flows through the bilayer. If this additional flow of water is such as to promote removal of water from between the bilayers, bilayer fusion is strongly promoted. For uncharged BLM's, there is no noticeable energy barrier to fusion once the bilayers have approached closely enough. The first step in the fusion process is invariably the formation of a single central bilayer. The central bilayer may later burst to allow mixing of the two volumes originally bounded by the separate bilayers - the topological equivalent of exocytosis.

T-PM-D9 CALCIUM EFFECTS ON LIPID LATERAL DISTRIBUTION AND FUSION IN MIXTURES OF SYNTHETIC PHOSPHATIDYLSERINES, PHOSPHATIDYLCHOLINES AND PHOSPHATIDYLETHANOLAMINES. John R. Silvius* and Jeannine Gagné, Department of Biochemistry, McGill University, Montréal, Québec, Canada H3G 1Y6.

High-sensitivity differential scanning calorimetry has been used to determine the phase diagrams for mixing of dimyristoyl and dielaidoyl phosphatidylserine (PS) with the corresponding phosphatidylcholines (PC's) and phosphtidylethanolamines (PE's) in the presence or absence of 30 mM calcium ion. PS mixes well with PE and PC in the absence of calcium, but calcium addition induces lateral phase separation from the liquid-crystalline state in mixtures containing ~ 20-80 mole % PS in PE or ~ 40-70 mole % PS in PC. Calcium-induced fusion of vesicles composed of these lipids or the corresponding dioleoyl species was examined by assaying the mixing of vesicle-wall and aqueous compartments. The effects of lipid acyl chain composition on vesicle fusion are modest above the lipids' T_m. However as others have found, the nature and content of zwitterionic lipids in the vesicles, strongly influences the rate and calcium concentration dependence of fusion. Correlation of the fusion and calorimetric results suggests a strong correlation of fusion with lateral phase separation (except at very high PS contents) for PC-PS but not for PE-PS mixtures. PE-rich membranes containing low levels of PS can fuse without phase separation at calcium levels lower than those required to fuse pure-PS membranes.
Supported by Grants MA-7776 and ME-7580 from the Medical Research Council of Canada and Grant 820040 from le Conseil de la recherche en santé du Québec.

T-PM-D10 MONOVALENT CATION-INDUCED PHOSPHOLIPID VESICLE AGGREGATION: EFFECT OF ION BINDING. S. Ohki, S. Roy, H. Ohshima* & K. Leonards, Dept. of Biophysical Sciences, SUNY at Buffalo, NY 14214.

Aggregation of acidic phospholipid vesicles induced by monovalent cations was studied for vesicles of small and large sizes. Although the order of capability for monovalent cations to induce massive aggregation of small (250Å in diameter) phosphatidylserine vesicles was $Na+ > Li+ > K+ > Cs+ > TEA+$, the relative position of Li+ and Na+ in this order was reversed for the large phosphatidylserine vesicles (more than 1000Å in diameter) and phosphatidic acid vesicles regardless of their sizes (both large and small vesicles). The similar switch in the order was also observed in the surface potential studies on the phosphatidylserine monolayer with variation of area per molecule with respect to the strength of monovalent ion binding to the membrane surface; the order of the binding strength for monovalent cations is deduced from the changes in surface potential with respect to the change in Mg^{2+} concentration on the subphase solution containing monovalent salts. It is $Na+ > Li+ > K+$ for the monolayers of large area (>80Å^2) per molecule and is $Li+ > Na+ > K+ > Cs+$ for those of small area (>80Å^2) per molecule. It was also found that for large acidic phospholipid vesicles, there were two steps of adhesion processes; the initial adhesion took place spontaneously after the change in salt concentration in the region of 0.1-0.3M monovalent salt, and the second phase adhesion progressed gradually with time after a salt concentration change in the region of high salt concentration. The observed phenomena of monovalent cation-induced vesicle aggregation with variation of the size of vesicles were examined in terms of the variation of binding affinities and accessibility of monovalent cations to the binding sites of lipid polar groups. This work was supported by an NIH grant (NIGMS 5 R01GM2484006).

T-PM-D11 DIRECT VISUALIZATION OF EXOCYTOSIS IN MAST CELLS. Michael J. Curran, Malcolm S. Brodwick, Charles Edwards, Department of Physiology and Biophysics, University of Texas Medical Branch, Galveston, Texas 77550 and Department of Biological Sciences, SUNY, Albany, New York.

Exocytosis was examined under Nomarski optics using mast cells from rats (RM) and beige mice (BM) with "Chédiak-Higashi" syndrome. Vesicles of rat were ∿ 0.5 μ and numbered ≈250 per cell. BM vesicles were 1-7 μ and numbered 2-20 per cell! Vesicles were stationary in a time frame of minutes. When the secretagogue compound 48/80 or the ionophore A23187 is applied in the presence of external Ca^{++}, vigorous exocytosis is observed with ruthenium red staining. Vesicles do not move with observable translational motion. However the vesicle size does increase in BM cells by ∿ 20%. Vesicle shape does not change remarkably; nor is there evidence for vesicular flattening against the cell membrane. Vesicles release in a random sequence in BM cells. When BM cells were placed in hypotonic media (50 mOsm) the cell diameter increased. After a delay the vesicle diameter increased by ∿ 20%. The vesicles remained attached to the surface membrane. The attachment was unaffected by 10^{-4}M colchicine or 10^{-4} cytochalasin B. Spontaneous release in hypotonic solutions was sometimes observed. Hypertonic solutions (660 mOsm) made with NaCl or sucrose caused cell and vesicle shrinkage (∿ 10% decrease in diameter). In RM hypertonicity delays the onset and slows the rate of exocytosis. Spontaneous release was again observed even in the presence of 2 mM EGTA. The dipeptide, CBZ-ser-leu-amide, blocks secretagogue induced release and vesicle expansion. This research was funded by DHHS NS 13778 (MSB), a predoctoral McLaughlin Fellowship (MJC) and DHHS NS-07681 (CE).

T-PM-D12 EXOCYTOSIS IN PERMEABILIZED MAST CELLS. Michael J. Curran and Malcolm S. Brodwick. Dept. of Physiology and Biophysics, Univ. of Texas Medical Branch, Galveston, TX 77550.

Mast cells from rat (RM) and beige mice with Chédiak-Higashi syndrome (BM) were permeabilized with a brief exposure to digitonin in order to gain direct intracellular access. Exocytosis was monitored with Nomarski optics and ruthenium red staining. Proper permeabilization was determined by trypan blue staining of the nucleus. Exocytosis can be reliably induced by $5x10^{-5}$M Ca^{++} and 5 mM MgATP. Prolonged digitonin treatment causes RM vesicles to become leaky suggesting that the vesicles contain cholesterol. When 1 mg/ml chymotrypsin is added in the absence of Ca^{++} and ATP normally stationary vesicles move about freely and stream out of the cell. The vesicles exhibit a Brownian-like motion except that the vesicles occasionally meet, stick together for a short time, and come apart. When Ca^{++} is added this motion abruptly halts. Several seconds later the vesicles all lyse or fuse. Chymotrypsin added in the presence of 5 mM MgATP caused apparent fusion or lysis without vesicular motion. When 0.6 M KI with 6 mM NaS_2O_3 was added vesicles moved about freely as with chymotrypsin. In cells permeabilized with external ATP without digitonin, KI caused the vesicles to move about within the cell. This motion halted when the KI was diluted. Following digitonin treatment, alamethicin, a nonselective ionophore, caused RM vesicles to expand. In digitonin treated cells phorbol ester caused release in RM and BM cells even in the presence of 0 Ca, 2 mM EGTA. Phorbol-induced release requires ATP. These results suggest that vesicles are tethered by actin-like filaments. The release process appears to include an osmotic step. Ca^{++} and ATP may be involved in the osmotic and/or other steps in the fusion process.

T-PM-E1 HYDRODYNAMIC AND ELECTRON MICROSCOPIC STUDIES OF FIVE MONOCLONAL ANTI-DANSYL ANTIBODIES WITH IDENTICAL VARIABLE REGIONS. M. L. PHILLIPS AND V. N. SCHUMAKER. Dept. of Chemistry and Biochemistry, UCLA, L. A., CA 90024.

Oi et. al., J. Cell Biol. 91 752, 1981, have examined the nanosecond emission anisotropy kinetics of monoclonal anti-dansyl IgG1, IgG2a, and IgG2b antibodies with identical variable regions. We are studying these and two additional monoclonal antibodies which also have the same variable region, an IgE and an IgG2a with a deletion which apparently includes the entire CH1 domains, by analytical ultracentrifugation and electron microscopy. The $s_{20,w}$ determined in duplicate runs were as follows: IgG1, 6.86 and 6.80S; IgG2a, 6.72 and 6.62; IgG2b, 6.70 and 6.70S; IgG2a(CH1 deletion), 6.37 and 6.215; and IgE, 8.30 and 8.40S. All of the antibodies appeared homogeneous by ultracentrifugation with the exception of the IgE which had a small (~10%) slower moving contaminant. When mixed with an equimolar amount of α,ε-bis dansyl gly-gly-lysine, IgG1 showed predominantly 9.6S dimer, with some 11.3S trimer, in the ultracentrifuge. In the electron microscope the dimers were seen to be closed and circular. Unlike other published pictures of dimers formed between polyclonal rabbit antibodies with bivalent haptens (Seegan et. al., PNAS 76 907-911, 1979), the hinge angle between the Fab arms of these mouse IgG1 antibodies is not closed but rather open at an angle of about 60°. Use of the shorter bivalent hapten bis dansyl cadaverine did not change this appearance. This observation may be related to the structure of the hinge region of mouse IgG1 and, in particular, to its reported relative lack of flexibility in the nanosecond time range.

T-PM-E2 NUCLEOTIDE ANALOGS AS STRUCTURAL PROBES FOR E. COLI GLUTAMINE SYNTHETASE
A. Ginsburg and M. R. Maurizi, NHLBI, NIH, Bethesda, MD 20205

Glutamine synthetase (GS) from E. coli is a dodecamer composed of identical subunits (50,000 M_r) arranged in 2 superimposed hexagonal rings. Introduction of specific structural probes at active sites of GS is possible because various analogs of ATP that are modified at the 6 or 8 position of the adenine ring have been found to substitute for ATP in the autoinactivation reaction of Mn•GS at pH 7 with L-met-S-sulfoximine. With L-met-S-sulfoximine phosphate, 2 Mn^{2+}, and the corresponding analog of ADP tightly bound at a subunit active site both intra- and inter-subunit contacts are strengthened (J. Biol. Chem. 257, 4271, 7246, 1982). The distance between active sites of GS has been estimated to be 28-38 Å, using a highly fluorescent ADP analog as donor in 2-4 inactivated sites of the dodecamer and increasing numbers of an appropriate chromogenic ATP analog as acceptor in other active sites. Thus, energy transfer may occur predominantly between isologously bonded opposing subunits from each ring. Furthermore, 6-S ATP and 8-S ATP form stable complexes with aquoglycyl-L-methionyl platinum(II) and these analogs have been used to insert electron dense probes at active sites of GS for analyses by scanning transmission electron microscopy in collaboration with J. Hainfeld, J. S. Wall, P. Furcinitti, and J. J. Lipka at the Brookhaven Natl. Lab. Preliminary image analyses at 5-10 Å resolution of 18 unstained, inactivated molecules with either 6-S ADP•Pt(II) or with 6-S ADP at all active sites show positions of increased mass in the 6-S ADP•Pt(II)•enzyme near the outside edge of hexagonal rings viewed along the 6-fold axis of symmetry. A mapping of specific nucleotide binding sites of GS may now be possible.

T-PM-E3 PRESSURE-DISSOCIATION AND ENZYME ACTIVITY OF LACTATE DEHYDROGENASES: CONFORMATIONAL DRIFT OF THE DISSOCIATED MONOMERS. Lan King and Gregorio Weber. University of Illinois, 397 Roger Adams Laboratory, Urbana, IL 61801.

We have studied the dissociation under hydrostatic pressure of porcine and bovine lactate dehydrogenase (H_4) by methods previously used by Paladini and Weber [Paladini, A. and Weber, G. (1981) Biochemistry 20, 2587-2593]. The results show that hydrostatic pressures, in the range of 1bar-3Kbar, promotes the dissociation of these proteins in solution of 10 µg/ml to 1 mg/ml concentration (0.07 to 7 µM tetramer). The standard volume changes upon dissociation were in the range of 220 ml/mole to 280 ml/mole. The reversibility of the pressure effects was better than 95% as judged by recovery of either excitation-polarization spectrum of the intrinsic protein fluorescence or of the dansyl polarization. The initial polarization was regained upon release of the pressure, but recovery of enzyme activity took one hour to several days depending upon the highest pressure applied and the duration of pressure incubation, in agreement with previous work of Jaenicke et. al. [Miller, K., Lüdemann, H.D., and Jaenicke (1981) Biochemistry 20, 5411-5416]. The enzyme before and immediately after being subjected to pressure show the same gel electrophoretic mobility. The difference between the time necessary for the recoveries of polarization and enzyme activity indicates that the reassociation of subunits into tetramer after releasing the pressure is a fast process, but that the fine sturcture of active tetrameric enzyme requires a much slower process which involves an exacting accomodation of amino acid residues inside the protein. Furthermore, the effect of duration of pressure incubation upon the rate of activity recovery suggests continual change, i.e., conformational drift within the monomers under pressure.

T-PM-E4 FLUORESCENCE STUDIES OF THE EFFECT OF HIGH PRESSURE ON THE SELF-ASSOCIATION OF MELITTIN. Richard B. Thompson and Joseph R. Lakowicz, Department of Biological Chemistry University of Maryland School of Medicine, Baltimore, Maryland 21201

We used fluorescence emission spectra and anisotropies to measure the equilibrium between monomeric and tetrameric melittin at pressures ranging from 1-1800 bar. Increased pressure promoted dissociation of the tetramer into monomers, as shown by a red shift in the emission and a decrease in the fluorescence anisotropy. At sufficiently high NaCl concentration (2 molal), melittin remains undissociated to 1800 bar. The self-association reaction proceeds with a volume change (ΔV) of + 180 ml/mole near 1 atmosphere; this value drops to approximately 5 ml/mole at 1800 bar. Given the small size of melittin the aggregation reaction is extremely pressure sensitive at modest pressures, but practically insensitive at higher pressures. This behavior is quite different from that observed for other proteins under pressure, but mimics the pressure dependence of micelle formation. If ΔV is taken to represent the difference in partial molal volumes between reactants (monomers) and product (tetramer), then the melittin tetramer is highly compressible in comparison with other proteins. Alternatively, pressure may directly affect the (mainly entropy-driven) self-association of melittin by changing the hydrogen-bonded structure of the solvent water. Our data strongly suggest the former hypothesis, but we cannot rule out the latter.

T-PM-E5 EFFECTS OF IONIC STRENGTH AND STATE OF ASSEMBLY ON THE KINETICS OF EXCHANGE OF CALF THYMUS HISTONES. M.P. McCarthy, P.K. Steffen and N. M. Allewell, Department of Biology, Wesleyan University, Middletown, CT 06457; R.C. Benedict, E.N. Moudrianakis and G.K. Ackers, Department of Biology, The Johns Hopkins University, Baltimore, MD 21218.

The kinetics of hydrogen exchange of calf thymus histone (H2A-H2B) dimers and $(H3\text{-}H4)_2$ tetramers at pH 7 have been examined at low (0.16M NaCl) and high (2M NaCl) ionic strengths and after incorporation into $(H2A\text{-}H2B\text{-}H3\text{-}H4)_2$ octamers. Results for both species are very similar. Approximately 60% of the backbone amide protons are detectable in both low and high salt and at least three kinetic phases can be distinguished. Increasing the ionic strength from 0.16 to 2M accelerates exchange of some of the rapidly exchanging protons, while slowing exchange of others. Exchange of more slowly exchanging protons is virtually unaffected. Incorporation of dimers into octamers accelerates exchange of ~40 protons to such an extent that they can no longer be detected. The effects of assembly upon the tetramer are qualitatively similar, although less dramatic. These results indicate that both increasing ionic strength and assembly destabilize some regions of the structure while stabilizing others. Higher resolution studies aimed at identifying these regions would therefore be of interest.

Supported by NIH grants AM-17335 (NMA) and GM-24486 (GKA), NSF grant PCM-801453 (GKA) and ACS grant NP-287 (ENM).

T-PM-E6 DOES SELF ASSOCIATION PLAY A ROLE IN THE REGULATION OF RABBIT MUSCLE PHOSPHOFRUCTOKINASE? Michael A. Luther and James C. Lee, Dept. of Biochemistry, St. Louis University School of Medicine, St. Louis, MO 63104.

Rabbit muscle phosphofructokinase (PFK) has been demonstrated by sedimentation velocity to undergo rapid self association. Recent physical evidence shows that association-dissociation of PFK subunits is linked to conformational changes between an active and inactive tetrameric PFK. Hence, from a thermodynamic viewpoint self association must play a role in the regulation of PFK. However, the accepted model in the literature proposes that self association plays no role due to the apparently slow rates reported for the self association process. A potential cause of these contradictory observations is the differences in the purification procedures, namely, the omission of differential heat denaturation and alcohol precipitation steps in the procedure from this laboratory. In order to resolve the differences in literature reports, physical and kinetic studies were conducted on PFK purified by three methods.

Steady state kinetics showed that the stability, specific activity, requirement of DTT for full activation, and degree of inhibition by high concentrations of ATP are all different depending on the method of purification. Subunit molecular weights determined by SDS gel electrophoresis are also different. PFK samples purified by methods including the heat denaturation and alcohol precipitation steps can be resolved by sedimentation into two components. The slow-moving component possesses no measurable enzymic activity and it does not undergo rapid dynamic self association, however, the fast component can. Hence, it is evident that native PFK is regulated by self association.

T-PM-E7 CALORIMETRIC STUDY OF THE THROMBIN ALPHA-2-MACROGLOBULIN COMPLEX. P. Bhattacharya and D.K. Strickland (Intr. by T. Busby). Plasma Derivatives Laboratory, American Red Cross Blood Services Laboratories, Bethesda, MD 20814

The interaction of human α_2-Macroglobulin (α_2M) with thrombin has been investigated by differential scanning calorimetry. The calorimetric measurements were made in a buffer of 50mM HEPES, pH 8.0. At this pH the temperature induced denaturation of α_2M was characterized by a broad transition with a transition midpoint at 71.0°C, and an enthalpy of 3.91 cal g^{-1}. Upon complex formation with thrombin, two transitions, with Tm values of 73.0°C and 82.0°C and a total enthalpy of 4.10 cal g^{-1} were observed. Titration of α_2M with increasing amounts of thrombin resulted in a progressive increase in the 82.0°C transition, which was found to saturate at a mole ratio of thrombin:α_2M of 1.0. These results suggest that formation of a equimolar complex of α_2M with thrombin is sufficient to induce the conformational change occurring in α_2M measured by this technique. Upon interaction of α_2M with several proteases, it has been observed that a substantial increase in the fluorescence of 6-p-toluidino-2-napthalene sulfonic acid occurs. This fluorescence probe has been used to monitor the interaction of thrombin with α_2M. In the presence of 2 μM thrombin and 1 μM α_2M, the reaction appears to be biphasic. A more rapid phase appears to correlate with loss in the ability of antithrombin III and heparin to inhibit thrombin and also with the formation of two species with faster mobilities upon polyacrylamide gel electrophoresis in a Tris-borate system. This phase is followed by a much slower phase which correlates with alterations occurring in the complex that can be detected by a further increase in the mobility upon electrophoresis in the borate gel system. (Supported by NIH Grant HL-30200)

T-PM-E8 KINETIC AND PHYSICAL STUDIES OF THE INTERACTION BETWEEN HUMAN $C\bar{1}$-INACTIVATOR AND $C1\bar{s}$. M. Lennick, S.A. Brew and K. Ingham. Plasma Derivatives Laboratory, Bethesda, MD 20814.

Human $C\bar{1}$-Inactivator ($C\bar{1}$-Ina) is the only circulating protease inhibitor which is known to react with the activated proteases ($C1\bar{r}$ and $C1\bar{s}$) of the first component in the complement cascade. We have developed a continuous enzymatic assay, based on esterolysis of the synthetic substrate, α-N-Carbobenzoxy-L-lysine-thiobenzyl ester, to measure rates of $C1\bar{s}$ inhibition by $C\bar{1}$-Ina. The apparent first order rate constants, obtained under pseudo-first order conditions (6.7 nM $C1\bar{s}$ and 68-404 nM $C\bar{1}$-Ina), show a linear dependence on $C\bar{1}$-Ina concentration. Thus, we determine a second order rate constant of (4.0 ± 0.1) x $10^4 M^{-1}$ sec^{-1} while we find no evidence for a two-step inactivation mechanism of $C1\bar{s}$ by $C\bar{1}$-Ina. Heparin increases the second order rate constant, in a dose dependent fashion, with a maximal 28-fold enhancement above 100 ug/ml. High performance size exclusion chromatography of the proteins, in the presence of 100 ug/ml heparin, suggests that the muccopolysaccharide effector binds tightly to $C1\bar{s}$ and to the $C1\bar{s}/C\bar{1}$-Ina complex; however, if heparin binds to $C\bar{1}$-Ina it does so in a manner which does not increase the apparent molecular weight of the protein. We have also done physical studies which provide evidence of changes in protein stability and conformation occurring as a result of complex formation. Differential scanning calorimetry shows endotherms centered at 52 and 60°C for $C1\bar{s}$ and $C\bar{1}$-Ina; however, there is no detectable transition for the complex over the temperature range scanned (25-105°C). In addition, iodide quenching of intrinsic fluorescence and differential UV absorbance spectra are consistent with the net exposure of one tryptophan and two tyrosine side chains in the complex. (Supported by NIH Grant HL21791)

T-PM-E9 FLUORESCENCE RESONANCE ENERGY TRANSFER USED TO MONITOR POLYMERIZATION OF COMPLEMENT PROTEIN C9 WITHIN C5b-9 MEMBRANE LESION. Peter Jay Sims. Depts. of Pathology and Biochemistry, University of Virginia School of Medicine, Charlottesville, VA 22908.

Cytolytic damage by the serum complement system is thought to be initiated by the membrane insertion of polymers of component C9 -- C9 polymerization and membrane insertion catalyzed by the membrane-bound C5b-8 complex. In order to monitor the kinetics of C9 activation and polymerization in situ, we have covalently labeled C9 with fluorophores suitable for the real-time spectroscopic detection of its aggregation state. We report here on one of these derivatives, FITC-C9. Polymerization of this protein -- induced either by heating in solution or by incubation with the membrane-associated C5b-8 complex (forming the cytolytic C5b-9 membrane lesion) results in a large decrease in the steady state fluorescence of the chromophore, with only small changes in its absorbance spectrum or mean fluorescence lifetime. Evidence is presented that the measured changes in fluorescence upon FITC-C9 activation are due to self-quenching of the fluorophore, which occurs in the polymerized state of the protein due to fluorescein to fluorescein resonance energy transfer between apposing C9 monomers. By monitoring FITC-C9 fluorescence, a dynamic measurement of the aggregation state of the membrane-associated complement proteins is therefore made possible. The potential applications of this fluorescent derivative of C9 are considered. Supported by a Grant-In-Aid from the American Heart Association; and the Jeffress Memorial Trust. PJS is a John A. Hartford Fellow.

T-PM-E10 KINETICS OF FITC-C9 POLYMERIZATION BY MEMBRANE-BOUND COMPLEMENT PROTEINS C5b-8.
Therese Wiedmer and Peter J. Sims, Depts. of Pathology and Biochemistry, University of Virginia, Charlottesville, VA 22908.

The fluorescence self-quenching by energy transfer of human complement protein C9 labeled with fluorescein isothiocyanate (FITC-C9) has been used to monitor the kinetics of C9 polymerization induced by the membrane-associated complex of complement proteins C5b-8. Time-based measurements of the fluorescence change observed during incubation of FITC-C9 with C5b-8 treated sheep red blood cell membranes at various temperatures revealed that C5b-8-induced C9 polymerization exhibits a temperature dependence similar to that reported for complement mediated hemolysis of sheep red blood cells, with an Arrhenius activation energy of 13.3 ± 3.2 kcal $mole^{-1}$ (mean ± 2 S.D.). Similar studies were performed with C5b-8 treated unilamellar vesicles composed of either dipalmitoyl-, dimyristoyl- or egg yolk phosphatidylcholine. Activation energies of 20 to 25 kcal $mole^{-1}$ for FITC-C9 polymerization by C5b-8 bound to these membranes were observed, values significantly higher than that obtained for sheep red cell membranes. Furthermore, the temperature-dependent rate of C9 polymerization was largely unaffected by the phase state of the lipid. These results suggest that the rate-limiting step in C5b-9 assembly is the activation and polymerization of C9 rather than the insertion of the C5b-9 complex into the membrane.
Supported by NIH-grant GM-26894; a Grant-In-Aid from the American Heart Association; and the Jeffress Memorial Trust; PJS is a John A. Hartford Fellow.

T-PM-F1 THE BEHAVIOR OF NOISY NEURAL NETS

P. Anninos, M. Kokkinidis and A. Skouras. Dept. of Physics, University of Crete, Iraclion, Crete, Greece

Previous studies with probabilistic neural nets in which the neural connections are made up by means of chemical markers revealed the existence of simple and multiple memory domains in the form of hysteresis loops. We generalized the above studies by considering the intrinsic noise of the system caused by the spontaneous release of synaptic transmitter substance. With this assumption the postsynaptic potentials (PSP's) will undergo spontaneous random fluctuations. The PSP's which will be generated by presynaptic activity will be added linearly to those fluctuations and the total PSP will determine whether or not a neuron will fire. In this approach by considering that the random PSP's are functionally equivalent to fluctuations in the firing threshold of the neurons, we developed a simple mathematical model which yields analogous characteristics of multiple hysteresis effects as noiseless neural nets.

T-PM-F2 A THEORETICAL STUDY OF DISORDERED MEMBRANE MULTILAYERS WITH APPLICATION TO X-RAY ANALYSIS. MITA GUPTA AND C.R. WORTHINGTON, CARNEGIE-MELLON UNIVERSITY, PA

There have been frequent references in the literature to disorder in oriented multilayers which contain a membrane pair within the unit cell. These systems may have both lattice disorder and substitution disorder. Lattice disorder refers to the disorder that results when the lattice constant follows a probability distribution peaked at some average lattice constant. On the other hand, substitution disorder results when the unit cells in the system are not identical. A particular form of substitution disorder occurs when the separation distance between membranes within the membrane pair follows a probability distribution that is peaked at some average width of the cytoplasmic region. Lattice disorder is associated with the broadening of the x-ray reflections whereas substitution disorder gives rise to diffuse scattering. Lattice disorder does not pose any problems for x-ray analyses while the diffuse scattering problem is only partially solved.

There are many ways of generating multilayers which contain a membrane pair within the unit cell that exhibits both kinds of disorder. A parameter that distinguishes one multilayer assembly from another is the correlation coefficient between the widths of the cytoplasmic and extracellular regions. The theoretical diffraction patterns corresponding to systems that have unequal correlation coefficients exhibit differences. These differences are significant only at relatively low values of the reciprocal space dimension. These differences however become negligible at higher values of the reciprocal space dimension, that is, when the normalized interference function tends to unity. Current work is concerned with directly determining the diffuse scattering parameters from experimental x-ray data.

T-PM-F3 A SLIDING-ELEMENT ALGORITHM FOR RAPID SOLUTION OF SPATIALLY DISTRIBUTED CONVECTION-PERMEATION MODELS. J.B. Bassingthwaighte, A.M. Lenhoff and J.L. Stephenson; Bioengineering, U. of Washington; Chem. Eng., Univ. of Wisconsin, Madison; and Theoretical Biophysics, NIH, Bethesda.

Analysis of data on tissue depositions obtained by NMR or positron tomographic imaging or of multiple tracer outflow dilution curves requires fitting data with models composed of aggregates of capillary-tissue units which account for heterogeneities of flows and multisolute exchanges between longitudinally distributed regions across capillary and cell barriers. Modern approaches to solving these partial differential equations numerically are accurate but slow, so that the cost of analyzing data is excessive. This is a severe problem even for models having analytical solutions. Our approach centers on using sliding fluid elements in the convected region, with the time step set equal to the length step divided by the fluid velocity; a single velocity must dominate to allow this. The exchanges between regions within each time step are calculated using local analytic approximations. The method enforces mass conservation unless there is regional consumption. Solutions for a 2-barrier, 3-region model accurate to within 0.5% are 100 to 1000 times faster than the analytic solution (Rose, Goresky and Bach: Circ. Res., 1977). There is even a 20 to 50% gain over the simplest single barrier model with an analytical solution (Sangren and Sheppard: Bull. Math. Biophys., 1953). The speedup is over 10,000 times for more complex models. Combining this efficient code with specialized optimizers giving rapid convergence fosters the development of families of such models serving diverse purposes. Immediate applications are to studies of kinetics and mechanisms of transport of substrates into cells of organs in vivo. (Supported by NIH grant RR01243)

T-PM-F4 MONTE CARLO CALCULATION OF PROTEIN PAC SPECTRA. C. Haydock (Intro. by F.G. Prendergast), Dept. of Pharmacology, Mayo Foundation, Rochester, MN.

Monte Carlo simulations of protein side-chain and main-chain motions are generated by a simple stochastic model. Perturbed angular correlation (PAC) spectra are calculated by averaging static hyperfine interactions over many sequences of stochastic states. It is assumed that the PAC probe nuclide is attached at a side-chain and that the motion of this side-chain can be simulated by a random walk through a set of allowed orientations. The resulting PAC spectra qualitatively resemble the well known spectra for isotropic rotational relaxation over the entire range of rotational correlation times. In particular, picosecond side-chain fluctuations result in a nearly unperturbed PAC spectrum. The effects of correlations between side-chain and main-chain motions are also investigated. These correlations are introduced by assuming that slower nanosecond main-chain fluctuations intermittently yield conformations virtually eliminating labeled side-chain mobility. Varying the percentage of time that side-chain motion is so hindered results in PAC spectra qualitatively differing from those above. Finally, experimental applications of these calculations to ^{111}In and ^{77}Br PAC spectroscopy are proposed.

T-PM-F5 INTERNAL AND EXTERNAL CURVATURE RELATIONSHIPS FROM SLIT-LAMP PHOTOGRAPHS OF THE HUMAN CRYSTALLINE LENS Jane F. Koretz[1] and George H. Handelman[2], [1]Biology and [2]Mathematics Depts., Rensselaer Polytechnic Institute, Troy, NY 12181

Accommodation, the process by which the eye focusses on near objects, occurs through systematic changes in lens curvature and thickness due to relaxation of externally applied forces. These changes can be seen both at the lens surface and at the interfaces between adjacent zones of discontinuity in the lens cortex. These curves were digitized for the entire accommodative range at 2 D intervals for four human subjects, aged 11, 19, 29, and 45, and fitted to polynomials. It was found that: all curves, independent of age, accommodative state, or location within the lens, could be fitted to parabolas with a χ^2 less than or equal to 0.001; for a given lens, a plot of the location of the curve within the lens versus the coefficient of the x^2 term gave two straight lines, one for the anterior and one for the posterior, with the same slope; the slope for a given age is maintained independent of accommodative state, but is shifted with accommodation; the slope changes progressively with increasing age. These results hold true for all lenses except the age 45 (presbyopic) lens, indicating a direct relationship between internal lens events and lens refractive power. Our accommodation model (Koretz and Handelman, 1982; 1984) is being modified to incorporate these relationships.

Supported by NIH grant EY02195.

T-PM-F6 STRUCTURE-FUNCTION RELATIONSHIPS IN BIOLOGICAL SYSTEMS. I. GLOMERULAR FILTRATION OF ALBUMIN. Guy K. Smith and Donald E. Oken.

Network thermodynamic models provide a means of studying the physical consequences of the structural organization of biological systems. This unique ability is inherent in the network thermodynamic paradigm as the informational content of a system's topology is automatically incorporated into a network thermodynamic model of that system.

Studies of glomerular albumin filtration illustrate the power of this approach on a relatively simple system. The glomerular filtration barrier has been modeled as a series of membranes with steady state coupled solute and albumin flow. Simulations using this relatively simple model and parameters of glomerular dynamics obtained experimentally have revealed that the albumin concentration in the glomerular filtrate is determined exclusively by the initial barrier of the composite membrane. The intramembrane protein concentration profile is then a function of the reflection coefficients (σ) of the more distal barriers as well as that of the entry step. This situation makes it theoretically possible to develop extremely high intramembrane protein concentrations and very irregular concentration profiles across the composite membrane. Changes in σ of the epithelial slit pore thus may cause alterations in membrane albumin concentration but are without effect on albumin concentration of the filtrate. Computer simulations of this model also indicated that if the σ for albumin of the initial glomerular barrier were to drop as low as 0.99 (normal $\geq$ 0.9999) the volume flow would drop to pathological levels, exclusive of any alteration in the hydraulic permeability of the membrane.

Dr. Smith is a USPHS postdoctoral fellow -- USPHS Training Grant #5T32AM07371-03.

T-PM-F7 ALGORITHMS FOR SENSITIVITY ANALYSES OF MONTE CARLO SIMULATION MODELS. Susan K. Seaholm and Eugene Ackerman. Division of Health Computer Sciences, Department of Laboratory Medicine and Pathology, University of Minnesota, Minneapolis, MN 55455.

Mathematical models are widely used in the Biophysical Sciences. One of the major considerations in evaluating such models is the sensitivity of the output or conclusions to the values of the parameters. For deterministic models with a single objective function, specifying such sensitivities is relatively easy. Often closed-form analytical expressions can be developed. Frequently the interactions between two or more parameters must be included, since this leads to a quite different analysis of the model than considering each parameter separately. For stochastic (Monte Carlo) models with multiple outputs derived from the simulations, the problem is even more complicated. This type of model is used in studying the scattering of electrons in tissues, in error analyses, and in population studies. Algorithmic formulations can be used for the automatic testing and analysis of Monte Carlo model sensitivities. Due to the strong interactions between the various parameters, they must be examined both univariately and in sets. Algorithms may also be employed to select strategies for succeeding sets of sensitivity tests, based on the preceding analyses. These methods are illustrated using the VESPERS programming system for the simulation of epidemics due to virus infections. This programming system provided the basis for a biotechnology pre-resource for the simulation of stochastic population models. Sensitivity tests are an essential part of a group of studies involving such population models. However, the results are more general and can be applied to other Monte Carlo model simulations. This work is supported in part by NIH grant RR 1632 and also by NIH grant LM 160.

T-PM-F8 A DYNAMICAL MODEL OF SWITCHING BEHAVIOR AT THE RIGHT OPERATOR OF LAMBDA John Aldridge, Genetics Division, Children's Hospital, Boston, Massachusetts.

The interactions of repressor and cro proteins at the right operator of bacteriophage lambda help mediate the switching between lysogeny and lysis. Elucidation of both the relative affinities of each protein for the operator and the relative activities of the two flanking promoters suggests a two dimensional differential equation model for the behavior of this network. A conceivable range of parameter values indicates that repressor and cro interactions with operator DNA may easily generate two stable steady states separated by an unstable saddle point. The network functions as a bistable switch. Alterations in binding affinities, dimerization constants, and degradation rates for both proteins suggest how known mutants can change the qualitative dynamics of the network, as well as how second site reversion may occur. In addition, the disparate promoter activities would predict that switching between steady states should be only under repressor control.

T-PM-F9 CONCENTRATION AND ELECTRIC POTENTIAL PROFILES IN INTERFACIAL REGION. V.S. Vaidhyanathan, Dept. Biophysics, SUNYAB, Buffalo, New York, 14214.

If, the concentration of an ion σ, C_σ, with valence Z_σ, in interfacial region is given by eqn.(1), and the local value of Debye-Huckel parameter, K(x) is given by eqn.(2),[x is position variable, $\epsilon(x)$local value of dielectric coefficient],and one imposes the electroneutrality condition, that at x = d, $\sum_\sigma Z_\sigma C_\sigma(d) = 0$, $C_\sigma(d)$ is concentration of σ at d, d being extent of inhomogeniety, one may verify that K(x) is always greater than K(d) for most values of $\beta(x)$. Thus, if the expression for chemical potential of ion σ, is given by eqn.(3), where ion-ion interaction contribution is included, $(H \neq 0)$, for equilibrium in interfacial region, one has the exact result, $[\phi'(x)/Y'(x)] = [K(d)-K(x)]/[K(d)K(x)]$, a negative definite quantity (the primes denoting differentials). $Y(x) \equiv -(4\pi e)\sum_\sigma Z_\sigma C_\sigma(x)$. Eqn.(3) leads to the result, $[e\Delta\phi/kT] = \beta - [\sum_\sigma Z_\sigma C_\sigma(x)]/[\sum_\sigma Z_\sigma^2 C_\sigma(d)]$, a result different from Nernst expression. When $\phi(d) = 0$, $\beta(o)$ and $\phi(o)$ must have similar signs, opposite to the sign of Y(o). Hence, eqn.(3) require that $\phi(x)$ and $C_\sigma(x)$ for positive ions must have schematically similar profile, another result at variance with conclusion from classical electrochemical expression.(1) $C_\sigma(x) = C_\sigma(d)\exp[Z_\sigma\beta(x)]$:(2) $K(x) = \varkappa^2\epsilon(x) = (4\pi e^2/kT)\sum_\sigma Z_\sigma^2 C_\sigma(x)$:(3) $\mu_\sigma(x) = \mu_\sigma^* + kT \ln C_\sigma(x) + Z_\sigma e[\phi(x)-(H/4\pi)Y(x)]$ e is protonic charge, k Boltzmann constant, T temperature.Classical result, if $H = 0$.

T-PM-F10 DEDUCTIVE APPROACH TO THE HORMONAL CONTROL OF AGEING, O.E. Rossler, R. Rossler (University of Tubingen, W. Germany).

Medawar's 1955 "reproductive value as a function of age" principle gives a lower bound to viability as a function of age in deductive adaptation theory. We give a new quantitative formulation and show that it constitutes an upper bound as well. Moreover, the resulting necessity of frequent readjustments of longevity under minor environmental changes implies that the existence of an "ageing hormone" can be predicted. Specifically, if reproductive delay is 15 years; if there is a probability of survival through that age of 1/2; and if the mean number of live-born offspring per year thereafter is 1/5 for a number of years, then the average newborn individual is supplemented by a first mature descendant after about 35 years, by 2 after about 45 years, by 3 after 55, by 4 after 65, by 6 after 75, by 9 after 85, and so on. In the same proportion, the individual's extinction or non-extinction makes less and less of a difference for the survival of its genes. There are corrections necessary if there is no chance of population growth, leading to a more complicated self-consistent (recursive) formula. Secondly, any larger (say, constant) viability function reduces the maximum possible speed of evolutionary adaptation and is, therefore, selected against under conditions of continual, near-maximal environmental change. Thirdly, under the same conditions, there is a selection pressure for frequent readjustments of ageing rate if the environment vacillates (as is likely) between conditions requiring a change in any of the 3 parameters that enter the above formula. Fourthly, the required simultaneous adjustments of many bodily traits (certainly more than two, which is the upper limit to coevolution; G.P. Wagner, Preprint, BioSystems) make a common morphogenetic control variable mandatory. Its value (averaged over weeks) as a monotonic function of time is to affect gene switches in most cells. Monotonic increase is safer - and may facilitate the biochemical hunt.

T-Pos1 TEMPERATURE EFFECTS ON WHOLE CELL AND SINGLE CHANNEL CA CURRENTS. D.L. Wilson, H.D. Lux*, W.R. Schilling and A. M. Brown. UTMB, Galveston, Texas & *Max-Planck-Institut, 8 Muchen 40, FRG.

The effect of temperature, T, on whole cell and single channel Ca currents in Helix neurons were studied. Single channels were obtained from a patch electrode applied to a neuron which was voltage clamped by two microelectrodes; this system allows measurement of whole-cell currents and transmembrane potential. In some experiments a combined suction-pipette-microelectrode system for voltage clamp and internal perfusion was used to measure whole-cell Ca currents. At low T turn-on of whole cell Ca currents is slowed, but turn-off or tail currents are only slightly affected; inactivation is very much decreased. Average patch and whole cell currents overlayed when scaled, and no change in the size of the unitary Ca events, i_{Ca}, during a pulse was detected. Peak current IV's appeared to be simply scaled by changes in T. Changing T from 29 to 9°C decreased I_{Ca} by ∿1/3 at OmV. This was due to decreases in i_{Ca} by .67 (.33 pA (9°C) & .49 pA (29°C) Q_{10}=1.2) and peak Po by 1/2 (Q_{10}=1.5). Kinetic properties of activation appeared to be much more affected than did steady-state properties; the time-to-peak increased by a factor of 4-6 and the single channel times-to-first-opening were markedly slowed. Open times were not markedly affected (1.05 ms (29°) and 1.2 ms (9°)). Closed times were fit by a sum of two exponentials; the fast time constant was relatively little affected (1.9 ms (29°) and 1.8 ms (9°)) whereas the slow time constant was much more affected (4.9 ms (29°) & 11 ms (9°)). These results are consistant with a temperature-dependent transition near the rest state that may be re-traversed from the open state; this may be consistent with a metabolic dependent step in activation.

T-Pos2 INACTIVATION OF SINGLE CHANNEL CA CURRENTS. D. L. Kunze, H. D. Lux*, and A. M. Brown. UTMB, Galveston, Texas 77550 and *Max-Planck-Institut, 8 Munchen 40, FRG.

Inactivation of Ca currents may be due to or modified by Ca influx. We studied the process in single channels of two excitable tissues from two widely divergent species: Helix neuron and Rattus ventricular myocyte. The gigaseal patch clamp method was used and in Helix the whole cell was simultaneously voltage clamped. Extracellular Ca concentration in the patch pipette was 40 mM. Holding potentials in Helix neurons were -50 mV; they were about -50 mV in cell-attached myocyte patches. Potentials were stepped by 30 to 50 mV and held for as long as 500 msec. As reported previously (Brown et al, Nature, 299, 1982) unitary Ca currents between different phyla were remarkably similar - brief bursts of openings of low amplitude with about 10pS slope conductance. At potentials of -15 to 0 mV activity was greater during the first 25 msec than at subsequent times. Single channel currents averaged from ensembles of 50-100 epochs rose to a peak value early in the record and subsequently declined. Neither mean open times nor unitary amplitudes changed across each epoch. Inactivation occurred because the average closed times duirng the rising phase of the averaged current were smaller than values at later times. Estimates of Ca influx may be obtained from the open events; longer openings should be associated with more Ca influx. Scattergrams of closed times versus preceding open times were uncorrelated. Burstergrams also showed no correlation between bursting and subsequent closed times. These results were obtained even when the rate of inactivation was maximum. Elimination of Ca currents from extra-patch membranes did not change these results. We conclude that Ca influx is not required for inactivation of Ca currents to occur.

T-Pos3 EFFECT OF CAFFEINE AND DANTROLENE SODIUM ON Ca CHANNELS IN FROG SKELETAL MUSCLE FIBERS. G. Cota and E. Stefani. Department of Physiology and Biophysics, Centro de Investigación del IPN, Apartado Postal 14-740, México, D.F. 07000, MEXICO.

Three microelectrode voltage clamp and current clamp experiments were performed in intact twitch skeletal muscle fibers of Rana moctezuma at 23°C. Slow Ca^{++} currents (I_{Ca}) were recorded in (mM/l): TEA-CH_3SO_3 120, $Ca(CH_3SO_3)_2$ 10 and sucrose 350 to abolish contraction. To further reduce K^+ currents 5 mM 3,4-diaminopyridine was added or muscles were preincubated in (mM): TEA-Cl 60, CsCl 60 and $CaCl_2$ 1.8. The decay of I_{Ca} during a maintained depolarization followed a single exponential time course. The figure shows that the corresponding rate constant $1/\tau_d$ became faster for larger depolarizations (•). The change in $1/\tau_d$ was not related to changes in peak current amplitude. The addition of 10-15 μM-dantrolene sodium to the recording solution, which reduces Ca^{++} release from sarcoplasmic reticulum (SR), did not significantly modify the voltage dependence of $1/\tau_d$ (o). Furthermore, neither the I-V curve nor the steady-state inactivation curve for I_{Ca} were modified by dantrolene, but the maximal value of I_{Ca} (ca. to 0 mV) decreased from -35±2 mA/cm^3 (6) to -25±1 mA/cm^3 (14). In other experiments we used the maximum rate of rise ($\dot{V}_{max}$) of Ca action potentials as a measure of I_{Ca}. The addition of caffeine 4 mM which increases the myoplasm Ca^{++} concentration, increased $\dot{V}_{max}$ from 1.20±0.04 V/sec (12) to 1.51±0.05 V/sec (7). Thus, Ca^{++} released from SR do not inactivate slow Ca channels.

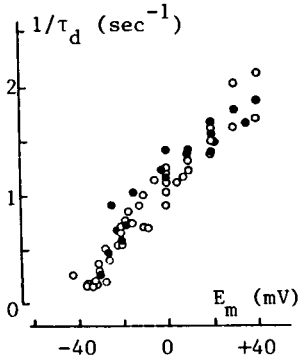

T-Pos4 REGIONAL CALCIUM ENTRY IN NEURONS OF THE GIANT BARNACLE. L.A.Lewenstein, N.Stockbridge, W.N.ROSS Dept. of Physiology, New York Medical College, Valhalla, NY 10595.

Absorbance changes of the dye Arsenazo III were measured with an array of photodiodes to detect variations in the magnitude and time course of intracellular calcium changes among different regions of neurons in the supraesophageal ganglion of Balanus nubilus. The preparation was mounted on the stage of a compound microscope and imaged onto a 10x10 photodiode array (each element detecting either a 25x25 μm^2 or a 40x40 μm^2 area in the ganglion). After the iontophoresis of Arsenazo III into the cell, absorbance changes at 660 nm were monitored in each position simultaneously in response to a depolarizing stimulus. Spectral measurements confirmed that the changes were due to calcium concentration increases. Optical signals disappeared upon replacement of normal saline (20 mM Ca) with saline containing 2mM Ca, 18 mM $CoCl_2$, suggesting that calcium entered from the extracellular medium. Anatomical correlations to the optical signals were made by the injection of Lucifer Yellow and subsequent examination with fluorescence optics.

In the photoreceptor, calcium entry was localized to the final 50 μm of the presynaptic terminal with at least 50 times less entering along the axon. However, another cell had calcium entry in its soma, axon and dendritic fields. This correlated with the finding that the cell supported a propagating calcium action potential in sodium-free saline. Other examples will be presented.

Supported by UPSH grant NS16295, Fellowship NS07172, and the Irma T. Hirschl Foundation.

T-Pos5 CALCIUM MEDIATED LIGHT EMISSION FROM THE EGGS AND EMBRYOS OF THE HYDROMEDUSAN PHIALIDIUM GREGARIUM. E. B. Ridgway and G. Freeman. Department of Physiology and Biophysics, Medical College of Virginia, Richmond; and Department of Zoology, University of Texas, Austin.

The egg of Phialidium gives a flash of light in response to KCl. This light is presumed to come from an endogenous calcium-sensitive photoprotein because EGTA extracts of the egg give light flashes on the addition of calcium, and because the adult Phialidium is known to produce phialidin, a calcium-sensitive photoprotein similar to aequorin. After a KCl response, the egg can be induced to give further light flashes by DMSO, A23187, and the detergent TritonX-100. The total light output from an egg amounts to roughly 5 billion photons. Assuming a quantum yield of 0.25 and uniform distribution throughout the egg volume leads to an estimate of 6 micromolar as the initial photoprotein concentration in unfertilized eggs. The total light that can be elicited decreases over several days after fertilization and is further reduced by about half during CsCl induced metamorphosis. This gradual decrease is probably due to consumption of the photoprotein during calcium mediated spontaneous light emission.

Spontaneous light emission accompanies a number of the important events in early development, and is particularly prominent and complex during metamorphosis which can be induced by treatment of 4 day planulae with a number of agents including Cs, K, and Li. Supported by NIH grants NS10919 and GM20024.

T-Pos6 POSSIBLE INVOLVEMENT OF ACTOMYOSIN IN Ca^{++} TRANSPORT ACROSS THE PLASMA MEMBRANE OF CHROMAFFIN CELLS. O.E. Harish, K. Rosenheck*, R. Levy and A. Oplatka, Departments of Polymer and *Membrane Research, The Weizmann Institute of Science, Rehovot 76100, Israel.

We have recently demonstrated that the introduction of the F-actin depolymerizing agent DNase-I (Friedman et al, BBRC 96, 1717 (1980)) or of the mechanochemically active heavy meromyosin (HMM) (Friedman et al, submitted) into chromaffin cells (by fusion with protein-containing liposomes) led to increase in secretion of catecholamines and to depolarization of the plasma membrane. As is well known, secretion induced by acetylcholine (ACh) is accompanied by an increase in Ca^{++} influx and the presence of Ca^{++} in the external medium is sufficient in order to cause secretion in leaky cells. Furthermore, the above-mentioned proteins did not affect secretion by leaky cells. We therefore checked $^{45}Ca^{++}$ uptake by cells (both un-stimulated and after stimulation with ACh) which had been loaded with DNase-I or HMM, as compared to control cells fused with liposomes containing only the medium in which the proteins had been dissolved and to untreated cells. The introduction of each of the proteins caused a marked increase in Ca^{++} uptake. The effect could be abolished by the Ca^{++}-channel blocker Co^{++} . We speculate that plasma membrane-associated F-actin, in combination with cellular myosin, by virtue of their capability to give rise to cytoplasmic streaming, and hence also to electroendoosmotic effects, may "pump' out ions, including Ca^{++}, thus controling the level of Ca^{++}. Both DNase-I and HMM (which is less effective mechanochemically than competing, cellular myosin) will diminish this pumping activity, thus leading to increased Ca^{++} uptake.

T-Pos7 SULFHYDRYL REAGENTS INDUCE CALCIUM SPIKES IN CRUSTACEAN MUSCLE. C. Zuazaga, M. Martínez and J. del Castillo. Lab. of Neurobiology, U. of Puerto Rico Med. Sch., San Juan, P.R. 00901

The ventroabdominal flexor muscle of the freshwater shrimp Atyas occidentalis normally responds passively to depolarizing current pulses. After exposure to α,β-unsaturated carbonyl compounds, depolarization evokes a train of overshooting action potentials. The following compounds (2mM; 5-10 min) induce this repetitive spike activity: N-ethylmaleimide (NEM), maleimide, 4-cyclopentene-1,3-dione and 2-cyclopentenone. The saturated analogs of some of these compounds do not induce this effect. Organic mercurials do not induce electrical activity and previous exposure of the muscles to them blocks the action of the unsaturated carbonyl compounds. These results suggest that the effect of the unsaturated carbonyl compounds is due to the modification of cysteinyl residues to polar thioethers and the interaction of these new side chains with existing amino or hydroxyl groups of membrane proteins. To test this hypothesis, several group-specific protein reagents were tested and it was found that only glyoxal and dinitrofluorobenzene altered the chemically-induced spike activity. These reagents, which are specific for arginine and amino groups respectively, modify repetitive activity to the firing of a single action potential. The following results strongly suggest that Ca^{2+} is the main carrier of current in the chemically-induced action potentials: a) the overshoot increases with increasing external Ca^{2+} concentration, b) the spikes disappear when external Ca^{2+} is replaced by Mg^{2+} and c) the spikes are blocked by 3-5 mM Co^{2+}, Mn^{2+}, Cd^{2+} and La^{3+}. We propose that the activation of these Ca channels involves the interaction, via hydrogen bonding, between the newly formed polar thioethers and existing arginine residues of muscle membrane proteins. (Supported by NIH grants NS07464,14938 and RR-08102.

T-Pos8 SPATIO-TEMPORAL CHARACTERISTICS OF Ca^{2+} DISPERSAL FOLLOWING ITS INJECTION INTO APLYSIA NEURONS. J. Chad, J. W. Deitmer and R. Eckert. Dept. of Biology, UCLA, Los Angeles, CA 90024

Calcium ions were injected into voltage-clamped neurons of A. californica while the Ca activity, $\bar{a}Ca_i$, was measured with a neutral-carrier-type Ca^{2+} electrode positioned near the injection site. The neurons were held at -40 mV at 13°C in ASW, and $\bar{a}Ca_i$ transients were elicited with pulses of electrophoretic current (0.2-0.5 μA for 1 to 24 s). The 90% response time of the Ca-sensitive electrode was below 5 s, and appeared not to limit the time course of decay of recorded $\bar{a}Ca_i$ transients. Injection of 4 pmol of Ca^{2+} produced a peak $\bar{a}Ca_i$ of 1.3 μM from a resting level ≈0.1 μM, measured at a distance of ≈20 μm. The $\bar{a}Ca_i$ decay transient could be approximated by a minimum of two summed exponentials having τ's of about 7 s, and 37 s. With increased distance between injecting and recording electrode, peak $\bar{a}Ca_i$ declined and the time course slowed. These results were compared to a model of Ca^{2+} dispersal based on the assumptions that i) Ca^{2+} buffer is uniformly distributed, and ii) Ca^{2+} diffuses between buffer sites at the rate calculated for an aqueous solution (Hodgkin & Keynes, 1957). Parameters of Ca^{2+} binding to a 'calcium binding protein' of Aplysia neurons (Bredderman & Wasserman, 1974; Christakos et al., 1983) were used, along with a transport number of 0.2. The model includes decreased probability of buffering due to saturation at increased $\bar{a}Ca_i$. Modeling of $\bar{a}Ca_i$ originating from a point source revealed steep spatial gradients of $\bar{a}Ca_i$ which flattened with time, similar to the behavior of $\bar{a}Ca_i$ transients measured experimentally. This study provides further evidence for development of buffer-dependent steep spatio-temporal gradients of cytoplasmic free calcium. Supported by USPHS NS 8364, NSF BNS 80-12346, BNS 82-03843, and a Max Kade Foundation Fellowship to J.W.D.

T-Pos9 NOREPINEPHRINE MODULATION OF CALCIUM CHANNELS IN INTERNALLY DIALYZED SENSORY NEURONS. Paul Forscher* and G.S. Oxford. The Neurobiology Program, Univ. of N.C., Chapel Hill, NC.

Calcium channel properties in chick dorsal root ganglion (DRG) cells grown in tissue culture were studied using the patch clamp technique in the whole cell configuration. External solutions contained NaCl and 300nM TTX. TEA^+ was sometimes added to block outward currents. Typical internal solutions contained K-aspartate with varying amounts of added EGTA, Mg-ATP, and cAMP.

Initial current clamp studies on cells dialyzed with Cs or K-aspartate solutions were hampered by spontaneous rundown of Ca-dependent action potential (AP) duration and amplitude. Addition of EGTA to internal solutions retarded AP rundown. Voltage clamp experiments in which internal K was replaced by either N-methylglucamine (NMG) or Cs were similarly hampered by Ca current rundown even in the presence of internal EGTA. Rundown was significantly decreased by addition of intracellular ATP (5-10mM) and cAMP (0.5-1mM), therefore voltage clamp studies were usually conducted in the presence of these added intracellular components.

After establishing stable recording conditions, the effects of norepinephrine (NE) on calcium channels were assessed (cf. Dunlap and Fischbach, J. Physiol. 1981). NE (1-10uM) reversibly decreased AP duration and peak inward current in K-aspartate dialyzed neurons in 5-20mM TEA^+, indicating that dialysis does not eliminate the response. However, AP's and currents from cells dialyzed exclusively with Cs or NMG exhibited little or no reversible response to NE.

Experiments are in progress to elucidate the basis of the apparent internal cation dependence of Ca channel modulation by NE in DRG cells. (Supported by NIH NS-18788 and NSF BNS82-11580.)

T-Pos10 ANTIBODY LOCALIZATION OF SODIUM CHANNELS IN DEVELOPING RAT SKELETAL MUSCLE. B. Haimovich, A. Horwitz and R. Barchi, University of Pennsylvania, Philadelphia, PA 19104

We have generated a polyclonal antiserum against the purified voltage dependent sodium channel from rat skeletal muscle sarcolemma. This antiserum bound specifically to purified sodium channel protein in a solid phase RIA and precipitated the sodium channel from a crude mixture of solubilized sarcolemmal proteins. On immunoblots of membrane proteins the antiserum reacted predominantly with a diffuse band in the high molecular weight region comparable in migratory characteristics to the large glycoprotein subunit of the purified sodium channel.

The antiserum specifically labelled surface membranes of mature and fetal rat skeletal muscle as well as the Nodes of Ranvier in rat peripheral nerve. Cross reaction was found with mouse, human and guinea pig skeletal muscle sarcolemma. This antiserum was then used to study developmental changes in the distribution of the sodium channel on the surface of fetal rat skeletal muscle cells grown in tissue culture. In primary cultures two types of surface staining were observed. Starting on day two, and continuing until the completion of fusion, all myoblast-like cells exhibited bright patches of immunoreactivity on their surface membranes. Following fusion (day 4-5), however, a diffuse pattern of immunofluorescence developed on the surface membrane that was subsequently associated with all growing myotubes. The ends of myotubes, or regions in which active fusion was taken place, were only dimly stained. A uniform diffuse staining was seen on all myotubes at later stages (day 7-15) that appeared lower in intensity than that observed with earlier myotubes. No staining was associated with fibroblast cells.

Supported in part by NS-18013 and the MDA.

T-Pos11 INTERNAL Cs^+ SUPPRESSES GATING CURRENT IN THE PRESENCE OF EXTERNAL TTX.
John G. Starkus*, S. T. Heggeness & M. D. Rayner, University of Hawaii, Honolulu, HI 96822

In a variety of preparations, cesium (Cs^+) is commonly utilized as a replacement cation for K^+ during internal perfusion. This substitution eliminates ionic current through potassium channels and reduces nonlinear leakage current, therefore, facilitating kinetic analysis of sodium and gating currents. Prior to a detailed kinetic study of sodium conductance control, we have carefully evaluated the effects of internal Cs^+ on perfused crayfish giant axons.

A comparison of sodium rising and falling phase condutance reveals no kinetic differences between axons perfused either with K^+ (plus 1 mM 4AP) or Cs^+ as the major internal cation. In addition gating currents (IgON) measured at E_{Na}, in the absence of external TTX, are not affected by this cationic substitution. However, with 100 nM TTX present in the external solution, internal perfusion with Cs^+ results in a suppression of intramembranous charge movement. This suppression of IgON occurs without any observable kinetic distortions, and demonstrates substantial hold potential dependence. At a hold potential of -80 mV, internal cation substitution of Cs^+ for K^+ results in at least 60% suppression of total charge movement. This suppression can be reversed by returning to K^+ internal perfusate. At more hyperpolarizing hold potentials, the Cs^+-TTX synergism is less apparent, producing approximately 10% suppression of gating charge movement at a hold potential of -120 mV.

One hypothesis consistent with these results is that Cs^+ may bind to TTX blocked sodium channels at less negative holding potentials, resulting in an interference with gating charge movement. Supported by NIRA award NS17202 and by University of Hawaii Research Council to JGS.

T-Pos12 COMPONENTS OF SODIUM CHANNEL BLOCK BY 9 AMINOACRIDINE IN CRAYFISH GIANT AXONS.
M. D. Rayner, S. T. Heggeness & John G. Starkus, University of Hawaii, Honolulu, HI 96822

Internal prefusion of non-pronased axons with 100 μM 9 aminoacridine (9AA) produces significant block of peak I_{Na} in single pulses to +80 mV. An additional 60% block of peak I_{Na} occurs during a twenty pulse stimulus train at 1 Hz. Neither IgON nor the hooked tail currents visible in such records are affected by the development of cumulative "use-dependent" block.

Comparison of pronased and non-pronased records indicates that the hooked tail currents reflect a "time-dependent" component of open-pore block with similar kinetics in both pronased and non-pronased axons. Non-pronased axons also show a tonic "initial" block which underlies the time dependent component. Comparison of recovery rates in 100 μM 9AA following a single test pulse or a twenty pulse, 1 Hz, stimulus train suggest that use-dependent block may reach equilibrium within a single 5 msec test pulse to +80 mV. Multipulse protocols indicate that use-dependent block is not strongly voltage-dependent in these axons.

9AA block in a non-pronased axon can thus be represented as the sum of time-dependent, use-dependent and initial block. Time-dependent block generates hooked tail currents, prevents normal inactivation and immobilizes IgOFF. Use-dependent binding blocks sodium channels without affecting the gating current generator. Initial block appears to reflect equilibrium binding to the use-dependent receptor at hold potential. It is not yet clear whether or not use-dependent block develops in a single pulse at a rate associated with the fast inactivation rate.
(Supported in part by NIH grant No. GM29263 to MDR and NIRA award NS17202 to JGS).

T-Pos13 VOLTAGE- AND USE-DEPENDENT BLOCK DUE TO INTERACTION OF SAXITOXIN WITH CALCIUM IONS IN NERVE MEMBRANE SODIUM CHANNELS. Vincent L. Salgado, Jay Z. Yeh and Toshio Narahashi. Dept. Pharmacol., Northwestern Univ. Med. Sch., Chicago, IL 60611.

Block of nerve membrane sodium channels by saxitoxin (STX) has been found to be dependent on calcium concentration, membrane potential, and stimulation in internally perfused crayfish axons. STX block was intensified by decreasing the external Ca concentration, with an apparent dissociation constant (K_d) of 18.8, 6.5 and 3.6 nM in 50, 10 and 2 mM Ca^{2+}, respectively. These changes in K_d are accounted for by changes in membrane surface potential due to Ca concentration changes. STX block was also voltage dependent; block was intensified by increasing the holding potential from -80 mV to -180 mV. The voltage dependence of STX block was enhanced by increasing Ca concentration in the range of 2 to 50 mM. At 10 mM Ca, however, STX block was minimal at -120 mV and was intensified with both depolarization and hyperpolarization. STX also produced use-dependent block, which developed with a 5-10 sec delay following a conditioning pulse, and recovered with a time constant of about 20 sec. Use-dependent block was enhanced by hyperpolarized holding potentials and high calcium concentration. The use-dependent block required channel opening for a short period (1 msec), longer depolarizing pulses being no more effective. Voltage- and use-dependent block by STX are explained by a model in which STX binding to a site at the external mouth of the channel is dependent upon calcium binding to one of two sites within the channel pore. Supported by NIH grants NS14144 and GM24866.

T-Pos14 INHIBITION OF INACTIVATION BY SCORPION TOXIN AND TRYPSIN IN NEUROBLASTOMA CELLS WITH NORMAL OR MUTANT Na CHANNELS. T. Gonoi, B. Hille, and W. Catterall, Depts. of Pharmacol. and Physiol./Biophys., Univ. of Washington, Seattle, WA 98195 (Intr. by D.K. Blumenthal)

Na^+ currents in N18 cells were measured using a whole cell patch clamp method from a holding potential of -75 mV. Intracellular application of trypsin through the pipette removed inactivation and increased peak I_{Na} 2.3 fold for pulses to +15 mV. The mid-point of the G_{Na} vs. V curve ($V_{0.5}$) was shifted from -12.5 mV to -35.6 mV. Extracellular application of Leiurus quinquestriatus toxin (Lqtx, 100 nM) increased τ_h from 0.6 msec to 5.7 msec and increased peak I_{Na} 2.0 fold. $V_{0.5}$ was shifted from -8.6 mV to -15.7 mV. The effects of Lqtx and trypsin on peak I_{Na} were not additive. These results resemble those in nonmammalian preparations except that peak I_{Na} values were not increased in those studies. The increase in peak I_{Na} values is compatible with either a Hodgkin-Huxley mechanism or certain coupled mechanisms of inactivation.

Some neuroblastoma cell lines selected for resistance to the cytotoxic effects of veratridine plus Lqtx have mutant Na^+ channels with reduced affinity for Lqtx as measured in biochemical experiments. In Lqtx-resistant cell lines LV10 and LV30, the time course of I_{Na}, G_{Na} vs. V curves, and h_∞ vs. V curves were identical to those for N18 except that the amplitude of I_{Na} was reduced. The action of Lqtx was voltage-dependent. At -75 mV, K_D values were 24 nM and 5.4 nM for LV10 and LV30 compared to 1.7 nM for N18. Apparent K_D values increased e-fold for each 15 to 21 mV depolarization between -90 mV and -30 mV for all three cell lines. These biophysical results verify that Lqtx-resistant cell lines have mutant Na^+ channels with reduced affinity for Lqtx and also show that this is a specific alteration which does not impair normal channel function.

T-Pos15 LIGHT MICROSCOPIC IMMUNOCYTOCHEMICAL LOCALIZATION OF SCORPION TOXIN BOUND TO AMPHIBIAN NODE OF RANVIER. Shepley M.P., Strichartz G.R., and Wang G.K. Anesthesia Research Laboratories, Brigham and Women's Hospital, Harvard Medical School, Boston, MA 02115

The high specificity of scorpion toxins for the sodium channel underlies their use as probes to localize and identify sodium channel proteins. In this study, scorpion toxin bound to nodes of Ranvier was localized with affinity purified rabbit-anti-scorpion toxin antibodies (RαTOX), and subsequently visualized with rhodamine conjugated goat-anti-rabbit antibodies (GαR-Rho). The RαTOX antibodies were derived from antiserum, produced by immunizing a rabbit with purified toxin from Leiurus quinquestriatus (LQIIα) emulsified in complete Freund's adjuvant. The affinity purified fraction of the serum was prepared on a column containing 210 µg of LQIIα bound to Affi-Gel 10 (Biorad). Desheathed frog sciatic nerves were incubated with 0, 60 or 120 nM LQIIα washed, and fixed with 1% paraformaldehyde. Nerves were made permeable to antibodies and incubated with RαTOX for 18 h at 4°C, followed by incubation with GαR-Rho for 2 h at room temperature. The tissue was examined with phase contrast and fluorescence microscopy. Loci of intense fluorescence were associated with intact nodes in LQIIα-treated nerves, whereas no such fluorescence appeared in the absence of toxin. Comparison of phase contrast and fluorescence micrographs of isolated fibers indicated that the nodal surface was the source of the fluorescence. Micrographs of bundles of fibers showed densities of fluorescing nodes comparable to the density of nodes observed by phase contrast. Preliminary results indicate that a competitive inhibitor of LQIIα, Anemonia sulcata toxin, partially inhibits scorpion toxin-associated fluorescence. Supported by a grant from the Multiple Sclerosis Society.

T-Pos16 PATCH CLAMP ANALYSIS OF VERATRIDINE-INDUCED SODIUM CHANNELS. Mitsunobu Yoshii and Toshio Narahashi (Intr. by Raymond F. Novak), Dept. Pharmacol., Northwestern Univ. Med. Sch., Chicago, IL 60611.

Modification of Na channels by veratridine has been studied in neuroblastoma cell line N1E-115 using patch clamp techniques. In our preliminary study, veratridine was shown to prolong the mean open time of single Na channels at low temperatures (12-14°C) (Yoshii et al., 1983, Neurosci. abstr. 9, 674). In order to further characterize the veratridine-modified Na channels, the sodium currents were recorded from both whole cells and single channels. The experiments were performed at room temperature (22°C) to augment the effect of veratridine (30-100 μM) applied extracellularly. In veratridine, a depolarizing clamp step elicited, following a peak Na current, a slowly rising Na current. The tail current associated with step repolarization was greatly increased in amplitude and decayed very slowly with a voltage-dependent time constant of 1.2 sec at -80 mV and 0.35 sec at -140 mV. The instantaneous current-voltage relationship for the slow component of the tail current showed a rectification, increasing at negative membrane potentials between -20 and -120 mV. Single Na channel currents were prolonged in duration up to several hundred milliseconds. The prolonged openings of the veratridine-modified Na channels were also observed upon repolarization. The veratridine-modified single Na channel currents exhibited a slight inward rectification at negative potentials. The amplitude of the modified single channel current was reduced to 0.7 pA at -30 mV, about half of the normal value. This reduction became less obvious at membrane potentials more negative than -120 mV where Ca block occurs in normal Na channels (Yamamoto et al., Biophys. J., in press). Supported by NIH grant NS14144.

T-Pos17 INTERACTION OF BATRACHOTOXIN WITH SODIUM CHANNELS IN SQUID AXONS. Joëlle Tanguy, Jay Z. Yeh and Toshio Narahashi, Lab. Neurobiol., École Normale Supérieure, Paris, France, and Dept. Pharmacol., Northwestern Univ. Med. Sch., Chicago, IL 60611.

The mechanism by which batrachotoxin (BTX) modifies the Na inactivation process was studied in internally perfused and voltage clamped squid axons. Internally applied BTX (1-10 μM) had little or no effect on Na channels when the membrane was held at either -150 mV or +40 mV. When repetitive pulses were applied from a holding potential of -80 mV to open channels, both activation and inactivation kinetics were affected: Na channels opened at large negative potentials and Na inactivation was completely removed. The removal of Na inactivation differed from that caused by pronase: In the pronase-treated axons, octylguanidine caused a time-dependent block of Na currents simulating the Na inactivation, whereas it failed to cause such block in BTX-modified axons whether or not the channel was treated by pronase. After removal of Na inactivation with pronase, BTX was still able to modify the Na channels, and the sustained depolarization to +40 mV was as effective in inducing BTX modification of the channel as the protocol with repetitive pulses. However, when octylguanidine and BTX were applied together to the pronase-treated axons, the sustained depolarization became less effective in producing the BTX effect. The situation is similar to that in normal axons, and octylguanidine appears to act like an inactivation gate. In summary, when conducting, the Na channels become available for BTX modification. The Na channel, once modified, loses its affinity for the inactivation gate or simulators. Supported by NIH grants NS14144 and GM24866.

T-Pos18 MODIFICATION OF SQUID SODIUM CHANNELS BY A RED-TIDE BREVETOXIN. James M.C. Huang and Chau H. Wu, Department of Pharmacology, Northwestern University, 303 E. Chicago Avenue, Chicago, Illinois 60611.

T17 toxin isolated from the red-tide dinoflagellate Ptychodiscus brevis causes a partial depolarization in squid axons. This depolarization can be blocked by tetrodotoxin (TTX), suggesting that T17 affects sodium channels. To investigate T17 mode of action, we performed voltage clamp experiments on internally perfused axons using the axial wire technique. During 4-sec depolarizing pulses from -180 mV to various potentials and in the presence of 1 μg/ml T17, sodium currents with very slow activation and inactivation kinetics could be clearly distinguished from the normal fast currents. Also, for membrane potentials less negative than -180 mV, T17 increased the holding current necessary to maintain the holding potential. For membrane potentials more negative than -180 mV, the holding current was same as controls. The voltage dependence of activation and reversal potential were shifted in the hyperpolarizing direction by 100 and 15 mV, respectively. However, tail currents were not significantly affected. TTX (300 nM) or procaine (30 mM) completely blocked the T17-induced slow currents. In the presence of TTX, T17 did not affect potassium currents. These results indicate that T17 induces depolarization by causing TTX-sensitive sodium channels to open at very negative membrane potentials. The modified sodium current produced by T17 activates and inactivates with a very slow time course. The brevetoxin appears to modify the ion permeability without affecting the sensitivity to TTX or procaine.

T-Pos19 AN IMPROVED "LOOSE-PATCH" VOLTAGE CLAMP FOR MUSCLE FIBERS AND NEURONS. W.M. Roberts and W. Almers. Dept. of Physiology & Biophysics, Univ. of Washington, Seattle, WA 98195

A previously described "loose-patch" method (Stühmer, Roberts & Almers, in Single Channel Recording, p. 123, eds. B.Sakmann & E.Neher, Plenum, 1983) is useful for recording under highly physiologic conditions, but has two disadvantages: (1) large leak currents across the 0.3-2 MΩ seal between pipette and cell surface and (2) contamination by active currents across uncontrolled membrane under the pipette rim. Both are avoided by using concentric pipettes (Fig A) pulled from an inner tube held in the center of an outer tube by three equally spaced support capillaries. The pipette tip is pushed against a nerve or muscle cell; potential steps are applied to both inner and outer barrels, but current is collected from the inner barrel only. Analog circuitry holds the tips of both barrels isopotential, preventing current across the rim of the inner pipette. This solves problem (1). Collecting currents only from the center of a larger isopotential patch solves problem (2). In response to a voltage step applied to a network of resistors simulating pipettes, membrane and seals, the recorded current rises with a time constant of 20 μs. We have recorded successfully from frog, rat and human skeletal muscle. The voltage and time dependence of Na and delayed K currents in frog muscle fell within the range of results obtained with other methods. Fig B shows membrane currents from a leech P-neuron in response to depolarizations of 40 to 140 mV from the resting potential (15°C), so the method may be used for neurons as well.

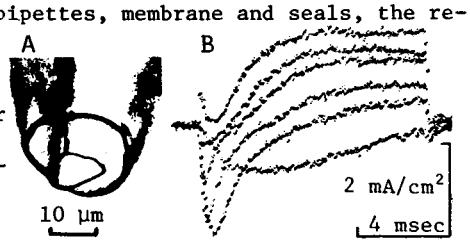

Supported by NIH grants AM17803 and NS 18748.

T-Pos20 **TWO COMPONENTS OF SINGLE NA CHANNEL INACTIVATION IN PATCH RECORDINGS FROM DISSOCIATED CARDIAC CELLS.** **Joseph Patlak**, Department of Physiology, U. of Vermont, Burlington, VT 05405.

Na currents from dissociated rat ventricular myocytes were studied with the patch clamp technique. Cells were bathed in a high $[K]_o$ solution at 11 °C, the patch electrode contained a HEPES buffered Ringer's, and recordings were made in the 'on cell' configuration. The high $[K]_o$ depolarized the cells to a resting potential of 0 to -5 mV, which was neglected during these recordings. The rate of inactivation during pulses from a holding potential of -120 mV to test potentials was measured. The fastest phase of inactivation was exponential, with time constant for decay, τ_h, described by $\tau_h = \exp[-(V_m+48)/9] + 0.46$ where V_m is in mV and τ_h is in ms. For pulses between -60 and -30 mV, a second, slower inactivating component was observed. Its time constant increased from 4 ms at -60 to >20 ms at -30 mV. Single channel observations in the same patches show that both components are due to current through the Na channel. The relative amplitudes of the fast and slow inactivating components during test pulses to -40 mV could be reversibly altered by changing the holding potential: The magnitude of the slowly inactivating currents increased at -100 mV holding potential, while the magnitude of the rapidly inactivating currents decreased. Changes in the opposite direction were observed for holding potentials of -140 mV. The variance of pulse ensembles was measured at each time point and analyzed using the method of Sigworth [J. Physiol. 307:97]. Plots of the variance vs. mean current showed substantial hysteresis at large current amplitudes: The variance was greater for currents on the rising phase than for currents of equal magnitude on the falling phase. Small currents had equal variance, regardless of the time during the pulse. A model explaining these data adds a state, which has slow, voltage dependent transitions, to the left of the normal closed states used for models of Na channel activity in nerve.

T-Pos21 SODIUM CHANNELS FROM MAMMALIAN HEART MUSCLE INCORPORATED INTO PLANAR LIPID BILAYERS. M.T. Nelson, R. Reinhardt & W.J. Lederer. Dept. Physiology, Univ. Maryland, Baltimore, MD & II. Physiol. Inst., Univ. des Saarlandes, D-6650 Homburg/Saar, FRG.

Sarcolemmal vesicles prepared from calf ventricular muscle (c.f. Jones et al., J.B.C. 254:530) were added to one ("cis" side) of the two solutions bathing a lipid bilayer (PE:PS). The solutions on both sides of the bilayer contained 250 mM NaCl and 0-1 mM $CaCl_2$. The "trans" side also contained 600 nM batrachotoxin. After the addition of these vesicles, there was a discrete change in membrane current that presumably reflected the incorporation of channel containing vesicle into the bilayer (Figure 1). The channel was open most of the time and voltages between -60 mV and +60 mV had little influence on the probability of the channel being open. The single channel conductance under the experimental conditions was about 17 pS. Reversal potential experiments suggest that the observed channel selects for Na over other monovalent ions. We have also seen other cardiac channels incorporated into lipid bilayers by this technique. (Supported by the American Heart Ass., NIH(HL25675), U.S. Army Res. Dev. Cont. & DFG-SFB38 (project C1)).

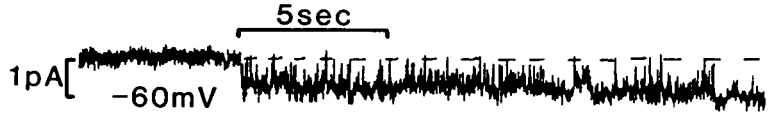

T-Pos22 SODIUM CHANNELS IN PLANAR LIPID BILAYERS: EFFECTS OF DIVALENT CATIONS ON ION PERMEATION.
Jennings F. Worley III. Dept. of Physiology, U of MD School of Medicine, Baltimore, MD 21201.

Saxitoxin-sensitive, voltage-gated sodium channels from rat brain were incorporated into planar lipid bilayers as described by Krueger, Worley, and French (Nature 303:172 1983). Variation in the conductance (γ) of single, batrachotoxin-activated channels was determined as the sodium ion concentration on both sides of the bilayer were altered. The conductance saturated at a maximum value of 30pS (half-maximum conductance at 25mM Na). At high sodium concentrations ($\geq$250mM) a reduction in γ was observed by addition of calcium or strontium. The figure illustrates the reduction of γ by addition of strontium. In the presence of 250mM NaCl, 200mM $SrCl_2$ added on both sides of the membrane reduced γ to 7-8pS. These current-voltage relationships are virtually identical using either neutral or negatively-charged, phosphatidylserine-containing bilayers. Thus, under saturating conditions surface charge on the phospholipid appears to have little effect on ion permeation. The linearity of the current-voltage relationships obtained at high strontium concentrations suggests that any direct blocking effect by strontium is either voltage-independent or weakly voltage-dependent. In addition, strontium may bind to, or screen charges which are associated with the channel protein at or near the mouth of the pore. (Supported by NIH; US Army Med.Res.Dev.Comm.)

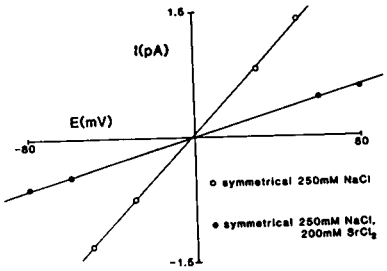

T-Pos23 STRUCTURAL AND FUNCTIONAL KINETICS OF ISOLATED SARCOPLASMIC RETICULUM. J.K. Blasie, D.H. Pierce, D. Pascolini, A. Scarpa, Depts. of Chemistry and Biochemistry/Biophysics, University of Pennsylvania, Philadelphia, PA 19104, and L.G. Herbette, Depts. Medicine and Biochemistry, University of Connecticut, Farmington, CT 06032.

Correlated time-resolved structural determinations using X-ray diffraction and functional measurements utilizing spectrophotometric techniques made it possible to associate structural changes of the sarcoplasmic reticulum (SR) membrane with Ca^{2+} "occlusion" and E∿P formation. The Ca^{2+} uptake reaction by SR membranes in oriented multilayers was initiated by flash photolysis of caged ATP and monitored using spectrophotometric techniques with a Ca^{2+} metallochromic indicator. The reaction profile was biphasic with a fast phase associated with Ca^{2+} "occlusion" and E∿P formation, and a subsequent slow phase which was identified as Ca^{2+} transport across the membrane profile. Time-resolved X-ray diffraction utilizing flash photolysis of caged ATP to synchronously initiate the Ca^{2+} transport process in SR membranes has shown that structural changes do occur in the membrane profile on a subsecond time scale following photolysis. Previous X-ray and neutron diffraction studies (∿10 Å resolution) of oriented multilayers of SR membranes have provided the separate time-averaged (resting state) profile structures for the protein, mainly Ca^{2+}-ATPase, and lipid bilayer of the SR membrane. Model calculations of the separate time-resolved protein and lipid bilayer profiles indicated that the observed membrane profile changes arose mainly from a redistribution of protein mass within the membrane profile on the order of ±5-10% of the total protein mass. This protein redistribution was correlated with calcium occlusion and E∿P formation, which occur before calcium translocation, and relaxed to the resting state protein profile following calcium transport. Support: NIH HL-18708, -27630 and -22135.

T-Pos24 ADP-INDUCED, RUTHENIUM RED-SENSITIVE, RAPID RELEASE OF Ca^{2+} FROM SARCOPLASMIC RETICULUM OF SKELETAL MUSCLE. László Mészáros and Frank A. Sreter, Department of Anesthesia, Mass. General Hospital and Harvard Medical School and Department of Muscle Research, Boston Biomedical Research Institute, Boston, Mass. 02114.

Ca^{2+} which had been actively loaded into rabbit skeletal sarcoplasmic reticulum (SR) by an ATP-dependent process was found to be released rapidly upon addition of ADP (0.2-1.0 mM) in the presence of low $[Mg^{2+}]$ (0.2 mM). The release of 5-30% of the loaded Ca^{2+} was followed by a spontaneous Ca^{2+} reuptake by SR indicating that the ADP-induced release was reversible. The Ca^{2+} fluxes were monitored using arsenazo III as Ca^{2+} indicator in a dual-wavelength spectrophotometer. When passively loaded (i.e. overnight incubated in 5 mM $^{45}Ca^{2+}$) was used, addition of ADP failed to induce Ca^{2+} release. The observed Ca^{2+} release was completely blocked by 2 μM ruthenium red (RR) and was reduced either by decreasing or by increasing the $[Mg^{2+}]$ (I_{50} = 0.1 mM and 0.5 mM, respectively). In parallel with the ADP-induced release of Ca^{2+}, ATP was synthesized through the back reaction of the Ca-pump as evidenced by the conversion of [^{14}C]-ADP to labelled ATP with concomitant reduction of the phosphorylated intermediate of the Ca-ATPase enzyme (EP). Both the synthesis of ATP and the decrease of the steady-state EP level after ADP addition was also blocked by 2 μM RR. (RR itself significantly increased the steady-state EP level.) The existence of a ruthenium red-sensitive, Ca-ATPase mediated Ca^{2+} release pathway is suggested. Supported by NIH grants (GM 15904-16, HL 23 961).

T-Pos25 FURTHER STUDIES ON THE ALKALINE pH INHIBITION OF Ca^{2+} TRANSPORT IN SARCOPLASMIC RETICULUM. **C.A. Tate, R.J. Bick, A. Chu, W.B. Van Winkle, and M.L. Entman. Section of Cardiovascular Sciences, Baylor College of Medicine, Houston, Texas 77030.**

We previously demonstrated a "Ca^{2+} sensitive factor" in SR related to the influx of Ca^{2+} to the intravesicular space. This factor is sensitive to preincubation conditions at alkaline pH (pH 7.4-7.6): When the SR is first exposed to alkaline pH without added Ca^{2+} (control), the subsequent rate of oxalate-supported Ca^{2+} uptake is 5-10% of that at pH 6.8. This alkaline pH inhibition is reversible. However, when the SR is exposed to both alkaline pH and Ca^{2+} (protected), the subsequent Ca^{2+} uptake rate is 70-90% of that at pH 6.8. CaATPase activity is not affected by preincubation conditions. Since concomitant oxalate transport is less affected than Ca^{2+} uptake under control conditions, we postulated that an increased Ca^{2+} efflux may occur under control at alkaline pH, leading to a reduced net Ca^{2+} uptake. Further work revealed: (1) Increased Ca^{2+} efflux occurs during the linear portion of Ca^{2+} uptake at alkaline pH under control conditions, whereas Ca^{2+} efflux is minor at pH 6.8 or alkaline pH under protected conditions. (2) Acylphosphate formation is not affected by preincubation condition at alkaline pH. (3) The content of membrane-bound calmodulin and the calmodulin-dep. phosphorylation of the 60K protein are not affected by preincubation conditions or pH. Added calmodulin has no effect on Ca^{2+} uptake under any condition. The results suggest that after the initial translocation of Ca^{2+}, Ca^{2+} efflux occurs from a membrane-bound compartment at alkaline pH under control, thus reducing the net rate of Ca^{+} uptake. Ca^{2+} efflux apparently is not related to calmodulin under these conditions.
Supported by AHA (Texas Affiliate and NIH (HL 13870).

T-Pos26 DECOMPOSITION OF PHOSPHORYLATED INTERMEDIATES OF Ca^{2+}-DEPENDENT ATPase OF SARCOPLASMIC RETICULUM BY TWO ROUTES. Yoichi Nakamura and Giuseppe Inesi. University of Maryland, Department of Biological Chemistry, Baltimore, Maryland 21201.

The decomposition of the phosphorylated intermediate (EP) in purified Ca^{2+}-ATPase from sarcoplasmic reticulum was measured by stopping the formation of radioactive EP from ^{32}P-ATP by adding twenty volumes of a solution of non-radioactive ATP, 0.5 mM $CaCl_2$, 5 mM $MgCl_2$, and 90 mM KCl at pH 7.0 and 0°C. The time course of decomposition consisted of an initial fast phase followed by a slow phase. The two components of EP, EP_{fast} (1.1 nmol/mg) and EP_{slow} (2.8 nmol/mg) decompose independently with rate constants of 6 and 0.4 min^{-1}, respectively. The rate of Pi liberation (7.3 nmol/mg/min) was in good agreement with the summation of the decomposition of the two components of EP (7.7 nmol/mg/min). After immediate formation of EP, the amount of EP_{slow} increased gradually, suggesting that EP_{slow} is converted from EP_{fast}. The increasing EP_{slow} fraction during the initial phase is consistent with the intial burst of Pi liberation. The ratio of the two components could be altered by changing $[Ca^{2+}]$. The conversion from EP_{slow} to EP_{fast} was inhibited by removing ADP, while the reverse conversion was not inhibited.

The fraction of EP_{slow} and the rate of decomposition, k_{slow}, were measured at various $[Ca^{2+}]$ and $[Mg^{2+}]$, pH, and temperatures. The fraction of EP_{slow} decreased at low $[Ca^{2+}]$ or high $[Mg^{2+}]$. k_{slow} decreased as $[Ca^{2+}]$ increased, but was unaffected by changes in $[Mg^{2+}]$. The fraction of EP_{slow} was minimal at pH 7.0, and k_{slow} decreased with an increase in pH. The fraction of EP_{slow} decreased with increasing temperature. Supported by USPHS (HL27867) and the Muscular Dystrophy Association of America.

T-Pos27 SR Ca-ATPase: AN ALTERNATIVE METHOD OF PURIFICATION. by Hector Barrabin, Helena Scofano and Giuseppe Inesi. (Intr. by D. Kosk-Kosicka) University of Maryland, School of Medicine, Department of Biological Chemistry, Baltimore, Maryland 21201.

Several methods based on selective protein solubilization with ionic detergents have been used to purify SR ATPase. We developed an alternative method of purification using non ionic detergents. SR vesicles were dissolved in $C_{12}E_8$, filtered through Millipore and passed through a DEAE cellulose column using a discontinuous NaCl gradient. The bulk of phospholipids and some contaminant proteins were eluted with 0.05 M NaCl. The Ca-ATPase protein was selectively eluted with 0.12 M NaCl. Increasing the ionic strength resulted in the elution of the other contaminant proteins. The purified ATPase presented only one band of 115K when submitted to polyacrylamide gel electrophoresis and one symmetrical peak when analysed by HPLC size exclusion chromatography.

The eluted ATPase has 10-15 mole of phospholipids/mol protein and low specific activity. The enzyme is then relipidated by incubation with phosphatidylcholine in the presence of detergent. After relipidation the specific activity attained was 19.5 ± 0.5 μmol Pi/mg protein min^{-1} (37°C, 10 mM ATP). The levels of phosphoenzyme obtained by phosphorylation with [γ-^{32}P]ATP or ^{32}P-Pi are 6.15 ± 0.40 and 7.30 ± 0.44 nmole E ~ P/mg protein respectively. The enzyme binds 14.2 ± 1.1 nmoles of calcium/mg protein. These values indicated that each 115 K polypeptide chain has one phosphorylation site and two calcium binding sites.

Advantages of this method of purification are: The short time of preparation, (2 hours) stability of the enzyme, and lack of inactive aggregates. Supported by USPHS (HL27867), Fogarty International Center, and Muscular Dystrophy Association of America.

T-Pos28 TRANSIENTS OF INTRINSIC FLUORESCENCE DURING THE TRANSPORT CYCLE OF SARCOPLASMIC RETICULUM ATPase. Francisco Fernandez-Belda, Mark Kurzmack and Giuseppe Inesi. Department of Biological Chemistry, University of Maryland School of Medicine, Baltimore, Maryland 21201.

Detection of intrinsic fluorescence transients in stopped-flow experiments allows monitoring the behavior of SR-ATPase during the transport cycle. For this purpose, fluorescence transients, enzyme phosphorylation, radioactive calcium displacement by lanthanum and Pi production were compared in rapid kinetic experiments using SR-vesicles, purified ATPase or solubilized enzyme.

A decrease in intrinsic fluorescence was observed following enzyme phosphorylation when ATP was added to enzyme preincubated with Ca^{2+} and was related to a change in the affinity and orientation of the calcium sites, independent of whether Ca^{2+} actually dissociated from the site. When substrate and Ca^{2+} were added to enzyme preincubated with EGTA a sequential relationship was shown between fluorescence rise and phosphoenzyme formation in appropriate experimental conditions.

The observations can be explained considering three states of different fluorescence level: a "low fluorescence" state of the enzyme in the absence of calcium and ATP, a "high fluorescence" state of the enzyme activated by calcium, and an "intermediate fluorescence" state of the enzyme with ATP bound or in the phosphorylated form with low affinity for calcium. The fluorescence transients and the final steady state level observed upon addition of ATP and calcium to the enzyme, are determined by the distribution of these enzyme states. Supported by USPHS (HL27867) and Muscular Dystrophy Association of America.

T-Pos29 THE RECONSTITUTED Ca^{2+}-ATPase FROM SARCOPLASMIC RETICULUM MEDIATES Ca^{2+}:nH^+ EXCHANGE: Theresa R. Byers (Intr. by Charles W. Carter, Jr.), Department of Biochemistry, University of North Carolina, Chapel Hill, NC 27514

The hypothesis that the Ca^{2+}-dependent ATPase from skeletal muscle sarcoplasmic reticulum catalyzes H^+ efflux during active Ca^{2+} uptake has been investigated using reconstituted proteoliposomes with defined permeability properties. Sarcoplasmic reticulum membrane is solubilized and reconstituted by hollow fiber dialysis in an excess of asolectin phospholipid. The small unilamellar vesicles prepared by dialysis are rapidly frozen, thawed and sonicated. Vesicles prepared by this technique are unilamellar, approximately 600A in diameter, contain an average of 3-5 ATPase molecules/vesicle, and support active Ca^{2+} uptake at an initial rate of 600 nmole Ca^{2+}/mg·min. Radioisotope efflux, the voltage-sensitive fluorescent dye, diO-C_5-(3), and the pH-sensitive flourescent dye, 8-hydroxy-1,3,6-pyrenetrisulfonic acid (pyranine), have been used to demonstrate that the time course of H^+ and K^+ equilibration across the membrane is slow compared with that of active Ca^{2+} uptake. The relative impermeability of these vesicles to small cations makes them suitable tools for the study of H^+ fluxes mediated by the Ca^{2+}-ATPase. Using entrapped pyranine to visualize pH changes, alkalinization of the vesicle interior has been observed upon addition of ATP to a proteoliposome suspension. Formation of this pH gradient can be prevented by a combination of the ionophores CCCP and valinomycin, but not by either ionophore alone. In addition, active uptake is maximally stimulated only if the vesicles are rendered permeable to both H^+ and K^+. These results suggest that the SR Ca^{2+} pump functions via a Ca^{2+}:nH^+ (n=1,2) exchange mechanism. (Supported by USPHS Grant AM 18687)

T-Pos30 TRANSMEMBRANE DISPLACEMENT OF THE CALCIUM ATPase IN THE SARCOPLASMIC RETICULUM MEMBRANE D.J.Scales[1] and S.R. Highsmith[2]. Depts. of Physiology[1] and Biochemistry[2], University of the Pacific, San Francisco, CA and Dept. of Biological Chemistry[1], University of Maryland, Baltimore, MD.

The native sarcoplasmic reticulum (SR) membrane is assembled asymmetrically as reflected in freeze fracture replicas. The Ca-ATPase appears only on concave fracture faces as a dense population of 9 nm particles. Corresponding depressions, or pits, on convex faces are never seen.

Recent studies have shown that vanadate binds rapidly to low affinity phosphate binding sites and stablizes the Ca-ATPase in a vanadate-enzyme structure. We find as soon as 15 minutes after the addition of vanadate that the enzyme aggregrates into two-dimensional arrays in the plane of the membrane. We also find the effects of vanadate to be completely reversible. When SR was incubated in 5 mM vanadate, 100 mM KCl, 0.5 mM EGTA, 10 mM Imidazole, pH7 solutions and then diluted into a buffer containing calcium, magnesium and ATP, the ATPase activity was normal for several hours and only somewhat reduced after 3 days.

Following vanadate treatment, convex fracture faces show pits for the first time. These pits are always aligned in rows and are never found in random arrangement. This suggests that the vanadate-ATPase complex moves in the transmembrane direction <u>after</u> alignment within the plane of the membrane.

We conclude that vanadate induces a spatial redistribution of the enzyme perpendicular to as well as in the plane of the membrane. The redistribution in the plane occurs first. This work was supported by N.I.H. grants 1-PO-1-HL27867, AM25177 and AM00509.

T-Pos31 OXIDATION IN SARCOPLASMIC RETICULUM. Nancy M. Scherer and David W. Deamer, Department of Zoology, University of California, Davis, CA 95616.

We have used several oxidants (O_2, iron/ascorbate, H_2O_2, $(NH_4)S_2O_8$) to investigate oxidation effects on functional parameters of isolated sarcoplasmic reticulum microsomes. Lipid peroxidation does not appear to be responsible for enzyme inhibition at the level of oxidation used in these experiments. Ca^{2+}-ATPase activity was greatly reduced or abolished when less than 1% of the total lipid was reactive with TBA. The degree of lipid peroxidation did not correlate well with changes in Ca^{2+}-ATPase activity, ^{45}Ca transport or the rate of ^{45}Ca efflux. The lack of effect of lipid in altering enzyme activity was supported by observations that exchange of lipoxidase-damaged lipid for lipid in undamaged SR or undamaged lipid for lipid in oxidized SR had little or no effect on Ca^{2+}-ATPase activity. Furthermore, several lipid antioxidants, including Mn^{2+}, α-tocopherol, mannitol, thiourea, propyl gallate, BHT or DMF did not prevent oxidative inhibition of the Ca^{2+}-ATPase. However, the SH reducing agents DTT, glutathione and mercaptoethanol did prevent inhibition of the Ca^{2+}-ATPase, even though modest lipid peroxidation occurred. DTT also activated Ca^{2+}-ATPase activity, ^{45}Ca transport and reduced the rate of ^{45}Ca efflux in undamaged SR. These data suggest that inhibition occurs by oxidation of an "essential" SH group in the Ca^{2+}-ATPase. This is supported by a decline in SH content, measured by DTNB, which parallels the decline in Ca^{2+}-ATPase activity and ^{45}Ca transport. In most cases, the oxidation of the SH group(s) was not reversible, as addition of reducing agents after SR was exposed to the oxidant typically did not reactivate the enzyme. This indicates that oxidation probably does not involve the formation of disulfides, but rather higher oxidation states. Supported by NSF grant PCM 80-01953 and a Jastro Shields grant from UCD.

T-Pos32 FLUORESCENCE STUDIES OF ATPase INTERACTIONS IN SARCOPLASMIC RETICULUM. George R. Kracke and Anthony Martonosi, Dept. of Biochemistry, SUNY Upstate Medical Center, Syracuse, N. Y. 13210

Interactions between ATPase molecules in sarcoplasmic reticulum (SR) have been studied by measuring the effects of detergents on the excimer fluorescence of pyrenemaleimide (PM) covalently bound to the Ca^{2+}-ATPase, essentially as described by Ludi and Hasselbach (Eur. J. Biochem. 130, 5-8, 1983). The excimer fluorescence in PM labeled SR is probably due to the intimate association of ATPase molecules into oligomers and this association is sensitive to detergents. The ability of zwitterionic detergents (Zwittergent 3-08, 3-10, 3-12, 3-14, 3-16) to abolish excimer fluorescence is a function of alkyl chain length. Zwittergent 3-08, with an 8 carbon hydrophobic tail, had no effect on the excimer fluorescence at concentrations up to 2 mg/ml, whereas Zwittergent 3-16, with a 16 carbon tail, almost entirely abolished excimer fluorescence at a concentration of 0.03 mg/ml; the effectiveness of Zwittergents of intermediate chain length, fell in between. Lysolecithin, SDS and deoxycholate markedly decreased excimer fluorescence at 0.1 mg/ml: $C_{12}E_8$, Brij 35, Triton X-100 and octylglucoside had only slight effect, even at 1 mg/ml concentrations. Increasing the molar ratio of PM/ATPase from 1:1 to 2:1 during labeling slightly increased the ratio of excimer fluorescence to that of the monomer. Fluorescence energy transfer was demonstrated between the protein tryptophan residues and the bound pyrenemaleimide. With Zwittergents of increasing chain lengths the inhibition of excimer fluorescence is paralleled by inhibition of Ca^{2+} dependent ATPase activity and the solubilization of microsomal proteins. $C_{12}E_8$ and octylglucoside do not significantly inhibit excimer fluorescence even at concentrations that solubilize microsomes and inhibit ATPase activity. (Supported by the NIH and the Muscular Dystrophy Association).

T-Pos33 H^+ ARE NOT COUNTER TRANSPORTED DURING ATP-DEPENDENT Ca^{++} UPTAKE BY SARCOPLASMIC RETICULUM VESICLES (SR). G. Salama and A. Scarpa, Dept. of Physiology, U. of Pittsburgh, Sch. of Medicine, Pgh, PA 15261 and Dept. of Biochem./Biophys., U. of PA, Phila. PA 19104.

The occurrence of either an obligatory or passive H^+ efflux during ATP-dependent Ca^{++} uptake by SR isolated from rabbit white skeletal muscle was investigated by spectrophotometric and polarometric techniques. The magnitude and time course of H^+ release and Ca^{++} uptake by SR were simultaneously recorded in a magnetically stirred cuvette with a fast-response pH electrode and arsenazo III (at 675-685 nm) respectively. Three protocols were designed to minimize and/or account for the acidification of the medium related to ATP hydrolysis rather than that due to net H^+ translocation across SR membranes. a) the magnitude and rate of acidification of the medium following ATP addition in intact SR was compared with that of lysed SR. The ratio of H^+ translocated to Ca^{++} taken up was measured at various ATP and SR concentrations at pH 7.0 with intact SR and SR lysed with various detergents. b) the ratio of H^+ release and Ca^{++} uptake was measured at various pH values, under conditions where different net pH changes occurred upon ATP hydrolysis. c) A fast ATP-regenerating system was used to maintain constant ATP concentration in the medium such that acidification attributable to ATP hydrolysis was negligible at pH 7.0 in the presence of SR or apyrase. The results obtained with the above protocols in 100 m HCl or 200 mM sucrose buffers indicate that there is no obligatory H^+ counter-transport, nor does H^+ efflux significantly balance the positive charge influx during ATP-dependent Ca^{++} uptake by SR. Supported by NIH NS 18590 and by AHA 821231.

T-Pos34 Mg^{++} PERMEABILITY OF SARCOPLASMIC RETICULUM VESICLES (SR); Mg^{++} IS NOT TRANSPORTED AS A COUNTERION DURING ATP-DEPENDENT Ca^{++} UPTAKE. G. Salama and A. Scarpa. Dept. of Physiol., U. of Pittsburgh, Pgh., PA 15261, and Dept. of Biochem./Biophys., U. of PA, Phila., PA 19104.

The Mg^{++} permeability and the counter-transport of Mg^{++} during ATP-dependent Ca^{++} uptake was investigated in SR isolated from rabbit white skeletal muscle with spectrophotometric techniques. The magnitude and time course of passive Mg^{++} efflux was recorded from Mg^{++}-loaded SR through the absorption changes of Antipyrylazo III or Arsenazo I at 575-600 nm. The half-time of passive Mg^{++} efflux from SR loaded with 2 to 20 mM Mg^{++} was 100 s in 100 mM KCl, 150 s in 100 mM KGluconate, and 370 s in either 100 mM Tris-Methanesulfonate or 200 mM sucrose buffers. The magnitude and time course of Mg^{++} released in the medium was measured during ATP-dependent Ca^{++} uptake monitored with Arsenazo I. Three experimental protocols were used to determine whether the increase in Mg^{++} in the medium was caused by Mg^{++} liberated from the hydrolysis of ATP or by the translocation of Mg^{++} from inside to outside. 1. After the addition of various concentrations of ATP to initiate Ca^{++} uptake, the rate and extent of Mg^{++} released was compared with that obtained from SR lysed with Triton X-100. 2. Mg^{++} released during ATP-dependent Ca^{++} uptake by SR was compared with that released during similar rates of ATP hydrolysis catalysed by apyrase. 3. Fast ATP-regenerating systems were used to maintain a constant ATP to ADP ratio, normal Ca^{++} uptake but no release of Mg^{++} in the medium. The results indicate that Mg^{++} is about 10 times more permeable than Ca^{++} and is not counter-transported during active Ca^{++} uptake even in reaction mixtures containing low (contaminating concentrations) of the more permeable ions: K^+, Na^+, and Cl^-. Supported by NS 18590 and AHA 821231.

T-Pos35 MOLECULAR INTERACTIONS IN IONENE-PHOSPHATIDYLGLYCEROL MIXTURES. D.A.Wilkinson, A.B.Turek, D.A.Tirrell, & S.D.Merajver. Departments of Physics and Chemistry, Carnegie-Mellon University, Pittsburgh, PA and Biophysics Research Division, University of Michigan, Ann Arbor, MI.

The gel to liquid crystalline transition of dipalmitoyl phosphatidylglycerol (DPPG) at pH 7.4 and the effects on this transition by ionenes (antibacterial polycations) and divalent cations have been studied by differential scanning calorimetry and dilatometry and by Raman spectroscopy. DPPG alone melts at T_m=41.2°C with a ΔH=9.96±0.18 kcal/mole and a ΔV=0.051±0.002 ml/g. The van der Waals interaction contribution derived from ΔV is 6.9± 0.3 kcal/mole. From the Raman spectra the rotameric contribution to ΔH is 2.64± 0.20 kcal/mole. Mixtures of DPPG with excess ionenes show that T_m varies inversely with polymeric charge density but is unaffected by the MW of the polymer in the range 3500 to 16000. At lower concentrations, ionene-6,10 (lowest charge density examined) induces phase separation between pure DPPG and a polymer-DPPG complex. Low MW di-ammonium analogues of ionene-6,10 appear unable to mimic the effect of the polymer. Mg^{++} raises T_m to 51°C but this effect is completely reversed by ionene-6,10. Ca^{++} increases T_m even more but addition of ionene-6,10 fails to reverse the effect completely (i.e. an ionene-lipid and Ca^{++} -lipid complexes are both present).

T-Pos36 INHIBITION OF AND DEHYDRATION-INDUCED FUSION BETWEEN LIPOSOMES BY A CARBOHYDRATE, Christopher Womersley, Paul Uster, Alan Rudolph & John Crowe (University of California, Davis).

Certain carbohydrates, particularly trehalose, are known to inhibit freezing and dehydration induced damage to biological membranes. We have studied the possibility that such carbohydrates inhibit fusion during freezing and dehydration, using fluorescence resonance energy transfer and freeze fracture as assays for the degree of membrane intermixing. Phosphatidyl serine:phosphatidyl choline (15:85) small unilamellar vesicles (SUV's) were frozen rapidly in liquid nitrogen, and allowed to thaw at room temperature. The extent of fusion (as measured by the quenching of donor probe fluorescence due to intermixing with the acceptor probe) was approximately 20%. Subsequent addition of trehalose up to a concentration of 1 g trehalose/g lipid had no effect on the freezing induced fusion during a single freeze-thaw cycle. Storage of frozen SUV's at -20°C without trehalose for 18 and 24 hours increased fusion to 60 and 70% respectively. Addition of trehalose (4 g/g) reduced this fusion by about 10%. Subjecting the SUV's to multiple freeze-thaw cycles reduced fusion in subsequent freezing trials to less than 5%. We suspect that this effect is due to the susceptibility of SUV's to mechanical stresses during freezing due to their acute radius of curvature; thus repeated freezing and thawing leads to the production of large unilamellar vesicles (LUV's) which are less susceptible to freezing damage. Lyophilization of both SUV's and LUV's resulted in nearly 100% fusion of the vesicles. Addition of trehalose in increasing concentration resulted in a decrease in fusion; complete inhibition was achieved at about 0.5 g trehalose/g lipid. We suggest that this technique may be useful for storage of liposomes for research and clinical applications. (Supported by NSF Grant PCM 82-17538 and National Sea Grant Ra/47.)

T-Pos37 A SPIN LABEL STUDY OF THE HYDROCARBON REGIONS OF DETERGENT PRODUCED PHOTOSYSTEM II PREPARATIONS FROM SPINACH THYLAKOIDS. Steven P. Berg and Charlene Waggoner, Department of Biological Sciences, University of Denver, Denver, Colorado 80208 and L. Andrew Staehelin, Department of Molecular, Cellular and Developmental Biology, University of Colorado, Boulder, Colorado.

A number of new methods for preparing oxygen evolving Photosystem II preparations have recently been published. These preparations are now being widely employed in studying the enzymology of oxygen evolution. We have concentrated our efforts on comparing the physical and biochemical properties of several of these preparations, in the hope that this information would be helpful in interpretting the oxygen evolution studies, and also that the information would be useful in understanding membranes in general.

We report here the use of a variety of spin labels, including 2,2,6,6-tetramethylpiperidine-N-oxyl (Tempo), 2-heptyl-2-hexyl-5,5-dimethyloxazolidine-N-oxyl (7N14), and 5-12-16-doxylstearic acids, to probe the lateral and transverse heterogeneity in hydrocarbon fluidity in several different oxygen evolving Photosystem II preparations. These preparations consistently demonstrate far greater spin label immobilization than do thylakoid membranes or vesicles prepared from the polar lipids extracted from thylakoids. This is presumably due to the high protein/lipid ratio present in most of these Photosystem II preparations. The high prote-n/lipid ratios in the Photosystem II preparations produced by detergent extraction may be due to detergent induced lipid depletion of the membranes. Curiously, however, when examined by freeze fracture electron microscopy, the protein complexes visible in the Photosystem II preparations do not appear closer together then they do in thylakoid membranes.

T-Pos38 THEORY FOR THE BINDING OF DIVALENT AND MONOVALENT CATIONS TO 2-COMPONENT PHOSPHOLIPID MEMBRANES. Michael Cohen and Joel A. Cohen. Dept. of Physics, Univ. of Pennsylvania, Philadelphia, PA 19104 and Dept. of Physiology, Univ. of the Pacific, San Francisco, CA 94115.

We previously treated the problem of divalent- and monovalent-cation adsorption by single-component charged phospholipid membranes, where the divalent cations adsorb with ion:phospholipid stoichiometries of 1:1 and/or 1:2, monovalent cations adsorb with a stoichiometry of 1:1, and divalent and monovalent cations either compete or do not compete for membrane binding sites [Biophys. J. 36 (1981), 623]. We now generalize this treatment to the case of membranes comprised of two kinds of phospholipids. The two phospholipid components are present at arbitrary mole fractions X and Y = 1-X. The phospholipids are assumed mobile and free to permute into the thermodynamically most favorable arrangement under any given ionic conditions. Since the X and Y sites rearrange upon divalent-cation binding, the numbers of XX pairs, XY pairs, and YY pairs on the lattice are not constant. The strengths of 1:2 divalent-cation binding to the 3 kinds of phospholipid pairs are given by the association constants K_{XX}, K_{XY}, and K_{YY}, respectively, and the strengths of 1:1 divalent-cation binding to X and Y sites are given by K_X and K_Y, respectively. By use of statistical mechanics we can calculate the number of bound complexes of each type on the membrane at equilibrium. That is, if D denotes a bound divalent cation, we can find the number of each of the complexes D_{XX}, D_{XY}, D_{YY}, D_X, and D_Y. The solution is given in terms of the solution to the previous problem of divalent-cation binding to single-component membranes. Monovalent-cation binding is readily included.

T-Pos39 THERMOTROPIC BEHAVIOR OF AQUEOUS DISPERSIONS OF PHOSPHOLIPID-CHOLESTERYLHEMISUCCINATE AND PHOSPHOLIPID-TOCOPHEROL HEMISUCCINATE MIXTURES. Ming-Zong Lai, Francis C. Szoka, Jr., and Nejat Düzgüneş. Dept. of Pharmacy and Pharmaceutical Chemistry and the Cancer Research Institute, University of California, San Francisco, CA 94143.

Differential scanning calorimetry has been used to characterize the influence of cholesteryl-hemisuccinate (CHEMS) and tocopherol-hemisuccinate (THEMS) on the phase transition of 1,2-dimyristoyl-3-sn-phosphatidylethanolamine (DMPE) and 1,2-dipalmitoyl-3-sn-phosphatidylcholine (DPPC) multilamellar dispersions at pH 7.4. The addition of 5 mole% CHEMS to DMPE reduces the transition temperature and significantly broadens the width of the endotherm. The sharp transition disappears upon the incorporation of 20 mole% CHEMS and at 50 mole% CHEMS the transition becomes so broadened as to be undetectable. At 35 mole% CHEMS the peak transition temperature is depressed from 48.6±0.5°C (DMPE) to 36±3°C and the enthalpy of the transition (6.5±0.3 Kcal/mol, DMPE) is reduced to 1.1±0.3 Kcal/mol. The addition of THEMS (10 mole%) reduces the peak transition temperature and asymmetrically broadens the transition, with the peak maximum at the high temperature end of the transition. Between 30 and 90 mole% THEMS, little additional change in transition width or shape occurs although the peak transition temperature is progressively reduced to 9°C at 80 mole% THEMS. This suggests that a THEMS-phospholipid complex is forming. Analogous results were obtained when the compounds were mixed with DPPC. A unique aspect of these compounds is that they can form mixtures with the phospholipids up to a derivative/phospholipid ratio of 9/1. Supported by NIH Grants GM29514, GM30163, GM28117.

T-Pos40 THE LECITHIN SURFACE BILAYER IS IN A STATE OF UNIFORM COMPOSITION. N. L. Gershfeld and K. Tajima*, LPB/NIADDK, National Institutes of Health, Bethesda, MD 20205.

Phospholipid dispersions in water form a bilayer at the equilibrium air-water surface (Gershfeld, N. L. and Tajima, K., Nature 279, 707[1979]). This surface bilayer is characterized by a maximum in the surface pressure-temperature phase diagram of the equilibrium dispersion. From the Gibbs equation for the surface film, and the Gibbs-Duhem equation for the equilibrium liquid crystal phase of the dispersion, a relation is derived for the surface pressure $\pi_e = \pi_e(T,p,\mu_i)$. At the temperature of surface bilayer formation, where the surface pressure is a maximum this relation indicates that the composition of the surface bilayer is identical to the composition of the liquid crystal phase in the dispersion. Experimental verification of this condition has been obtained with mixed dispersions of DMPC and DOPC that have been labeled with tritium, where the individual contributions of each lipid to the equilibrium surface film have been obtained as a function of temperature. At the temperature of surface bilayer formation the composition of the surface film equals that of the liquid crystal phase of the dispersion; but at temperatures above and below this temperature, the surface and bulk phase compositions differ significantly. Thus, the surface bilayer is in a state of uniform composition, and therefore shares thermodynamic properties with other states of uniform composition such as azeotropes (constant boiling mixtures). Like azeotropes the surface bilayer exists at a singularity in temperature. This confirms the results of recent studies that the barrier for water permeability across the surface bilayer exists only at the temperature of surface bilayer formation (L. Ginsberg and N. L. Gershfeld Biophys. J. 41, 357a[1983]).

*Present address: Tokyo Metropolitan University, Tokyo, Japan.

T-Pos41 RAMAN SPECTROSCOPIC STUDY OF THE INTERACTION OF POLY-L-LYSINE WITH DIPALMITOYLPHOSPHATIDYLGLYCEROL BILAYERS. Danielle Carrier and Michel Pézolet. Département de chimie, Université Laval, Québec (Québec) Canada G1K 7P4

The interaction of the basic polypeptide de poly-L-lysine with the negatively charged phospholipid dipalmitoylphosphatidylglycerol was studied using Raman spectroscopy. The nature of the interaction appears to depend on the molar ratio of the constituants. At up to one lysine group per lipid molecule, the bilayer is stabilized by the polypeptide that undergoes a conformational transition toward an ordered α-helical structure in which the electrostatic interactions are probably maximal. The stabilization of the bilayer is detected by both an increase of the temperature of the thermotropic transition of the lipid and of the inter-chain vibrational coupling of the methylene C-H vibrations. At higher poly-L-lysine concentration, hydrophobic interactions must be involved to explain the binding of excess of polypeptide. There seems to be a penetration of poly-L-lysine in the bilayer that increases with the polypeptide concentration. Under these conditions, the chain packing lattice gradually changes from hexagonal to either orthorhombic or monoclinic symmetry. We believe that this change of structure is associated with the interdigitation of the acyl chains.

T-Pos42 THERMOTROPIC BEHAVIOR AND NEURAMINIDASE ACTIVITY IN PHOSPHATIDYLCHOLINE BILAYERS CONTAINING GANGLIOSIDES Gd_{1a} AND Gt_{1b}. M. Myers, C. Wortman and E. Freire, Department of Biochemistry, University of Tennessee, Knoxville, TN 37996-0840

High sensitivity differential scanning calorimetry and steady state fluorescence spectroscopy have been used to study the thermotropic behavior of large unilamellar dipalmitoyl phosphatidylcholine vesicles containing the disialoganglioside Gd_{1a} and the trisialoganglioside Gt_{1b} on their outer surface. Experiments designed as a function of the ganglioside molar fraction and Ca^{2+} concentration indicate that both gangliosides have an ordering effect on the hydrocarbon portion of the bilayer which is enhanced by the presence of Ca^{2+} ions. Calorimetric studies also indicate that ganglioside Gt_{1b} tends to phase separate into compositional rich ganglioside domains in the absence of Ca^{2+}. Ca^{2+} concentrations of 10 mM or greater are necessary to induce a similar effect with ganglioside Gd_{1a}. Knowing this, we have been able to identify and evaluate factors affecting the rates of hydrolysis of gangliosides by the soluble neuraminidase of Clostridium perfringens and relate them to the physical state of the membrane and the state of aggregation of the ganglioside within the lipid bilayer. The data with membrane bound ganglioside indicate maximal activation energies at temperatures slightly lower than the lipid phase transition temperature. Additional studies with the soluble substrate sialyllactose and with micellar gangliosides indicate that the rates of hydrolysis of these substrates are independent of Ca^{2+} while those of membrane bound gangliosides are inhibited by Ca^{2+}. This suggests a preference of the soluble neuraminidase for dispersed ganglioside substrates rather than those forming part of largely aggregated clusters. (Supported by NIH Grant GM-30819.)

T-Pos43 HEAT SENSITIVE IMMUNOLIPOSOMES: PREPARATION AND CHARACTERIZATION. S.M. Sullivan and L. Huang, Dept. of Biochemistry, Univ. of Tennessee, Knoxville, TN 37996-0840.

We have prepared liposomes capable of binding to the target cell surface and releasing entrapped contents by brief heating. Fused dipalmitoylphosphatidylcholine (DPPC) unilamellar liposomes (FUVs) were prepared by the method of Wong et al. (Biochem. 21(1982), 4126). Monoclonal anti-$H2K^k$ was derivatized with palmitic acid by the method of Huang et al. (BBA 716(1982), 140). The palmitoyl antibody (pAb) was injected into a temperature regulated liposome suspension at a controlled rate (0.2 to 2 µl/min). The final protein to lipid ratio was dependent upon rate of injection and, to a lesser extent, on the physical state of the bilayer. Injection of pAb into a FUV suspension containing 50 mM carboxyfluorescein (CF) at 41°C resulted in simultaneous antibody incorporation and entrapment of dye. Liposomes with or without incorporated antibody exhibited very similar dye release properties with respect to temperature and osmolarity of the external medium. Release of dye at temperatures between pre- and main transition temperatures of DPPC was abolished by addition of calf serum (5%). This also resulted in a small increase in the maximal release temperature along with an increased rate of release. These immunoliposomes specifically bound to the target cells below the phase transition temperature of DPPC. Rapid release of the entrapped dye from bound liposomes was achieved upon brief (less than 3 minutes) exposure of cells at 41°C. These heat sensitive immunoliposomes may be useful in enhancing drug delivery to target cells. (Supported by NIH Grant CA-24553.)

T-Pos44 LIPID-CHOLESTEROL BILAYERS. COMPUTER SIMULATION STUDIES.

T. Lookman,* D.A. Pink,* M.J. Zuckermann† and N. Jan.*

We have studied the equilibrium properties of a model of a DMPC or DPPC bilayer containing cholesterol. We have represented lipid hydrocarbon chain states by an extension of a multi-state model used before, (e.g. Pink, Can. J. Biochem. (1984)), and cholesterol as a single-state system. Both "chains" and "cholesterol" occupy the sites of a triangular lattice and may move from site to site. We have used Monte Carlo methods, making use of both Glauber and Kawasaki dynamics to study the dependence of specific heat, enthalpy and other thermodynamic quantities upon cholesterol concentration.

We shall present a phase diagram together with an analysis of the dynamics which may be giving rise to a number of "peaks" in specific heat measurements.

* Theoretical Physics Institute, St. Francis Xavier University, Antigonish, N.S. Canada, B2G 1C0.

† Physics Dept. McGill University, 3600 University St., Montreal, P.Q. Canada, H3A 2T8.

Work supported by NSERC of Canada.

T-Pos45 RAMAN SPECTROSCOPIC STUDY OF THE MELTING BEHAVIOR OF ANHYDROUS DIPALMITOYL PHOSPHATIDYLCHOLINE (DPPC) BILAYERS. Timothy J. O'Leary and Ira W. Levin, Laboratory of Chemical Physics, NIADDK, National Institutes of Health, Bethesda, MD 20205.

The temperature dependence of the Raman spectra of anhydrous, polycrystalline DPPC was investigated in the 0° to 108°C temperature range. For this temperature interval, spectra of the C-H and C=O stretching mode regions reflect a significant lateral expansion of the lipid matrix and an increased motion of the sn-2 chain within the bilayer interface region, respectively. In the 100-108°C range, a cooperative phase transition occurs in which further lateral expansion of the bilayer is accompanied both by an increased number of gauche rotamers within the hydrocarbon chain region and by multiple conformers in both the headgroup and glycerol backbone moieties. When the polycrystalline samples are rapidly cooled, the acyl chain region reorders without a concomitant reordering of the headgroup and interface regions. For these samples the spectral features characteristic of the lipid headgroup and interface segments are similar to those of hydrated bilayers. With the exception of specific interface and headgroup region changes, which are caused directly by the addition of water in contrast to the temperature induced melting of hydrated bilayers, the melting behavior of anhydrous lipid systems is analogous to the completely hydrated dispersions. The spectral changes accompanying the melting of polycrystalline DPPC bilayers demonstrate the usefulness of investigating anhydrous lipid systems in understanding structural changes characteristic of hydrated systems, in clarifying the role of water in determining membrane bilayer organizations, and in assisting in the vibrational assignment of specific spectral features representative of liposomal dispersions.

T-Pos46 PALMITYL CARNITINE: PHASE DIAGRAM IN WATER AND INFLUENCE ON MEMBRANE STRUCTURE. R.H. Stinson. Biophysics Interdepartmental Group, Physics Department, University of Guelph, Guelph, Ontario, Canada, N1G 2W1.

Carnitine plays a necessary role in the transport of fatty acids into the mitochondrion. While much of the biochemistry of the process has been worked out, the actual physical process of transfer has not been investigated. A phase diagram of palmityl carnitine as a function of water content and temperature shows regions of lamellar, hexagonal and cubic structure. The presence of relatively small amounts (5% w/w) of palmityl carnitine can cause significant changes in the thickness and structure of model membrane structures, when investigated with X-ray diffraction. In general, addition of palmityl carnitine to DPPC/H_2O systems or DPPC/cardiolipin/H_2O systems results in increased disorder and reduction of bilayer thicknesses of about 15%.

T-Pos47 CARBOHYDRATE-PHOSPHOLIPID INTERACTIONS, John H. Crowe, Lois M. Crowe, Mary A. Whittman, & Dennis Chapman (University of California, Davis and Royal Free Hospital Medical School, London). Trehalose, a carbohydrate found at high concentrations in organisms capable of surviving dehydration, stabilizes dry biological membranes, a property shown to less extent by other carbohydrates. Interaction between lipids and carbohydrates has been investigated in the present studies. (1) Calorimetric studies on DPPC dried with carbohydrates show that without the carbohydrates T_c is elevated by ca. 30° K. With trehalose, T_c decreases with increasing trehalose concentration until at the highest trehalose concentration T_c is < that for hydrated DPPC. Similarly, ΔH increases with trehalose concentration. Other carbohydrates depress T_c of dry DPPC, but not nearly so much as does trehalose. (2) Monolayer preparations of DPPC spread on aqueous surfaces with carbohydrates in the subphase show that trehalose decreases packing density of the lipids. The other carbohydrates tested do likewise, but to less extent than does trehalose. Unlike some molecules known to expand monolayers by intercalating between head groups, trehalose expands even fully condensed monolayers. (3) Infrared spectroscopy suggests that the interaction between DPPC and carbohydrates is probably by means of hydrogen bonding between -OH groups of the carbohydrate and the phosphate head group; in the presence of trehalose the OH deformation and P=O asymmetric stretching bands are depressed, broadened, and shifted in frequency. The apparent strength of the interaction can be evaluated from the integrated intensity of the P=O asym. str. in DPPC. The strength of this interaction between DPPC and various carbohydrates (assessed with DSC, monolayers, and IR) is correlated with the ability of the same carbohydrates to preserve dry membranes. (Supported by NSF grant PCM 82-17538 and Sea Grant RA/47).

T-Pos48 PHASE PROPERTIES, INCLUDING SUBTRANSITIONS, AND PERMEABILITY CHARACTERISTICS OF PHOSPHATIDYLCHOLINE BILAYERS. Michael Singer, Medicine, Queen's Univ., Kingston, Ontario, Canada K7L 3N6 and Leonard Finegold, Physics, Drexel Univ., Philadelphia, PA., U.S.A. 19104

Aqueous dispersions of C14, C16, C17, and C18 phosphatidylcholines (PC, where Cn denotes diacyl of n carbons per chain), and mixtures of C14/C16 PC and C16/C17 PC were prepared and their thermal properties studied by d.s.c. after sample storage at 2-6°C for up to 22 days. C16 PC and C18 PC display subtransitions at 22°C and 29°C respectively as previously reported by Chen et al (Proc. Nat. Acad. Sci. USA 1980, 77:5060). C17PC shows two subtransitions at 21° and 26° respectively which are independent of each other. Although C16 and C17PC individually develop subtransitions, an equimolar mixture does not. Similarly, mixtures of C14/C16PC containing 10 or more mol % of C14PC do not display a subtransition. Efflux measurements in vesicles of C16 or C17PC prepared and stored under similar conditions reveal a) that the subgel phase has a very low permeability to ions and b) that the transition from subgel to gel phase may result in small but definite local permeability maxima at temperatures close to that observed by d.s.c. These results underscore 1) the primary dependence upon acyl chain structure of subtransition formation in phosphatidylcholine dispersions, 2) that the "crystalline" packing of the subgel phase acts as an effective barrier to ions, 3) subtransitions may be shown by permeability as well as d.s.c. measurements.

T-Pos49 IMPURITY EFFECTS ON THE PHASE BEHAVIOR OF LARGE, UNILAMELLAR VESICLES: R. A. Parente, and B.R. Lentz, Biochemistry Department, University of North Carolina, Chapel Hill, NC 27514.

Large, unilamellar vesicles (LUV) have been prepared by three procedures from several synthetic phosphatidylcholines. Reverse phase evaporation vesicles (REV) and fusion vesicles were prepared by established procedures. A published procedure for preparation of dialyzed octylglucoside vesicles (DOV) was modified to allow its use with synthetic phospholipids.

Negative staining and freeze-fracture electron microscopy were used to determine the vesicle size distribution (mean diameters 800 to 1000 Å) and extent of oligolamellar contamination in DOV preparations. Trapping of 6-carboxyfluorescein yielded measurements of internal volume (2.6±0.3μL/ μmol P_i) consistent with the size distributions determined by electron microscopy. An upper limit of less than 3 mol % oligolamellar vesicle contamination was indicated by calorimetric heat capacity profiles.

The phase behaviors of large, multilamellar vesicles and all three types of LUV were compared using high sensitivity differential scanning calorimetry. The most remarkable feature was the increased breadth of the main transition of DOV and of REV preparations relative to the multilamellar species and to fusion vesicles. Both the main and pre-transitions occurred at nearly the same temperatures in unilamellar and multilamellar species, but the unilamellar pre-transition involved less than half the enthalpy observed in the multilamellar transition. Control experiments indicated that the broadened main phase transition associated with DOV and REV preparations reflected bilayer impurities resulting from preparatory procedures. It is concluded that LUV prepared by procedures that avoid impurities undergo a highly cooperative phase transition, as demonstrated here for fusion vesicles. Supported by NSF, PCM-79-22733.

T-Pos50 CATION DEPENDENCE OF THE HYDRATION FORCE BETWEEN PHOSPHATIDYLCHOLINE BILAYERS, Wai Meng Kwok and L. J. Lis, Physics Dept., Kent State University; and J. M. Collins, Physics Dept., Marquette University.

We have used multiamellar arrays of phosphatidylcholine to study the effects of both cation species and concentration on the hydration force acting beteen lipid surfaces. The osmotic pressure technique of Rand and Parsegian (LeNeveu, et al, 1976, Nature 269: 601-603) and x-ray diffraction provided net repulsive pressure versus lamellar separation data for the same lipid in different salt solutions. Our initial results indicate that monovalent cations affect the force character between lipid surfaces in a manner different from that observed between mica surfaces (R. M. Pashely, 1981, J. Coll. Interface Sci. 80: 153-162); emphasizing the difference between molecularly heterogeneous and crystalline surfaces. Specifically we found a consistent decrease in the net repulsive force between dipalmitoylphosphatidylcholine bilayer surfaces as the concentration of the monovalent cation increased in solution. The effect of divalent cations on the hydration force shows a more complex behavior due to the appearance of the repulsive electrostatic force.

T-Pos51 RAMAN SPECTROSCOPIC STUDY OF CYCLOPENTANOID ANALOGUES OF DIPALMITOYL PHOSPHATIDYLCHOLINE MULTILAMELLAR DISPERSIONS. William H. Kirchhoff,[a] Anthony J. Hancock[b] and Ira W. Levin,[a] [a]Laboratory of Chemical Physics, NIADDK, NIH, Bethesda, MD 20205 and [b]Dept. of Chemistry, University of Missouri, Kansas City, MO 64110.

The thermotropic behavior of four cyclopentanoid analogues of dipalmitoyl phosphatidylcholine (DPPC) as hydrated multilamellar dispersions has been investigated by Raman spectroscopy in both the C-C stretching (1000-1200 cm^{-1}) and C-H stretching (2800-3100 cm^{-1}) mode regions. Since these analogues differ from DPPC in that they are derived from diastereoisomeric cyclopentane-1,2,3-triols, the resulting rigidity about the glycerol backbone is expected to affect the packing and conformational properties of both the crystalline material and fully hydrated bilayer dispersions. These differences are manifest particularly for the polycrystalline samples in spectra reflecting the structural properties of the headgroup, interface and acyl chain regions, respectively. Temperature profiles of the multilamellar dispersions indicate broader phase transition intervals in comparison to normal DPPC bilayers. Preliminary analyses indicate that the contributions of headgroup conformations to the phase transition enthalpies, which range from 7.8 to 19 kcal/mole, are significant. Further, the cyclopentanoid phosphatidylcholine derivatives exhibiting the greater acyl chain order in the gel phase, as defined by the C-H stretching mode interval, yield the higher enthalpies (∿18-19 kcal/mole) for the gel to liquid crystalline phase transition.

T-Pos52 INVERTED MICELLAR INTERMEDIATES AND THE TRANSITIONS BETWEEN LAMELLAR, CUBIC, AND INVERTED HEXAGONAL AMPHIPHILE PHASES

D. P. Siegel, Procter & Gamble Co., P. O. Box 39175, Cincinnati, OH 45247

A theory of the lamellar-to-inverse hexagonal phase transition is proposed. This transition can occur via two routes, one of which was suggested by Hui et. al. (1). When the lipid headgroups are poorly-hydrated and the lamellae can be easily apposed, line defect (1) formation is facile. These line defects represent H_{II} tubes or halves of H_{II} tubes lying parallel to the plane of the apposed bilayers: they aggregate sideways into H_{II} rod assemblies rapidly. $L \leftrightarrow H_{II}$ transitions in such lipids systems are rapid and comparatively non-hysteretic. When the lamellae are better-hydrated and close apposition of large areas of bilayer is rare, inverted micellar intermediates (IMI, (2)) form between the bilayers. IMI aggregate end-on into H_{II} rod precursors slowly. $L \leftrightarrow H_{II}$ transitions in such systems are slower and hysteretic, and can exhibit ^{31}P-NMR resonances because of the presence of micellar aggregates with small interfacial radii of curvature. IMI are also likely to be the first inverted-geometry structures formed when small bilayer vesicles are apposed. Finally, if the rate of IMI aggregation into H_{II} rods is nearly zero, it is shown that lamellar phases will form arrays of IMI that have the attributes of the cubic phase studied by others (1). The cubic phase is probably the product of a frustrated $L \leftrightarrow H_{II}$ transition.

1) S. W. Hui, T. P. Stewart, L. T. Boni, Chem. Phys. Lipids 33 113 (1983).
2) D. P. Siegel, Biophys. J. (in press).

T-Pos53 PHASE SEGREGATION BEHAVIOR OF PE/PS & PC/PS UPON ADDITION OF Ca^{++} OR CHOLESTEROL.
C.P.S. Tilcock, M.B. Bally, S.B. Farren and P.R. Cullis, Dept. of Biochem., Univ. of British Columbia, Vancouver V6T 1W5, Canada, and S.M. Gruner, Dept. of Physics, Princeton Univ. Princeton, NJ 08540.

The phase behaviors of mixtures of synthetic phosphatidylethanolamine (PE), phosphatidylcholine (PC) and phosphatidylserine (PS) have been examined via ^{31}P and ^{2}H-NMR and cross-checked by freeze-fracture and X-ray diffraction. It is shown that Ca^{++} can segregate dioleoyl PS into cochleate domains in equimolar PE/PS mixtures if dioleoyl PE is used, but not if the more unsaturated species dilinoleoyl PE is used. Cholesterol inhibits this segregation and facilitates the Ca^{++} induced formation of a hexagonal (H_{II}) lattice containing both PE and PS. In the absence of Ca^{++}, the thermotropic phase behavior of both the PE/PS and PE/PS/cholesterol systems is markedly dependent on the thermal history of the specimens. Ca^{++} abolishes much of the thermal hysteresis and the need for long equilibration times. In equimolar dioleoyl PC/dioleoyl PS mixtures, Ca^{++} induced lipid segregation is not affected by the presence of up to 33 mol% cholesterol. These results suggest that Ca^{++} induced phase separation of PS may not be readily achievable in multicomponent biomembranes containing both PE and cholesterol. Supported by the M.R.C. (Canada), the B.C. Heart foundation, the N.I.H. and the D.O.E.

T-Pos54 ^{13}C-NMR OF DIPALMITOYLPHOSPHATIDYLCHOLINE - PALMITIC ACID MIXTURES
Andrea B. Kohn and Stephen E. Schullery, Chemistry Department, Eastern Michigan University, Ypsilanti, MI 48197.

Mixtures of dipalmitoylphosphatidylcholine and palmitic acid in excess water were studied by ^{13}C-NMR. Twelve compositions containing from zero to 0.67 mole fraction palmitic acid were studied over the temperature range 29 to 73°C. Phase transition temperatures were obtained from plots of T_2^* versus temperature, where apparent spin-spin relaxation times T_2^* were estimated from half widths of the choline methyl and the alkyl methylene signals. The results are consistent with a previously published phase diagram (Schullery et al., Biochemistry 20 (1981)6818-6824) containing two peritectic transitions in the low-palmitic acid region. The NMR data provide direct evidence for the lower temperature peritectic transition which was not detected in previous differential thermal analysis studies but whose existence had been theoretically inferred.

T-Pos55 A DIFFERENTIAL SCANNING CALORIMETRY (DSC), X-RAY DIFFRACTION AND ^{31}P-NMR STUDY OF THE GEL PHASES OF DIHEXADECYL (DHPC) AND DIPALMITOYLPHOSPHATIDYLCHOLINE (DPPC). D.J.Siminovitch, M.J.Ruocco and R.G. Griffin. F. Bitter Nat'l Magn. Laboratory, M.I.T., Cambridge, MA 02139

DSC of hydrated (50 wt % H_2O) DHPC dispersions annealed at -4°C demonstrates a reversible low enthalpy transition (ΔH~0.5 kcal/mol) at 2°C in contrast to the conditionally reversible, high enthalpy subtransition (ΔH~3-7 kcal/mol) at 17°C for annealed DPPC dispersions. X-ray diffraction studies indicate that DHPC dispersions form a lamellar gel phase (d_{AVE} =46.3 Å) with wide angle reflections at 1/4.1 and 1/3.7 Å at -2°C. At temperatures above the low enthalpy transition, (20°C), a second lamellar gel phase (d_{AVE}=46.8 Å) with a single wide angle reflection at 1/4.04 $Å^{-1}$ is obtained. In contrast, at -2°C DPPC dispersions yield a lamellar phase (d=59 Å) and wide angle reflections at 1/4.4 and 1/3.8 $Å^{-1}$ characteristic of the L_c phase, while at 20°C the $L_{\beta'}$ gel phase (d=64 Å) with reflections at 1/4.2 and 1/4.1 $Å^{-1}$ is observed. We observe little difference between DHPC and DPPC in the magnitude of the chemical shielding anisotropy (CSA) in the L_α and $P_{\beta'}$ phases. However, in the low temperature gel phases the DHPC CSA is significantly reduced relative to the DPPC CSA. In the DHPC gel phase, axially symmetric powder patterns are observed until -20°C; remarkably, the CSA changes by ~5 ppm over the 60°C range from 40°C (58 ppm) to -20°C (62 ppm). Previous studies indicate that DPPC molecules cease long axis rotation near 0°C. [1] A possible explanation for the observed ^{31}P-NMR DHPC spectra may be that DHPC long axis rotation persists to much lower temperatures (~-30 C). The persistence of long axis rotation may in part result from the removal of any motional constraints imparted by the carbonyl group and molecular conformational and packing differences at the bilayer interface. 1) J.H. Davis, Biophys.J.(1979) 27, 330. Supported in part by the National Multiple Sclerosis Society (FG591-A-1) and the Natural Science and Engineering Research Council of Canada.

T-Pos56 PERTURBATION OF RED CELL MEMBRANE DIELECTRIC CONSTANT BY BUTANOL. R.I. Macey and F. Orme, Dept. of Physiology-Anatomy, Univ. of California, Berkeley, CA 94720.

Dielectric properties of the lipid bilayer portion of human red cell membranes were investigated through ion selective electrode measurements of the flux of the hydrophobic ion TPA^+ (tetraphenyl arsonium). Calculated TPA^+ permeability coefficients show a dramatic increase as a function of butanol concentrations. Corresponding membrane butanol concentrations were calculated from the red cell membrane/alcohol partition coefficient data of Roth and Seeman (Biochim. Biophys. Acta 255:207,1972) (binding of butanol to Hb was negligible). Treating the membrane as a bulk hydrocarbon slab, its dielectric constant at each butanol concentration was calculated using a modified form of the Clausius-Mossotti formula (extended to liquid mixtures). This data was then used to calculate the TPA permeabilities (normalized to untreated native membrane) using the Parsegian modification (Nature 221:884,1969) of the Born charging energy. All parameters used in the calculation are available from independent measurements. Using the following parameters: native hydrocarbon dielectric constant = 2.2, butanol dielectric constant = 17.5, thickness = 50 Å, butanol/membrane partition coefficient = 1.5, TPA ion radius = 4.2 Å, the calculated permeability ratios quantitatively account for the measurements over the entire concentration range of 0 to 400 mM butanol. Corresponding values of membrane dielectric constant ranged from 2.20 to 2.36 while permeabilities ranged from 8.8×10^{-7} to 9.9×10^{-6}. (Supported by NIH Grant #GM18819.)

T-Pos57 GLYCOPHORIN A ACTS AS A RECEPTOR FOR E. COLI K99 BINDING. Donald E. Brooks, Departments of Pathology and Chemistry, University of British Columbia, Vancouver, Canada, V6T 1W5. Application of a viscometric assay to the hemagglutination induced by an Escherichia coli strain producing a K99-positive adhesin suggests that shear forces can enhance the strength of bacterial adhesion. The reaction proceeds in two phases, an initial phase in which the degree of aggregation remains constant during shearing, as indicated by a plateau in the shear stress-time behaviour, and a second phase in which the aggregation is enhanced and the shear stress increases with time. The results strongly parallel those found in studies of concanavalin A-induced hemagglutination. The purified adhesive structures (pili) produce an identical response to that of whole bacteria indicating that no other membrane components are involved in the adhesion reaction. This hemagglutination is selective for MM and MN erythrocytes over NN erythrocytes. Competitive inhibition with isolated glycophorin of both the binding of ^{125}I-labelled purified adhesin and the hemagglutination detected viscometrically or on microtitre plates suggests strongly that the receptor for this adhesin is glycophorin A. We thank the Canadian MRC for support.

T-Pos58 THE MECHANISM OF FORMATION OF IRREVERSIBLY SICKLED CELLS. Kazumi Horiuchi, Kurumi Horiuchi and S. Tsuyoshi Ohnishi. Department of Hematology and Medical Oncology, Hahnemann University School of Medicine, Philadelphia, Pa. 19102.

It is known that certain percentage of red blood cells in sickle cell patients are permanently deformed. These irreversibly sickled cells (ISC) have higher density and less deformable membrane. ISC is considered to play a major role in causing anemia in the patients, since they are subject to sequestration by the spleen (although a direct relationship between the percentage of ISC in the circulation and the severity of the disease is not observed). The mechanism of ISC formation was not well understood, because a method to prepare ISC in vitro under physiological condition has not been established. We have recently developed a method to prepare ISC in vitro under physiological condition, namely, to expose cells to repeated sickling-unsickling process (S.T. Ohnishi, Brit. J. Haematol.; in press). We have found that when we expose cells to such cycles, the cell density starts to increase even after exposure to several cycles. Cell shape does not change immediately, but it does take ISC-form after several hours of such a process. It was found that "calmodulin-binding" drugs inhibit the formation of ISC, and that the potency is related to the affinity of the drug to calmodulin. A possible mechanism of ISC formation will be discussed. (Supported in part by NIH HL 23200).

T-Pos59 KINETIC INDEPENDENCE OF CHLORIDE, UREA AND WATER TRANSPORT IN HUMAN ERYTHROCYTES. S. C. Jones and O. Fröhlich. Dept. of Physiology, Emory University, Atlanta, GA 30322.

At 0°C, pH 7.6 and at concentrations of 1 and 2 M, equilibrium exchange of urea across human red cells has a half-time of about 2.5 s and 5 s, respectively, as determined by a rapid filtration technique (Dalmark and Wieth, J. Physiol. 244:583, 1972). We have measured 14-C urea fluxes to test the hypothesis of Solomon and coworkers (Biophys. J. 37:215a, 1982) that an aqueous pore constitutes a common pathway of chloride, urea and water transport. We have used two strategies to test for coupling between urea, chloride and water transport. In the first approach, we measured urea fluxes in the presence of different chloride concentration gradients which are known to recruit the anion transport protein into different conformational states. In the second approach, we measured urea transport in the presence of osmotic gradients to test for flux coupling between urea and water movements along the postulated common pathway. We found that urea exchange was not significantly altered when measured in chloride-free media in which the anion transport protein is locked into an empty, outward-facing conformation, while chloride net efflux is strongly affected by the conformational state of the transporter (Fröhlich, Biophys. J. 41:63a, 1983). Urea transport measured into media in which the osmolality was varied by adding different concentrations of sucrose or sorbose was not significantly different under conditions of net water influx or efflux. Therefore, water and urea do not appear to interact along their transport pathways. The data suggest that the transport pathways of chloride, urea and water transport are not kinetically linked. (Supported by a BRS Grant from Emory University).

T-Pos60 INHIBITION OF ANION TRANSPORT IN HUMAN ERYTHROCYTES BY CARBODIIMIDES. James D. Craik and Reinhart A.F. Reithmeier, Department of Biochemistry, University of Alberta, Edmonton, Alberta, Canada T6G 2H7.

Incubation of intact human erythrocytes with carbodiimides EDC (1-ethyl-3-(3-dimethylaminopropyl) carbodiimide hydrochloride or CMC (1-cyclohexyl-3-(2-morpholino ethyl) carbodiimide metho-p-toluenesulfonate) which are known to modify carboxyl residues leads to irreversible inhibition of anion uptake as measured by ^{32}P phosphate uptake in exchange for intracellular chloride. Inhibition is rapid at 37°C (maximal effect in less than 5 minutes, 10 mM EDC), temperature dependent, and concentration dependent (half maximal inhibition 2.5 mM EDC, 50% haematocrit, 37°C) but does not give total inhibition under any conditions tested. Inclusion of glycine ethyl ester, a nucleophilic reagent, in the incubation medium had little effect on transport inhibition.

Carbodiimide treatment of intact erythrocytes gives rise to intermolecular cross linking of many membrane proteins and ghost preparations from treated cells are pink indicating that haemoglobin has cross linked to the membrane. However substantial inhibition of anion transport may be attained before significant changes to the pattern of membrane proteins as seen on SDS-PAGE (Laemmli buffer system) become apparent. Digestion of carbodiimide treated cells by proteolytic enzymes papain and chymotrypsin have been performed to examine possible intramolecular cross linking within Band 3, the anion transport system.

(Supported by the Medical Research Council of Canada [RAFR] and an Alberta Heritage Foundation for Medical Research Fellowship [JDC])

T-Pos61 A SYNERGISTIC EFFECT OF PHOSPHATIDYLCHOLINE/ACIDIC PHOSPHOLIPID MIXTURES ON THE PURIFIED Ca^{2+} Mg^{2+} ATPase FROM HUMAN ERYTHROCYTE MEMBRANES. David R. Nelson, Donald J. Hanahan (Intr. by Barry B. Muhoberac) The University of Texas Health Science Center, San Antonio, TX 78284

Ca^{2+} Mg^{2+} ATPase was solubilized from human erythrocyte ghost membranes by detergent extraction with Triton N101(0.5mg/mg membrane protein) and purified by calmodulin affinity chromatography. Aliquots were then assayed in a cocktail containing 0.15mg/ml Triton N101 and various phospholipids or phospholipid mixtures. No activity was seen in the presence of detergent alone but the detergent was required for activity with phospholipids. At low levels(0.005mg phospholipid/ml) the ATPase activity was highly sensitive to the detergent concentration, with maximal activity occurring at or near the critical micelle concentration(0.053-0.061mg/ml). When phosphatidylcholine(PC) was varied from zero to 0.1mg/ml, activities in the range from 1-3μmol/min/mg were obtained. The same concentrations of the acidic phospholipids phosphatidylserine(PS) or phosphatidylinositol(PI) produced 5-8 times greater activity. However, when a less than optimal concentration of PS(0.02mg/ml) was included in the assays and PC was added, a synergistic effect was observed. The ATPase responded to the additional PC as if more PS were being added. PC did not produce this effect in the absence of PS, nor could the result be explained by an increase in the total phospholipid concentration. The stimulation of ATPase activity caused by the addition of PC did not continue beyond 0.01mg/ml (33% PC, 67% PS). After this, the ATPase activity decreased, apparently due to dilution of the PS by the PC. This observation may explain why some investigators have seen reactivation of the ATPase by PC in phospholipase delipidated ghosts, while others have claimed a requirement for acidic phospholipids. Supported in part by NIH grant AM-25547-04

T-Pos62 EFFECT OF THIOUREA ON DBDS BINDING TO BAND 3 IN HUMAN RED CELL MEMBRANES by Peter L. Dorogi* and A. K. Solomon, Biophysical Lab., Dept. of Physiology and Biophysics, Harvard Medical School, Boston, MA 02115 (*Present address: Gillette Research Institute, Rockville, MD)

Binding of DBDS(2,2'-dibenzamido-4,4'-stilbene disulfonic acid) to band 3 is followed by a conformation change in band 3 to produce band 3*-DBDS (Verkman et al, J. Gen. Physiol., 81, 421, 1983). pCMBS(p-chloromercuribenzene sulfonate) is a non-competitive inhibitor of DBDS binding (Lukacovic et al, Biophys. J., 37, 215a, 1982). We have found that thiourea (TU) modifies DBDS binding kinetics, both with and without pCMBS, and have proposed the following reaction scheme:

$$\text{DBDS} + \text{band 3} \overset{K_i}{\longleftrightarrow} \text{band 3-DBDS} \underset{k_{-j}}{\overset{k_j}{\rightleftharpoons}} \text{band 3*-DBDS}$$

When [band 3] << [DBDS] << 0.5 μM; TU = 0; pCMBS = 1.5 mM; K_i = 28 ± 5 μM, k_j = 4.0 ± 0.5 s^{-1} and k_{-j} = 0.10 ± 0.05 s^{-1} (Lukacovic et al, priv. comm.). Addition of 20 mM TU changes these values to: K_i = 0.6 ± 0.3 μM, k_j = 0.2 ± 0.2 s^{-1}, and k_{-j} = 0.20 ± 0.03 s^{-1}, indicating that TU stabilizes the bimolecular association. Without TU the high affinity form, band 3*-DBDS, is much more stable than the low affinity form; TU makes both forms equally stable. K_D for the TU effect on DBDS fluorescence is ~ 0.4 mM, much lower than the K_I of TU inhibition of urea transport of 15 mM (Chasan and Solomon, Fed. Proc., 39, 957, 1980). Without pCMBS, TU causes smaller effects. Since DBDS binds specifically to band 3 under our experimental conditions, these results indicate that TU can alter the band 3 conformation. (Funded by NIH: HL 14820).

T-Pos63 DTNB BINDING TO BAND 3 IN THE HUMAN RED CELL by Peter L. Dorogi, Michael F. Lukacovic, Michael R. Toon and A. K. Solomon, Biophysical Laboratory, Department of Physiology and Biophysics, Harvard Medical School, Boston MA 02115

Polyacrylamide gel electrophoresis by Brown et al (Nature 254, 523, 1975) shows that DTNB(5,5'-dithiobis(2-nitrobenzoic acid)) binds to band 3 in NEM (N-ethylmaleimide) treated human red cell ghosts with no evidence of binding to other membrane proteins. DTNB binding to NEM treated red cell ghosts, measured by optical absorption (412 nm) of the reaction product, is equivalent to a stoichiometry of 1.0 ± 0.2:1 with band 3 monomers. The time course of binding of the specific fluorescent stilbene anion exchange inhibitor, DBDS(2,2'-dibenzamido-4,4'disulfonic stilbene), to NEM treated band 3 was previously studied by stopped flow kinetics. The mercurial sulfhydryl reagent, pCMBS(p-chloromercuribenzene sulfonate), inhibits water transport into the red cell. Stopped-flow studies have shown that pCMBS is a non-competitive inhibitor of DBDS binding to band 3 (Lukacovic et al, Biophys. J., 37, 215a, 1982). In the presence of 1.0 mM pCMBS, DTNB increased the time constant for pCMBS binding from 3.5 ± 0.6 s to 6.7 ± 1.3 s ($p < 0.05$), thus showing that DTNB binding affects the band 3 conformation. In the absence of pCMBS there is a similar, but smaller, effect on the time constant. DTNB does not bind to the pCMBS site because equilibrium binding of DBDS to band 3, in the presence of pCMBS, is unaffected by DTNB. Furthermore, DTNB has no effect on the inhibition of red cell water flux by pCMBS. However, we have found that DTNB binding does inhibit ethylene glycol transport in NEM treated red cells. In view of the evidence indicating that the primary site for DTNB binding is band 3, this observation suggests that ethylene glycol transport is mediated by band 3. (Supported in part by NIH grant HL 14820).

T-Pos64 DIFFUSIONAL FLUX OF SOLUTE IS NOT COUPLED TO OSMOTIC FLOW OF WATER ACROSS THE ERYTHROCYTE MEMBRANE. W.R. Galey and J. Brahm, Dept. of Physiology, University of Mexico, Albuquerque, New Mexico, 87131 and Dept. of Biophysics, University of Copenhagen, DK 2200 N, Denmark.

The ratio of our recent determinations of diffusional and osmotic water permeabilities yield a calculated equivalent pore diameter of ~25Å which is inconsistent with the permeability characteristics of red cells. This casts doubt on the validity of the equivalent pore theory. This theory and the band 3 mediated common pathway for ions, nonelectrolytes and water proposed by Solomon et al.(Biophys.J.1982,37,215a) predict a solvent drag effect on solute fluxes. To test this, we measured the tracer efflux of H_2O, urea, Cl and ethanol in a continuous flow reaction apparatus under: Osmotic equilibrium and osmotic flow of water into and out of cells induced by mixing 100 mM KCl equilibrated cells with a 200 or 250 mM KCl solution, or vice versa. Taking into account that the efflux rate coefficient changes with cell volume during the experiment and comparing the fluxes to controls at the same equilibrium osmolality, neither an increase in solute flux with water flow, nor a decrease in flux against water flow is demonstrated for any of the solutes. Using urea as a test solute, we found that not only was the efflux independent of the direction of water flow but also independent of the magnitude of water flow. These results show no demonstrable solvent drag and thus no frictional interaction between solutes and water.

T-Pos65 MICROWAVES ELICIT THE IRREVERSIBLE SHEDDING OF PROTEIN FROM THE RABBIT ERYTHROCYTE DURING EXPOSURE AT THE MEMBRANE PHASE TRANSITION TEMPERATURE. R.P. Liburdy and A.Penn, Institute of Environmental Medicine, New York University Medical Center, 550 First Ave, NY, NY 10016

We have previously reported that short-term microwave exposure of rabbit erythrocytes(2450MHz, 60mW/g, 30 min) increases passive permeability to Na only for exposures conducted at the membrane phase transition temperature, T_c. This finding demonstrated that functional alterations in transport induced by microwaves are linked to the membrane phase transition. We have recently sought to identify structural alterations associated with microwave exposures by employing SDS-polyacrylamide gel electrophoresis and sensitive silver staining. Here we report that microwave exposure of erythrocytes at T_c(17.5°C) as described above results in the irreversible shedding of two proteins of molecular weight(MW) 26,000 and 24,000D into the cell-free supernantant, and that these proteins are not shed from sham-exposed, temperature-matched cells. In addition, microwave-treated samples display pronounced shedding of proteins of MW 28,000, 15,000, 14,400, 13,000, 11,000, 10,000, and 8,000D. In contrast, 20,000 and 18,000D proteins are more pronounced in the sham-treated samples. This differential shedding was not detected for exposures conducted at off-T_c temperatures. We estimate that only 450 fgm of proteins are shed per erythrocyte in response to microwave treatment. This corresponds to approximately 1/100th of the total protein mass of the erythrocyte membrane. These proteins are most likely peripheral proteins which are loosely bound to the outer leaflet of the cell membrane via cationic bridges.

This research was supported by the Office of Naval Research(RPL) and the NIEHS(AP).

T-Pos66 ENCAPSULATION OF HEMOGLOBIN IN PHOSPHOLIPID VESICLES: SURROGATE RED CELLS IN VITRO AND IN VIVO. Martha C. Farmer and Bruce P. Gaber, Biomolecular Optics Section, Optical Probes Branch, Code 6510, Naval Research Laboratory, Washington, DC 20375

Hemoglobin encapsulated in large unilamellar vesicles (LUV's) is being developed as an emergency resuscitation fluid. Oxygenation of the encapsulated hemoglobin is rapid and cooperative; oxygen affinity can be modulated by co-encapsulation of organic phosphates. The liposomal membrane is dimyristoyl phosphatidylcholine:cholesterol:dicetyl phosphate in a 5:4:1 molar ratio. Repulsive forces due to the negative charge on the dicetyl phosphate prevent significant aggregation or fusion during storage. Serum free Ca++ levels induce reversible aggregation but not fusion. No hemolysis is detected in a suspension of erythrocytes and hemoglobin-filled LUV's incubated at 37 C for 8 hours. Circulation half-life is generally a function of vesicle diameter and composition. Vesicle diameter and lamellarity are controlled by high-pressure extrusion through Nuclepore membranes. Precipitation of proteins onto the liposomal membrane during extrusion and circulation will be demonstrated and the consequences discussed. Infusion of the surrogate red cells into an isolated rabbit heart preparation yielded measurements of coronary resistance which paralleled that of infused erythrocytes. Initial toxicity studies are negative. Data on the survival of transfused animals will be presented. (Supported by the Office of Naval Research. MCF is a research fellow of the National Research Council.)

T-Pos67 FLUORESCENCE STUDIES USING SYNCHROTRON RADIATION ON NORMAL AND DIFFERENTIATED CELLS LABELED WITH PARINARIC ACIDS. T. PARASASSI, F. CONTI, N. ROSATO, O. SAPORA and E. GRATTON, Dept. of Chemistry University of Rome, CNR Pisa, Istituto Superiore Sanita Rome, Dept. of Physics University of Illinois at Urbana.

The fluorescence lifetime and polarization of fatty acids (cis- and trans-parinaric acids) have been used to study changes in membrane properties during the differentiation process in K562 cells. Fluorescence lifetimes have been measured using the multifrequency phase fluorometer at the ADONE facility at Frascati (Italy). The emission of cis- and trans-parinaric acid in K562 cells is doubly exponential. Resolution of the two lifetime values and the relative fractional intensities has been performed. The relative fraction of each exponential component as well as the lifetime values are different in normal and differentiated cells. Lifetime and polarization value changes are clearly associated with differentiation process indicating the involvement of the cellular membrane in the differentiation process. Also the decrease of lectin-induced agglutination has been revealed to be an early and sensitive test to monitor K562 cells induced differentiation. Our results suggest a structural rearrangement of the plasma membrane after differentiation, which we attribute to a greater extent of domains separation in the differentiated cells.

T-Pos68 BIEXPONENTIAL KINETICS OF DISULFONIC STILBENE BINDING TO HUMAN RED CELL GHOST MEMBRANES. Kevin R. Smith, and James A. Dix, Department of Chemistry, State University of New York, Binghamton, NY 13901.

The inhibitor of anion exchange in red cells, 4,4'-dibenzamido-2,2'-disulfonic stilbene (DBDS), undergoes fluorescence enhancement upon binding to band 3, the anion exchange protein. Kinetic studies of the binding of DBDS to band 3, done with a fluorescence stopped-flow photometer capable of 2 msec time resolution, reveal a biexponential time course: a fast time course that is approximately linear with DBDS concentration, and a slow time course that saturates with DBDS concentration. Analysis of the concentration dependence of the time course, either by pseudo-first order analysis or by numerical simulation, is consistent with a two-step binding mechanism consisting of a bimolecular association of DBDS and band 3 (forward rate constant 1-3 /uM s, reverse rate constant 3 /s), followed by a unimolecular rearrangement of DBDS-band 3 complex (forward rate constant 4 /s, reverse rate constant 0.1 /s). The inhibitors of anion transport, 4,4'-dinitro-2,2'- disulfonic stilbene (DNDS) and flufenamic acid, both reduce the forward rate constant for the bimolecular association of DBDS and band 3. In contrast, the transportable anion, chloride, increases the reverse rate constant for the unimolecular rearrangement. These studies suggest that DBDS has restricted diffusional access to its binding site on band 3, that the binding site is blocked by DNDS and flufenamic acid, and that chloride inhibits the unimolecular rearrangement of the DBDS-band 3 complex. Supported by NIH grant HL29488.

T-Pos69 CALCIUM-INDUCED IMMOBILIZATION OF GLYCOPHORIN IN THE HUMAN ERYTHROCYTE MEMBRANE. D.E. Golan, P.A. Singer, and W.R. Veatch (deceased). Departments of Pharmacology and Medicine, Harvard Medical School and Brigham and Women's Hospital, Boston, Massachusetts 02115.

Elevated intracellular calcium has profound effects on human erythrocyte shape and deformability, membrane associated properties that are governed by the erythrocyte cytoskeleton. Recent evidence suggests that glycophorin interacts with the cytoskeleton in a dynamic manner to control these properties. Fluorescence photobleaching recovery (FPR) was used to measure the lateral mobility of labeled glycophorin in intact erythrocyte membranes, in the presence and absence of elevated intracellular calcium. Specificity of labeling was achieved through limited periodate oxidation of extracellular, glycophorin-linked sialic acid moieties, and conjugation of the fluorescent probe fluorescein-5-thiosemicarbazide to the resultant aldehydes. The divalent cation ionophore A23187 was used for rapid calcium loading of intact erythrocytes. Control erythrocytes incubated either without A23187 or in the presence of both ionophore and EDTA manifested lateral diffusion coefficients for glycophorin of approximately 1 x 10^{-11} cm^2 sec^{-1} and fractional mobilities of 61-66%. Calcium treatment induced a 50% decrease in the fractional mobility of glycophorin without change in the diffusion coefficient of the mobile fraction, over the concentration range 10-100 μM. The immobilization was not due to ionophore alone, since erythrocytes incubated with ionophore and EDTA yielded results identical to those incubated without ionophore. It is likely that the immobilization of glycophorin induced by calcium is mediated by the erythrocyte cytoskeleton; this suggests, further, that calcium may be involved in the dynamic regulation of glycophorin-cytoskeleton interactions. Supported by NIH grant AI-15311.

T-Pos70 MEASUREMENT OF CYTOSOLIC FREE CA DURING VOLUME REGULATION IN AMPHIUMA RED BLOOD CELLS. Peter M. Cala, Elizabeth Murphy, and Lazaro J. Mandel. Physiology Departments, University of California School of Medicine, Davis, CA and Duke University Medical Center, Durham, NC.

Cytosolic free Ca (Ca_f) was measured in a suspension of Amphiuma red cells using the null point method (Murphy and Mandel, AJP 242:C124, 1982). Cells were pre-incubated for 1½ hours at 23°C in the control solution (1R) containing (mM): NaCl, 95; KCl, 3; MgCl, 1; CaCl, 1; imidazole,20; glucose, 10; sucrose, 30. Subsequently, cells were centrifuged and resuspended in the appropriate medium at a hematocrit of 1-1.5% modified to be nominally Ca-free and containing 40μM Arsenazo-III. Following a short re-equilibration, digitonin (1μg/mg protein) was added to permeabilize the cells to Ca and the uptake of Ca into the cells monitored optically with Arsenazo-III as a function of extracellular Ca (Ca_o) concentration. The Ca_o at which no net uptake or release of Ca is obtained (null point) measures Ca_f. In the control solution (1R, 240mosM), Ca_f=0.46±0.15μM. Shrinking the cells in 1.3 R (319mosM) activates an obligatorily coupled (1:1) Na/H exchange which restores volume to normal levels (RVI). Associated with cell shrinkage, Ca_f decreased to 0.16±0.11μM. In contrast, swelling cells in hypotonic medium (183mosM) activates a K/H exchanger which causes cell volume to decrease toward normal levels (RVD). Coincident with the swelling-induced activation of K/H exchanger, there is a large decrease in intracellular Ca binding sites, leading to a probable increase in Ca_f over control. These characteristics of RVD could be mimicked by addition of 5μM A23187. In other experiments, phenothiazines (20 and 50 μM), known calmodulin inhibitors, inhibited the RVD response in the presence and absence of A23187, while stimulating by 30% the RVI response. These results suggest that: 1) RVD may be mediated by an increase in Ca_f, 2) RVI may involve a decrease in Ca_f, and 3) Ca-calmodulin-mediated reactions may be responsible for activation of K/H exchange and inhibition of Na/H exchange.

T-Pos71 MOLECULAR ORDER AND CONFORMATION IN CHOLESTEROL-MODIFIED HUMAN ERYTHROCYTE MEMBRANES Michael W. Rooney, Yvonne Lange* and John W. Kauffman Northwestern U. Evanston, Il 60201 and *Rush University, Chicago, Il 60612

The effects of cholesterol on human red cell membrane architecture were analyzed with FTIR and Raman vibrational spectroscopies. Compared to normal erythrocyte membranes (0.8 mol cholesterol per mol phospholipid), acyl chain mobility is greater for the depleted (C/P ≈ 0.6) and less for the enriched (C/P ≈ 1.2) membranes as determined from shifts of the IR symmetric methylene C-H stretching band (2852 cm^{-1}) over the temperature range 5° → 40°C. There is a linear-like trend of the IR shifts, without any evidence of a phase change for any of the three cholesterol contents. Raman C-C stretching modes (1065-1130 cm^{-1}) reflecting trans-gauche isomerism in the lipid acyl chains indicate that depleted and control membranes have similar conformational contents. Enriched membranes, however, reveal a 20% increase in the intensity of the trans mode relative to the 1004 cm^{-1} line which is a stable reference in all three preparations. The IR and Raman data suggest that high cholesterol contents decrease acyl chain mobility as well as induce the gauche → trans isomer transition, while lower contents seem to only affect chain mobility. The relative intensity of the Raman protein skeletal band (940 cm^{-1}) is used to estimate the content of helical secondary structure of the depleted membranes at ≈ 40%, the control membranes at ≈ 55% and the enriched membranes at ≈ 75%. A strong contribution from the IR carbonyl mode (1726 cm^{-1}) of the enriched membranes was interpreted as an increase in order of the hydrate structure surrounding the 2-acyl chain carbonyl group. IR difference spectra of enriched relative to depleted membranes had similar ordering in choline and phosphate vibrational groups.

T-Pos72 INCREASED PASSIVE SODIUM FLUX ASSOCIATED WITH HUMAN ESSENTIAL HYPERTENSION. George D. Webb, Dept. Physiol. & Biophys., Univ. of Vermont Coll. Med., Burlington, VT 05405

Several laboratories have reported an increased passive flux of Na across red blood cell membranes from human hypertensives compared to red cells from normotensives. We report a confirmation of these findings in a preliminary study of 4 hypertensive subjects and 4 normotensive subjects of similar age and weight (all male). Intracellular Na and K were determined by flame photometry of lysed fresh red blood cells (washed 5 times with iced isotonic Mg-sucrose buffer). We also labeled intracellular Na by incubating cells overnight in a nutrient repletion medium containing ^{22}Na. This procedure did not alter significantly the intracellular Na and K concentrations from their fresh values. The rate of efflux of ^{22}Na from the labeled red blood cells into a physiological saline solution was measured with and without the presence of 10^{-4}M ouabain by counting timed samples of supernate for ^{22}Na. The results are presented below:

	Fresh intracellular Na conc. (mM)			"Passive" ^{22}Na efflux rate (mmol/l cells/hr)		
	individual values	mean	std. dev.	individual values	mean	std. dev.
normotensive	8.0, 7.3, 7.8, 6.9	7.5	.5	.85, .73, .71, .70	.75	.07
hypertensive	10.6, 10.9, 7.8, 13.2	10.6	2.2	.87, 1.16, 1.08, .97	1.02	.13

Both intracellular Na concentration and ouabain-insensitive ("passive") Na efflux are significantly greater in the hypertensive group than in the normotensive group (unpaired t-test $p<.05$). Note that there is no overlap of the individual "passive" Na efflux rates, thus raising the hope that passive Na flux across red blood cell membranes can be used as a genetic marker to detect young individuals with a predisposition for high blood pressure. Supported by BRSG and GCRC, both funded by USPHS.

T-Pos73 PHORBOL ESTER STIMULATED PHOSPHORYLATION OF ERYTHROCYTES MEMBRANE PROTEIN E. Ling and V. Sapirstein, Dept. of Biochemistry, E.K. Shriver Center, Waltham, MA 02254

Erythrocytes contain a submembrane cytoskeletal network consisting of spectrin, actin, and band 4.1. Numerous studies have shown that these proteins play important roles in determining erythrocyte shape, deformability and the lateral mobility of membrane proteins. It has been suggested that phosphorylation of these cytoskeletal proteins may be related to the control of these morphological properties. We have examined the in situ phosphorylation of erythrocyte membrane and the cytoskeletal proteins. Erythrocytes were preincubated with ^{32}Pi at 37°C for 1 hour. Membranes were prepared by lysis of the cells in the presence of 5mM EDTA and 1mM PMSF. Membrane proteins were analyzed by SDS polyacrylamide gel electrophoresis (SDS-PAGE) and autoradiography. We observed that addition of phorbol-12-myristate-13 acetate (PMA) 10 min prior to lysis dramatically increased the phosphorylation of a protein with molecular weight of 80-90 kD. In contrast, there was no increase in the phosphorylation of spectrin, band 3 or actin during the same period. 4 α-phorbol 12, 13-didecanoate, an inactive phorbol ester, failed to cause an increase in phosphorylation of the 80-90 kD protein. When the intracellular Ca^{2+} was elevated by A23187 in the prescence of high external Ca^{2+} (1.2mM), this protein was degraded as revealed by its abscence on SDS-PAGE and autoradiogram. The degradation of this protein appeared to be dependent on the intracellular Ca^{2+} concentration since addition of ionophore in the presence of low external CA^{2+} failed to promote degradation. The identity and the physiological role of this 80-90 kD protein is not known. However, the molecular weight and its susceptibility to Ca^{2+} dependent degradation suggests that it may be band 4.1. Experiments are being carried out to further characterize this protein. (Supported by NS16186 and HD05515).

T-Pos74 COLD SHOCK HEMOLYSIS STUDIED BY FREEZE-FRACTURE AND ESR. T. Takahashi*, E.F. Erbe**, R. L. Steere**, S. Noji*** and H. Kon***. (Intr. by R.J. Williams) *Cryobiology and Tissue Banking Laboratory, American Red Cross, Bethesda, MD; **Plant Virology Laboratory, United States Department of Agriculture, Beltsville, MD; ***Laboratory of Chemical Physics, NIADDK, National Institutes of Health, Bethesda, MD.

When human red cells are osmotically stressed or chemically treated, they hemolyze if they are cooled below +10°C (called "cold shock"). We studied the effect of osmotic stress and temperature change on membrane fluidity by ESR using various membrane probes. At constant temperature, membrane fluidity detected by 12-doxyl stearate decreased as the extracellular salt concentration was raised above isotonic, reaching a plateau at 900 mOsm. This fluidity remained constant to about 1800 mOsm. In contrast, hypertonic sucrose solution produced a peak splitting, indicating that a second, immobile phase had developed. The mobility of cholesterol did not change between 300 and 1200 mOsm but decreased abruptly above 1200 mOsm and then remained constant between 1800 and 2400 mOsm. When red cells in isotonic NaCl were cooled from 37° to -5°C, the Arrhenius plots of isotropic rotational correlation time consisted of two straight lines with a break point at 10°C. In contrast, the plots for hypertonic conditions (1800 mOsm) exhibited a stepwise change, indicating that some change, such as a phase transition, occurred in the cell membrane at approximately 10°C. This change was also observed visually by freeze-fracture electron microscopy. At 10°C, cells in 1800 mOsm became wrinkled and membrane particles were aggregated.

All the chemicals that induce isotonic cold shock are calmodulin antagonists, indicating that calmodulin may be involved in cold shock hemolysis.